Republic of Iraq
Ministry of Higher Education
and Scientific Research
University of Babylon

AN INVESTIGATION OF THE BEHAVIOUR OF SELF – LUBRICATED FLOATING RING JOURNAL BEARING USING AN IMPROVED BOUNDARY CONDITIONS

A Thesis
Submitted to the College of Engineering of University of Babylon in Partial Fulfillment of the Requirements for the Degree of Master of Science in Mechanical Engineering
(Applied Mechanics)

By
Lekaa' Hameed Abd – Al Shaheed
Al – Joubori
(B. Sc, 1996)
(November, 2005)

2005 A.M *1426 A.H*

﴿ بسم الله الرحمن الرحيم ﴾

﴿ يرفع الله الذين آمنوا مِنكم والذين أُتوا
العِلمَ دَرَجاتٍ والله بما تعملونَ خبيرٌ ﴾

صدق الله العلي العظيم

سورة المجادلة , الآية 11

SUPERVISOR CERTIFICATE

*We certify that this thesis entitled "**An Investigation Of the Behaviour of Self – Lubricated Floating Ring Journal Bearing Using An Improved Boundary Conditions**" was prepared under our supervision at the Mechanical Engineering Department, University Of Babylon, Babylon – Iraq, as a partial fulfillment of the requirements for the degree of Master of Science in Mechanical Engineering.*

Signature	*Signature*
Lecturer	*Asst. Prof.*
Dr. Basim A. Abass Al-Maksosi	*Dr. Alaa' M. Hussan Al-Jesany*
(Supervisor)	*(Supervisor)*
Date / /	*Date / /*

EXAMINING COMMITTEES CERTIFICATE

*We certify that this thesis entitled "**An Investigation of the Behaviour of Self – Lubricated Floating Ring Journal Bearing Using An Improved Boundary Conditions**" and as examining committee, examined the student "**Lekaa' Hameed Abd – Al Shaheed Al – Joubori**" in its contents and that in our opinion it meets the standard of thesis for the degree of Master of Science in Mechanical Engineering.*

Signature:

Name: **Lecturer**

Dr. Basim A. Abass Al-Maksosi

(Supervisor)

Date: / /2006

Signature:

Name: **Asst. Prof.**

Dr. Alaa' M. Hussan Al-Jesany

(Supervisor)

Date: / /2006

Signature:

Name: **Asst. Prof.**

Dr. Ahmed A. Al – Rajihy

(Member)

Date: / /2006

Signature:

Name: **Asst. Prof.**

Dr. Bahaa' I. Kazim

(Member)

Date: / /2006

Signature:

Name: **Prof.**

Dr. Hussan J. Al- alkawi

(Chairman)

Date: / /2006

Approval of the Mechanical Engineering Department
Head of the Mechanical Engineering

Signature:

Name: **Asst. Prof. Dr. Adil A. Alwan Al- Mosawi**

Date: / /2006

Approval of the College Engineering
Dean of the College of Engineering

Signature:

Name: **Prof. Dr. Abdul alwahid K, Rajih Al- Bakri**

Date: / /2006

DEDICATION

To my supervisors

To my father

To my mother

To my family

ACKNOWLEDGMENT

(In The Name of Allah, The Gracious, The Merciful)

First, of all I thank ***Allah*** *who helped me in carrying out this work.*

I wish to express my deep gratitude to my supervisors Dr. Basim A. Abass and Dr. Alaa' M. Hussein for their invaluable help, advice and encouragement during the various stages of the present work.

My thanks are due to Dr. Karima. E. Amori, the lecturer at the Mechanical Engineering Department, University of Baghdad, for her assistance and great support.

Finally, I record sincere gratitude to my family and all those who have helped me throughout this research.

Lekaa'

2005

ABSTRACT

The static characteristics of porous floating ring journal bearing under hydrodynamic lubrication conditions are theoretically analyzed. An isothermal finite bearing theory was adopted during this analysis. To investigate the behaviour of such bearing, it is assumed that oil is supplied through the outside diameter of the bearing under low supply pressure.

The computational treatment consists of numerical solutions for the governing equations of the problem. The effect of different parameters affecting the performance of the bearing, namely, permeability, supply pressure, the geometry of the ring and the bearing are taken into consideration. The steady state characteristics are obtained numerically by solving the modified Reynolds' equation and the Darcy's equation together with appropriate boundary conditions to obtain the leading and trailing edges of the oil – films. The governing equations are transformed to discrete form using finite difference technique. A program written in (FORTRAN – 90) language has been prepared to solve the resulted simultaneous equations.

The angular extent of the oil – film formed in journal – ring and ring – bearing oil films is obtained by applying the integral momentum equation at the leading edge of the oil – film to define the beginning of the oil extent while, the continuity of flow across the trailing edge is used to define the end of the oil extent.

The analysis of the bearing performance shows the occurrence of a negative film pressure before the trailing end of the oil – films region

as expected when compared the results with the behaviour of porous bearings obtained by different workers. Numerical results show that the bearing performance is affected by different parameters namely, dimensionless oil – fed pressure, permeability, eccentricity ratios of inner and outer oil – film, clearance ratios, and the radii ratios.

LIST OF CONTENTS

NOMENCLATURE

The following symbols are generally used throughout the text. Others are defined as when used during the articles.

Symbol	Description	Units
c	Mean Radial Clearance	m
c_1	Journal – Ring Mean Radial Clearance	m
c_2	Ring – Bearing Mean Radial Clearance	m
$(D)_{ii}$	Inside Diameter, $(D)_{ii}= (2*R)_{ii}$	m
e_1	Journal Eccentricity	m
e_2	Floating Ring Eccentricity	m
$(F_r)_{ii}$	Frictional Force	N
$(F^{\wedge}_r)_{ii}$	Dimensionless Frictional Force, $(F^{\wedge}_r)_{ii}=(F_r\, c/\eta\ \omega R^2\, L)_{ii}$	-
$(F_{P\theta 1})_{ii}$	External Pressure Force Acting on Oil – Film Surface at Inlet End of Oil – Film Region at $(\theta=\theta_1)_{ii}$	N
$(F_{P\theta 2})_{ii}$	External Pressure Force Acting on Oil – Film Surface at Trailing End of Oil – Film Region $(\theta=\theta_2)_{ii}$	N
$(F_{\tau j})_{ii}$	External Shear Force Acting on Oil – Film Surface Adjacent to Journal and the Outer Surface of Ring i.e. $(y=h)_{ii}$	N
$(F_{\tau b})_{ii}$	External Shear Force Acting on Oil – Film Surface Adjacent to Inner Surface of Ring and Bearing i.e. (y=0)	N
$(h)_{ii}$	Oil – Film Thickness	m

$(h_{\theta 1})_{ii}$	Oil – Film Thickness at Inlet End	m
$(h_{\theta 2})_{ii}$	Oil – Film Thickness at Trailing End	m
$(h^{\wedge})_{ii}$	Dimensionless Oil –Film Thickness,($h^{\wedge}=h/c)_{ii}$	-
k_1	Permeability of the Porous Matrix	m^2
L	Length of the Ring and the Bearing	m
$(M_{\theta 1})_{ii}$	Circumferential Momentum Flow Rate across Oil Film Surface at Inlet End of Oil – Film Region, i.e. at $(\theta = \theta_1)_{ii}$	N
$(M^{\wedge}_{\theta 1})_{ii}$	Dimensionless Circumferential Momentum Flow Rate across Oil – Film Surface at Inlet End of Oil– Film Region, i.e. at $(\theta = \theta_1)_{ii}$, $(M^{\wedge}_{\theta 1}= M_{\theta 1}/(\rho c(R*\omega)^2 L)_{ii}$	-
$(M_{\theta 2})_{ii}$	Circumferential Momentum Flow Rate across Oil – Film Surface at Trailing End of Oil – Film Region, i.e. at $(\theta = \theta_2)_{ii}$	N
$(M^{\wedge}_{\theta 2})_{ii}$	Dimensionless Circumferential Momentum Flow Rate across Oil – Film Surface at Trailing End of Oil–Film Region, i.e. at $(\theta = \theta_2)_{ii}$, $(M^{\wedge}_{\theta 2}=M_{\theta 2}/(\rho c(R*\omega)^2 L)_{ii}$	-
$(M_{\theta c})_{ii}$	Circumferential Momentum Flow Rate across Oil – Film Surface at Both Axial Ends ($z = \pm L/2$)	N
$(M^{\wedge}_{\theta c})_{ii}$	Dimensionless Circumferential Momentum Flow Rate across Oil – Film Surface at Both Axial Ends i.e. at ($z = \pm L/2$), $(M^{\wedge}_{\theta c}= M_{\theta c}/(\rho c(R*\omega)^2 L)_{ii}$	-
$(M_{\theta b})_{ii}$	Circumferential Momentum Flow Rate across Oil – Film Surface Adjacent to Inner Surface of Ring and Bearing, i.e. (y=0)	N

$(M^{\wedge}_{\theta b})_{ii}$	Dimensionless Circumferential Momentum Flow Rate across Oil – Film Surface Adjacent to Inner Surface of Ring and Bearing , i.e. (y=0) $(M^{\wedge}_{\theta c}= M_{\theta c}/(\rho c(R*\omega)^2 L)_{ii}$	-
N_j	Journal Rotational Speed	r.p.m
N_r	Floating Ring Rotational Speed	r.p.m
N_r/N_j	Ring to Journal Speed Ratio	-
$(P)_{ii}$	Oil – Film Pressure	N/m^2
$(P^{\wedge})_{ii}$	Dimensionless Oil – Film Pressure, $(P^{\wedge} =c^2P/(\omega R^2 \eta))_{ii}$	-
$(P^*)_{jj}$	Oil – Film Pressure Inside the Porous Matrix	N/m^2
$(P^{\wedge *})_{jj}$	Dimensionless Oil – Film Pressure Inside the Porous Matrix, $(P^{\wedge *} =c^2P^*/(\omega R^2 \eta))_{jj}$	-
P_s	Supply Pressure	N/m^2
$P_s^{\wedge}$	Dimensionless Supply Pressure, $P_s^{\wedge} = P_s (c_2)^2/(\omega R^2 \eta))_{ii}$	-
$(q_{\theta p})_{ii}$	Poiseuilles' flow	m^3/s
$(q_{\theta c})_{ii}$	Couettes' flow	m^3/s
$(Q)_{ii}$	Flow Rate	m^3/s
R_j	Journal Radius	m
R_1	Ring Inner Radius	m
R_2	Ring Outer Radius	m
R_3	Bearing Inner Radius	m
R_4	Bearing Outer Radius	m
r	Radial Coordinate with Origin at the Center of the Bearing	-
$(S)_{ii}$	Sommerfeld Number , $(S= (R\omega \eta L / W)*(R / c)^2)_{ii}$	-

$(T)_{ii}$	Frictional Torque	N.m
$T^{\wedge}_{inner}$	Dimensionless Frictional Torque at the Inner Surface of Ring, $T^{\wedge}_{inner}= T_{inner}\, c_1 / \eta\omega_j R^3{}_1 L$	-
$T^{\wedge}_{outer}$	Dimensionless Frictional Torque at the Outer Surface of Ring, $T^{\wedge}_{outer}= T_{outer}\, c_2 / \eta\omega_r R^3{}_2 L$	-
$(U)_{ii}$	For ii=1 $U = U_j$ (Journal Velocity) For ii=2 $U = U_r$ (Ring Velocity)	m/s
$(u, v, w)_{ii}$	Oil – Film Velocity Components in θ,r,z Directions Respectively	m/s
$(u^*,v^*,w^*)_{jj}$	Oil Velocity Components inside the Porous Matrix in θ,r,z Directions Respectively	m/s
$(u_z)_{ii}$	Axial Velocity of Oil in Clearance Gap	m/s
$(u^*_r)_{jj}$	Radial Filter Velocity of Oil in Porous Matrix	m/s
$(u_\theta)_{ii}$	Circumferential Velocity of Oil in Clearance Gap	m/s
$(u_{\theta m})_{ii}$	Circumferential Velocity of Oil across the Control Surface at Inner Surface of Ring and bearing, i.e. (y=0)	m/s
$(W)_{ii}$	Load Carrying Capacity	N
$(W^{\wedge})_{ii}$	Dimensionless Load Carrying Capacity, $(W^{\wedge})_{ii}=(W\, c^2 / \eta\omega R^3\, L)_{ii}$	-
$(W_r)_{ii}$	Component of Oil – Film Force Along the Line of Centers	N
$(W^{\wedge}_r)_{ii}$	Dimensionless Component of Oil – Film Force Along the Line of Centers, $(W^{\wedge}_r)_{ii} =(W_r\, c^2 / \eta\omega R^3\, L)_{ii}$	-
$(W_T)_{ii}$	Component of Oil – Film Force Perpendicular to the Line of Centers	N

$(W^{\wedge}_{T})_{ii}$	Dimensionless Component of Oil – Film Force Perpendicular to the Line of Centers, $(W^{\wedge}_{T})_{ii} = (W_T\, c^2 / \eta\omega R^3\, L)_{ii}$	-
z	Axial Coordinate with Origin at middle of Bearing Length	-
y	Coordinate in the Direction of Oil – Film Thickness with Origin at Inner Surface of Floating Ring and Bearing	

Greek Symbols

Symbol	Description	Units
$(\beta)_{ii}$	Angular Extent of Oil Film, $(\beta)_{ii} = (\theta_2 - \theta_1)_{ii}$	Degree
$(\Delta r)_{ii}$	Increment in r – Direction	m
$(\Delta\theta)_{ii}$	Increment in θ– Direction	m
Δz	Increment in z – Direction	m
ε	Eccentricity Ratio	-
ε_1	Journal –Ring Eccentricity Ratio	-
ε_2	Ring –Bearing Eccentricity Ratio	-
$£_{P^{\wedge *}}, £_{P^{\wedge}}, £_{M^{\wedge}}, £_{q^{\wedge}}, £_{T^{\wedge}}, £_{W^{\wedge}}$	Errors Ratios	-
η	Absolute Viscosity of Oil	pa . s

θ	Angular Coordinate from Maximum Film Thickness Position	degree
$(\theta_1)_{ii}$	Angle from Line of Centers to Inlet End of Oil – Film Region	degree
$(\theta_2)_{ii}$	Angle from Line of Centers to Trailing End of Oil – Film Region	degree
$((R/c)\mu)_{ii}$	Coefficient of Friction	-
$(\hat{\mu})_{ii}$	Dimensionless Coefficient of Friction $= (R_1/c_1)\mu_1$ in case of journal –ring oil film $= (R_2/c_2)\,\mu_2$ in case of ring –bearing oil film	-
ρ	Density of Oil	kg/m^3
$(\hat{\tau})_{ii}$	Dimensionless Shear Stress	-
$(\Phi)_{ii}$	Permeability Parameter, $(\Phi)_{ii} = (k_1 R / c^3)_{ii}$	-
ψ_1	Journal –Ring Attitude Angle	degree
ψ_2	Ring –Bearing Attitude Angle	degree
ω_j	Journal Rotational Speed	rad/s
ω_r	Floating Ring Rotational Speed	rad/s

Subscripts

b	Referring to Bearing
ii	=1 referred for Journal – Ring Oil – Film =2 referred for Ring – bearing Oil – Film
jj	=1 for Porous Matrix of Floating Ring =2 for Porous Matrix of Bearing
j	Referring to Journal
i,j,k	Grid Number in Radial, Circumferential and Axial Direction, Respectively
r	Referring to Floating Ring
s	Supply Condition

Superscripts

^	Dimensionless Quantity
*	Porous Parameters

INTRODUCTION

1.1 Introduction

With the introduction of high speed turbochargers, gas turbines and compressors, vibration problems and instability were raised. Design improvement and modifications of journal bearing arrangement were made to decrease the excessive vibration and increase the stability range; one of the arrangements was the enhancement of damping characteristics of the journal bearing by introducing a floating ring between the rotating journal and the fixed bearing.

Porous journal bearings impregnated with oils are widely used in industrial applications. Since these bearings have more advantages than the non – porous bearings because they do not need continuous lubrication, hence their structure is simple and they also have low cost. In spite of their wide usage, their performance can vary from one application to another because of the complex conditions under which these bearings operate, **[1].**

The porous floating ring journal bearings, such as that shown in Figure (1-1) seem to have both advantages mentioned above (self – lubrication and high damping characteristics). Although, the solid floating ring journal bearing has been extensively investigated but there seems to be no work in literature dealing with the performance of the porous floating ring journal bearing. Hence, the present work represents an attempt to study the performance of such bearings.

This work consists of theoretical investigation of this type of bearing using improved boundary conditions suggested by some Japanese workers in the last decade, (Kaneko et, al. as be described later), to define the leading and trailing edges of the oil film. The experimental analysis carried out by these workers on the performance of porous bearings shows that the oil film is formed mainly in the loaded part of the bearing and the oil film is significantly smaller than that formed in solid journal bearing, even under hydrodynamic lubrication conditions. The theoretical analysis of the problem is based on the assumption that the bearing receives subsequent lubrication from an external source, to ensure that the bearing system operates under hydrodynamic lubrication conditions.

The analysis is carried out to a finite length bearing working under isothermal condition. A steady state solution has been obtained using the finite differences technique to solve the governing equations namely, the Reynolds' equation, which has been modified to include the slip velocity effect at the porous surface, to evaluate the pressure distribution through the journal – ring and the ring – bearing oil films and the Darcy's equation to evaluate the pressure distribution of the oil through the porous matrix (porous ring and porous bearing). The above equations are solved together with appropriate boundary conditions required to evaluate the oil film extent.

The momentum theorem is applied in the clearance gap of the oil films and the integral momentum equations are derived and used to determine the extent of the oil film at the inlet boundary, while the continuity of flow is used to determine the trailing edge at the outlet boundary line.

A computer program has been prepared and written in (FORTRAN 90) language and executed on a personal computer (Pentium 4) of 256 MB Ram, to solve the governing equations of the problem. An iterative scheme with successive under relaxation has been adopted to solve the problem numerically. The outer loop

of the iterations has been stopped when the equilibrium conditions which characterize the bearing performance (load and frictional torque about the inner and outer surfaces of the ring) are satisfied.

As the pressure distribution through the oil films are determined, all the parameters related to the performance of the bearing such as friction coefficient, attitude angle, load carrying capacity…etc, can be calculated. The computer program has been tested on the bases that the solution of the floating – ring bearing problem merely consists of parallel solution of two ordinary porous journal bearing problems. Hence, a problem related to a porous journal bearing with specified dimensions has been solved by the computer program and the results are compared to that published in literatures, a good agreement has been obtained during the comparison.

1.2 *The Objectives of the Present Work*

The following are the main objectives of the present work;

1- Using an improved boundary condition to analyze the porous floating ring journal bearing and put forward the mathematical model for a finite length of such bearing.
2- Solving the governing equations of the problem by using a suitable numerical. A computer program had been put forward to solve these equations.
3- Calculation of the main steady state performance parameters.

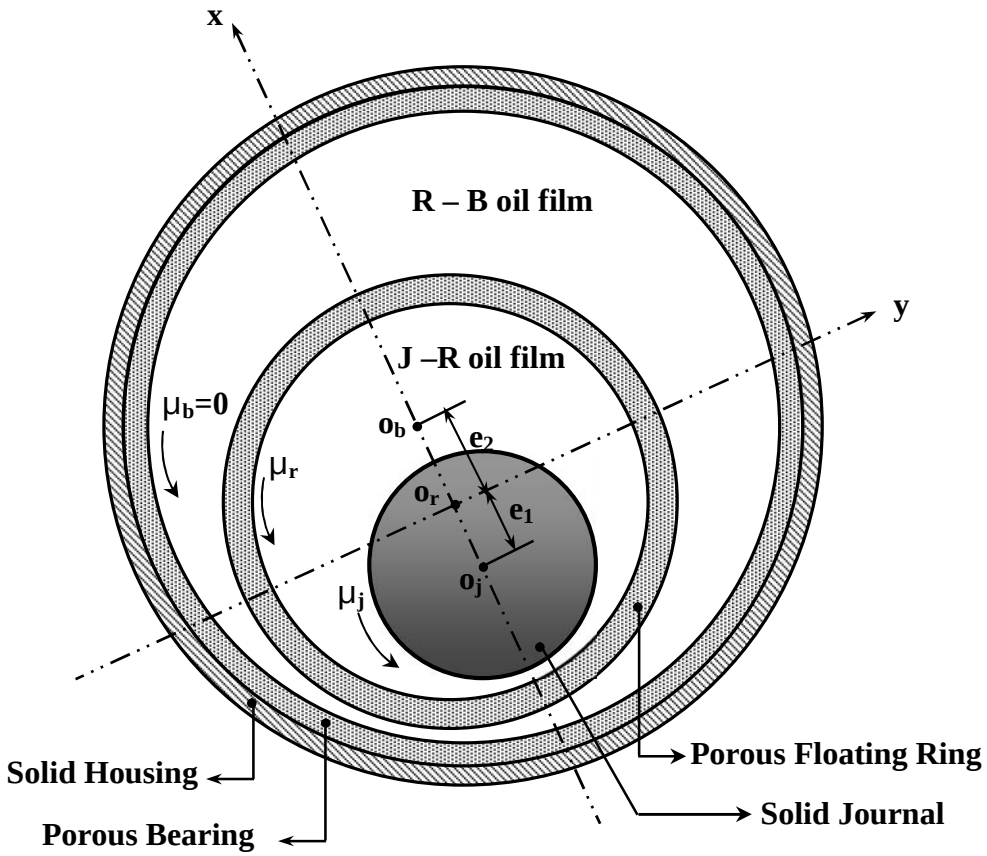

O_j Journal Center
O_r Floating Ring Center
O_b Bearing Center

Figure (1-1) Porous Floating Ring Journal Bearing

CHAPTER TWO
LITERATURE SURVEY

2.1 Porous Journal Bearings

Porous oil bearings can be defined as bearings in which the oil comes out of pores to lubricate fractioning surface (self-lubrication) and, on shut-down of the operation, oil would penetrate back to the pores. As such, lubrication of porous oil bearing is efficiently realized with comparatively small amount of oil. This type of bearing system is widely accepted for audio-visual (Av.) equipment, domestic electric applications and automobile electric components.

The most common type of bearings in category of porous oil bearing is the oil impregnated sintered bearing, which is made of Cu-base alloy, Cu-Fe base alloy, Fe base alloy or AL-base alloy. The Cu-base alloy bearings have superior fitness, while these of Fe-base alloy possesse superior mechanical strength and these of Cu-Fe base alloy are characterized by well balanced fitness and mechanical strength, AL-base alloy bearings are characterized by superior fitness and thermal conduction with comparatively light weight. Regimes of surface temperature of these bearings would vary depending on the type of oil employed, (0 – 80 °C) with mineral oils and (-30 to 120 °C) with synthetic oils. The porous bearings are mainly characterized by the permeability, which can be defined as the property that characterized the ease with which a fluid may be made to flow through the material by an applied pressure gradient or in other word it is the fluid

conductivity of the porous material, the porosity which is defined as the fraction of the bulk volume of the material occupied by the voids, **[2].**

The performances of porous bearings have been widely studied. The review of literature related to this field can be classified into the following categories:-

2.1.1 *Oil Flow in Porous Journal Bearings*

Morgan and Cameron, (1957), [3], studied the oil flow in porous journal bearings; they used dyed oil for impregnation of porous bearing. They covered the bearing surrounding with felt cloth in order to see oil emergence pattern from the bearing surface. They observed that the oil emerged towards load side of the felt cloth cover and the weight of the bearing and felt unchanged before and after the oil emergence, which led them to conclude that the oil must have penetrated into counter – loaded side of bearing from the felt. Evidences reported by this work seem to ensure the presence of oil flow in the porous oil bearing system due to pumping effect.

Kaneko, S., (1989), [4], applied porous materials to study the behaviour of the annular plain seals. The porous material was employed in pump by insertion into the inlet part of the seal. The static characteristics of such seals have been analyzed in the laminar – flow regime. The effect of the porous materials were found to increase the hydrostatic force since these materials performed as a hydrostatic bearing, and reduced the hydrodynamic force owing to the seepage of liquid between the seal clearance and the porous matrix. These effects consequently yield large film force component along the line of centers and small one perpendicular to the line of centers

for the porous seal compared to that for the equivalent solid seal. The total side leakage flow from the outlet end was also significantly affected by the porous materials, which took larger values for the porous seals than for the solid one and increased with the axial length of the porous matrix.

Kaneko and Obara, (1990), [5], arranged an experimental model, using small diameter packed glass spheres to explicate the mechanism of lubrication in porous bearings, by using the dye – injection method as a flow visualization technique. They showed a circulation of oil existing through the porous matrix, which contributed to the lubrication in porous bearings, and under boundary lubrication conditions, the oil feed pressure (P_s) from an external source significantly affected the flow pattern, while under hydrodynamic lubrication conditions, the oil in the porous matrix flew away from the position of the load line towards the unloaded region. For small pressure supply (P_s), the oil moved towards the region where the oil film pressure would be minimum.

Kaneko et al., (1994), [6], arranged an experimental model in order to investigate oil film formation in bearing clearance to explicate the mechanism of lubrication in porous bearings. They visualized the oil film in porous bronze bearing impregnated with fluorescent – dyed oil by using a pair of ultraviolet lamps. They observed that the oil film was formed in the loaded part of the bearing and it extended over a wide range for the relatively small static load and high oil feed pressure, and the angular extent of the film for the porous journal bearing was significantly small as compared to that for the solid journal bearing.

Kaneko et. al., (1994), [7], studied the effect of the oil supply pressure on the mechanism of lubrication in porous journal bearing. In this

analysis the angular extent of the oil film formed in bearing clearance has numerically been obtained on bases of the postulate that the oil film extent remains constant when a balance is established between oil fed into the clearance and that from the clearance. The computed results indicated that the dimensionless oil feed pressure has a marked effect on static characteristics, and an increase in supply pressure yield higher value of the angular extent of the oil film and load carrying capacity, and lower the coefficient of friction.

Kaneko and Hashimoto, (1995), [8], carried out an experimental investigation of the effect of oil supply pressure on the frictional characteristics under hydrodynamic and mixed lubrication regimes. They observed that under the same value of dimensionless oil – feed pressure (P_s), the relationship between the coefficient of friction and the Sommerfeld number was represented by a single friction curve extending from the hydrodynamic regime to the mixed regime, even for the different combinations of oil – feed pressure and shaft speed, and the friction factor decreased in hydrodynamic regime and then steeply increased in the initial stage of the mixed regime. The supply pressure was found to be effective at the transition point from hydrodynamic to boundary lubrication.

Kaneko et al., (1998), [9], made an experimental investigation of the static and dynamic characteristics for annular plain seals with porous materials applied to the seal surface by insertion into the middle of the seal. Experimental results showed that the annular plain with porous materials had a higher leakage flow rate, large main stiffness coefficient and smaller cross – coupled stiffness coefficient and main damping coefficient than conventional annular plain seals with solid surfaces, i.e. an increase of approximately 30 percent in the leakage flow rate while, the main stiffness

coefficient for the porous seals were four to six times as much as those for the solid seals due to the increase in the hydrodynamic force induced by a friction of the hydrodynamic porous bearing, and reduction of approximately 30 percent in the main damping coefficient were obtained. When porous materials were applied to the seal surface, a high stable operation speed by a stiffer rotor support was obtained.

Shah and Bhat, (2003), [10], studied a porous exponential slider bearing with a Ferro – fluid lubricant whose flow was governed by Jenkins flow behaviour considering slip velocity at the porous interface. They obtained that exponential porous slider bearing had more load carrying capacity, and coefficient of friction than the corresponding inclined plan porous slider bearing, and the decrease in load capacity of the bearing owing to the slip velocity as well as the material parameter could be made good by increasing the magnetization of the fluid.

2.1.2 *Boundary Conditions Used in Porous Bearings*

Bevers and Joseph, (1967), [11], showed in their experimental study that the adherence boundary condition, which was valid for impermeable surface, was not valid at the nominal surface of permeable material due to the migration of fluid tangent to the boundary within the porous matrix and an alternative boundary condition was proposed by them which admit a nonzero tangential velocity at the porous surface, i.e. slip velocity which could be defined as the slip boundary condition which expresses that there is oil flow in tangential direction in the porous material.

Prakash and Vij, (1973), [12], analyzed an inclined plane infinite slider bearing with an impermeable slider and a porous – faced stator backed by a solid wall. They concluded that the effect of porosity was to decrease the load – carrying capacity and friction when the coherent boundary condition in their analysis used.

Prakash and Vij, (1974), [13], presented an analytical solution for the performance characteristics of a narrow journal bearing using the modified Reynolds' equation which included the effect of slip velocity. Results were presented for various bearing characteristics and compared with results obtained by using no – slip condition. The analysis indicated that in the no – slip case, the load increase with eccentricity ratio but decreased as the permeability parameter took large values, and coefficient of friction increased with permeability parameter, while, in the slip case, the effect of slip decreased the load capacity, however, with increasing the eccentricity ratio, the trends were reversed and the load capacity increased, and the coefficient of friction decreased at large value of permeability parameter and it would be increased at small value of permeability parameter. It was seen that porous bearing had higher attitude angle than nonporous ones, and there was a relative error due to neglecting the of slip in the calculation, i.e. the results showed that the occurring error could be reach 70 percent.

Rouleau and Steiner, (1974), [14], developed a practical and accurate numerical method for the calculation of bearing performance. This method used Reynolds' boundary conditions to analyze the porous bearing performance. The results, in their analysis, were based on a modified form of the Reynolds' equation for the film and also accounted for slip at the film – bearing interface by means of Darcy's law. The analysis showed that

there were less load capacity and more friction coefficient than that given by the often used Sommerfeld boundary conditions. Also they concluded that the sealing of the axial ends of practical porous bearing, in order to increase load capacity, had little practical effect.

Cusano, (1979), [15], implemented and developed an analytical solution for the performance characteristics of starved porous journal bearing. The solution was based on a finite bearing using modified Reynolds' equation which included the effect of slip velocity. He concluded that the porous bearings would operate under steady starved condition in cases where the bearings received subsequent lubrication from external source. The results are presented for active film arc from 20 to 90 degrees. Bearings of active film arc less than 20 degree were not obtained since the load capacity for such values would be very small if hydrodynamic conditions were to be maintained. The values of active film arc greater than 90 degree were not obtained since there were few porous bearing applications where such film extents exist. For higher operating eccentricity ratios and higher permeability parameters, the flow from the porous matrix was a large proportion of the total side flow. These values suggested that for such eccentricity ratios and permeability parameter, it would be advantageous to close the pores at the ends of the bearing, with such closure, given oil – film extent could be maintained with a smaller oil supply to the bearing.

Patel and Gupta, (1983), [16], analyzed an inclined porous slider bearing with slip velocity at the porous boundary was considered in this work. They obtained expressions for dimensionless load carrying capacity, friction coefficient and center of pressure in the form of integrals. Their results showed that the minimization of the slip parameter was essential to

increase the load capacity, and the friction force decreased as the slip parameter decreased and the permeability parameter increased, while the friction coefficient increased as the permeability parameter increased and decreased as the slip parameter increased. The parameters which affected the performance of the bearing were the permeability parameter, and the slip parameter, although, these were not independent of each other.

Kaneko et al, (1994), [17], made an experimental investigation of the oil film formed in porous bearings. The results of their analysis showed that the oil film under hydrodynamic lubrication conditions extended over a wider range than that under boundary lubrication conditions. Under hydrodynamic lubrication conditions, the angular extent for the porous bearing was considerably small compared with that for the solid journal bearings.

Kaneko et al, (1997), [18], used an improved boundary condition to analyze theoretically and experimentally the oil film pressure distribution in porous bearings under hydrodynamic lubrication conditions. In this analysis they concluded that the integral momentum equation obtained by applying the momentum theory to the oil film region was proposed for the circumferential boundary condition of the oil film pressure, and the oil – film pressure distributions were numerically solved using both the integral momentum equation and the continuity equation based on the balance of the oil film across the clearance gap. The study yielded negative pressure before the trailing end of the oil – film region, which was confirmed in the measured oil – film pressure distributions, and the location of the trailing end of the oil – film region obtained in the study moved toward the down region as compared to the analysis based on the quasi – Reynolds' boundary condition yielding better agreement with the measured oil – film region.

Yousif, Nacy and Abass, (1999), [19], performed a full theoretical analysis of the problem of two non conformal porous surfaces in line contact under conditions pertinent of elstohydrodynamic lubrication. Their work consisted of a computational and experimental treatment for the behaviour of machine elements made of a porous material. The Reynolds' equation was modified to include the slip velocity effect at the porous boundary. They observed that the maximum oil film pressure increased with increasing the permeability of the porous material, whilst the oil film thickness decreased, and the oil film pressure increased and film thickness decreased with increasing the applied load with porous disks of certain permeability and at a constant specific speed. The shear stress generated at the permeable surface increased with increasing the permeability of the porous material, also they showed that the coefficient of traction increased with increasing the permeability, and the slip velocity increased with increasing the permeability.

Erno¨ Baka, (2002), [20], used pressure functions to calculate load carrying capacity of the porous journal bearings under hydrodynamic lubrication conditions. Pressure functions were determined and compared to each other to show the difference of several simplification, assumptions, and boundary conditions. The porous material was assumed to be isotropic and homogenous. Four pressure functions [”Cameron”, ”Rouleau”, ”Beavers and Joseph”, ”Murti” and ”Prakash and Vij”] were analyzed using the short bearing approximation and one pressure distribution [Capone function] with the infinitely long bearing assumption. The load carrying capacity and the coefficient of friction were calculated and compared to one another. The solutions presented above of the equation of the hydrodynamic lubrication for porous bearings and the calculated load carrying capacities showed that the solution of equation of hydrodynamic lubrication for porous bearings

were more complicated than for the solid sliding bearings, and the short bearing assumption gave more simpler solution than the infinite long bearing assumption. There were many new boundary conditions taken into consideration with the influence of the porous bearings on the hydrodynamic effect.

Saha and Majumdar, (2004), [21], studied the steady – state and the stability characteristics of hydrostatic two – layered porous oil journal bearings. The effects of the eccentricity ratio, slenderness ratio, bearing number, feeding parameter and anisotropy of permeability on load carrying capacity, attitude angle, and friction variable and oil flow rate were investigated. Stability analysis was performed using linearized perturbation method. It was observed that a two – layered porous bearing gave higher stability than a single – layered porous bearing.

2.1.3 *Oil Film Formation in Porous Bearings*

Yung and Cameron, (1979), [22], studied the sliding surface of pad type oil impregnated sintered bearing possessing convex shape surface, using optical interference technique. They showed that the temperature gradient must be induced in the micro taper lands rising from the entry to exit of the bearing due to shearing friction, and the temperature gradient in micro – lands must lead to comparatively large rear end of the micro – land, and this must function as the load supporting point of the porous oil bearing.

Braun, (1982), [23], observed the oil film formation in journal type oil impregnated sintered bearing from the interior of a hollow glass shaft,

using while light. He showed that about 1/7 of the total circumference of the porous bearing was covered by oil film, which must support the load of the bearing.

Terril, (1983), [24], obtained an axisymmetric solution of the Navier – Stokes equations for potential flow superimposed on Poiseuille flow. The results were used to obtain fully developed solution for flow in a porous pipe with variable suction or injection, and the suction distribution needed to change a specified axial velocity distribution at one cross – section to a specified axial velocity distribution at another cross – section.

Yoken – Doh, (1987), [25], showed that two effects were considered to be responsible for film formation in the clearance of porous oil bearing, namely, the oil feed effect known as pumping effect from pressure in the clearance, and the oil seepage from pores to bearing surface by reduced oil viscosity and by increased oil volume due to thermal expansion induced by friction heat generated at the bearing sliding surface.

Kaneko et al, (1991), [26], made an experimental investigation of the state of oil film formation in journal type oil – impregnated sintered bearing made of bronze under different conditions. They used fluorescent dyed oil fed into the bearing, where this was made visible by irradiation with UV light. Constant oil supply through the outside diameter of the porous bearing was delivered to the bearing in order to hold the oil content in the porous bearing constant. They noticed that the oil film formation in porous bearing was rather limited to 65° under hydrodynamic lubrication condition as compared with that in solid bearing, while the oil film formation in porous bearing was rather limited to 30° under boundary lubrication condition as compared with that in solid bearing. Also they concluded that commonly

assumed range of oil film formation, namely 180°, for theoretical analysis of hydrodynamic lubrication condition was not justifiable for porous oil bearing possessing no oil fed hole.

Kaneko and Ohkawa (1992), [27], theoretically analyzed the oil film extent under hydrodynamic lubrication condition in porous bearing. When the oil film extent reached steady state, the inflow of oil into the bearing clearance through the porous matrix due to the oil – feed pressure must make up for the oil leakage from the clearance to both ends and to the porous matrix due to the hydrodynamic pressure generated in the oil film. The results showed that the oil film region extended over a wide range for the higher dimensionless oil – feed pressure and smaller Sommerfeld number, which could be explained by the balance between the inflow and outer flow across the oil film region, and the data on the oil film extent were confirmed to be in agreement with the experimental results.

2.2 *Lubrication of Floating Ring Journal Bearings*

A floating – ring bearing is a special type of hydrodynamic lubricated journal bearing in which a bush (ring) is maintained floating in the lubricating fluid between the shaft journal and rigid housing.

The floating ring journal bearing has long been considered as a high damping bearing for rotor support. It was used extensively by the British in the connecting rods of Bristol aircraft engines in 1920 – 1930. Since that time many researchers have worked on the field of floating ring cylindrical journal bearing.

Shaw and Nussdrofer, (1947), [28], analyzed the operating characteristics of the floating ring journal bearing. Their analysis indicated that the floating ring operated over a wide range of speeds for a given shaft speed and the failure of the floating ring bearing to start from rest under load was an important point in designing this bearing. Also they showed that less total heat was generated in the two oil films of the floating ring journal bearing than the heat generated in an equivalent journal bearing and the load carrying capacity of the floating ring bearing was less than that of an equivalent journal bearing.

Kettleborough, (1954), [29], studied the frictional behaviour of different ring operating with different clearance ratios assuming an infinite length and no film rapture theory. In his experimental work he concluded that increasing the clearance ratio (c_2/c_1) increased the speed ratio (N_r/N_j), and thus reduced the journal friction and there was a reduction in the running temperature for the floating ring journal bearing compared with that for conventional bearing, due to an increase in oil flow.

Orcutt and Ng, (1968), [30], carried out theoretical analysis which gave some design data including the steady state and dynamic load properties for the floating ring journal bearing with pressurized lubricant supply. They showed that there was a good agreement between the measured and the calculated journal eccentricity (since the Sommerfeld number decreased with increasing the eccentricity ratio) a large decrease in Sommerfeld number occurred for lower values of clearance ratio while the friction factor increased with Sommerfeld number and it was lower for higher values of clearance ratio. The floating ring bearing had about (40 %) lower power loss than a comparable tilted pad bearing, but the load capacity

based on minimum film thickness was considerably less than that of a tilting pad bearing because the clearance was split between two films.

Tanaka and Hori, (1972), [31], derived a theory based on the assumption of infinitely short bearing and the film rapture in negative pressure region. The experimental work carried out to study the suppressing effect of the floating ring journal bearing concluded that the floating ring bearing had better stability than the conventional cylindrical bearing, that was attributed to the high damping effect of the outer film and the stability of the floating ring journal bearing was improved by using a stiffer shaft and larger radii and clearance ratio.

Rohde and Ezzat, (1980), [32], analyzed the performance of the floating ring journal bearing under highly loaded and dynamic conditions and they investigated its feasibility for automotive applications. The results showed that the frictional power losses decreased with increasing the outer clearance (c_2), and there existed a clearance beyond which there was a minor reduction in power losses, the floating ring concept resulted in an average friction reduction of (35%). The ring speed dropped with increasing inner clearance (c_1), since under this condition the inner film frictional torque available to drive the ring was decreased.

Mokhtar, (1981), [33], theoretically investigated the performance characteristics and design data for floating ring journal bearings based on the convenient boundary conditions. Results obtained indicated that the ring dimensions were the dominant factor indicating the final bearing behaviour and the oil film thickness between the ring and the bearing housing was much thinner than between the journal and the ring. The floating ring

bearing showed less frictional power loss than the ordinary bearing, but that might be achieved at the expense of the load carrying capacity.

Li and Rohde, (1981), [34], analyzed the steady – state and dynamic characteristics of floating ring journal bearing. They employed the finite bearing theory rather than short bearing assumption in their study which concluded that the ring speed decreased with decreasing values of Sommerfeld number, it decreased more rapidly with increasing the load for larger value of clearance ratio and for small value of clearance ratio (c_2/c_1) the outer film became considerably stiffer, hence it could operate at smaller eccentricity ratio than the inner film.

Li, (1982), [35], analyzed and gave some information about the design of the floating ring journal bearing supporting a high speed flexible rotor. The conclusions in this analysis were that the ring rotated faster when the inner clearance was reduced and the power consumption in floating ring journal bearing was lower than that in conventional journal bearing due to the rotation of the floating ring which caused lower shear force acting on the journal.

Wilkock, (1983), [36], investigated the load carrying efficiency of floating ring journal bearings, and examined the general case of the floating ring bearing under the requirement that capacity number and the load should be the same as for the single film bearing for both inner and outer films. The results obtained showed that the floating ring design made possible significant power savings over the full range of laminar and turbulent therefore if the reference bearing was laminar, a reduction in the power loss of (42%) was achieved by increasing the total clearance while, if the reference bearing was turbulent reduction of (51 to 64%) was achieved by

reducing the bearing length, the amount of reduction depends on the level of turbulence.

Yousif and Abass, (1989), [37], made theoretical and experimental investigations of the behaviour of the floating – ring journal bearing lubricated with bi – phase (liquid – solid) lubricant. Solid additives used in this work were in the form of wood and graphite particles of various particle size and concentration. The theoretical and experimental investigations showed that the existence of solid particles in suspension in liquid lubricant improved the performance of the floating – ring journal bearing, giving an increase in load carrying capacity and a reduction in friction factor and attitude angle together with a reduction in ring eccentricity ratio and the bearing operation became more stable when using rings having smaller clearance ratios. Also they indicated that the ring speed increase linearly with the journal speed and that there was a slight increase in friction force and frictional torque when the bearing was lubricated with bi – phase lubricant in comparison with that lubricated with pure oil.

Dong and Zhao, (1991), [38], presented an analysis of the performance of floating – ring journal bearing with non – stationary load. Their observation showed that the experiment, in which floating – ring bearing replaced the main bearing in an S195 diesel engine, was successful, and it had invariably insisted that floating – ring bearings were only suitable to a relatively high – speed and light – load rotating machinery. Floating – ring bearing could also be in good working order, even when subject to low speed and heavy, non – stationary loads, however, the use of floating – ring bearings, had great significance for the reduction of bearing power – loss and giving longer operating life.

Yousif and Nacy, (1993), [39], predicted the steady state performance characteristics for the floating ring conical journal bearing and comparison had been made with the equivalent conical journal bearing. They indicated that the load carrying of the floating ring conical journal bearing was less than that of an equivalent conical journal bearing, and the floating ring conical journal bearing exhibited less frictional losses when compared to an equivalent conical journal bearing. Therefore the floating ring conical journal bearing posses superior stability characteristics as compared with an equivalent conical journal bearing.

Cheong and Kim, (2001), [40], analyzed the steady state performance of the counter – rotating floating ring journal bearing with isothermal finite bearing theory. They confirmed that the counter – rotating floating ring journal bearings properly designed had considerable load capacity at equal counter – rotating speeds, and the operating characteristics of the counter – rotating floating ring journal bearing according to the method of acceleration and deceleration of the rotational speeds of the journal and sleeve were clarified. It was theoretically confirmed that floating ring journal bearing could be used in counter – rotating journal – bearing system and had the potential to become a good substitute for rolling bearing in counter – rotating systems.

Andres and Kerth, (2004), [41], put forward a physical model and fast computation programs in order to improve the design and performance of turbochargers. They made a thermal analysis to study the performance of floating ring bearing used in turbochargers. Prediction for the exit lubricant temperature, power losses and floating ring speeds a greed well with measurements obtained in an automotive turbocharger test rig, therefore,

floating ring bearings offer lower power consumption and cooler operating conditions than plain journal bearing or semi – floating ring bearings.

Although there is a number of theoretical and experimental work related to the analysis of the performances of the floating ring bearing as shown in previous articles, however, there is no work (to the best of our knowledge) dealing with the performances of porous floating ring journal bearing. So, the present work represents an attempt to analyze such bearing theoretically using improved boundary conditions as suggested by Kaneko et. al., 1997, [18] which state that the integral momentum equation obtained by applying the momentum theorem and the continuity equation to the oil – film region are proposed for the circumferential boundary condition of the oil – film pressure to obtain the leading and trailing ends of the pressure distribution of the oil – film regions.

CHAPTER THREE

THEORETICAL ANALYSIS

3.1 Introduction

The theoretical analysis in this chapter forms an attempt to build up a mathematical model to investigate the behaviour of the porous floating ring journal bearing.

The main governing equations with appropriate assumptions and boundary conditions used to solve this problem are described in the following articles.

3.2 Geometry of The Bearing

The geometry of the porous floating ring journal bearing with the coordinate system used in this work is shown schematically in Figure (3-1).

The journal rotates with a constant angular velocity (ω_j) about its center (O_j).When the floating ring bearing works smoothly, the hydrodynamic action would eventually force the porous ring to rotate at an induced speed (ω_r) which is less than that of the journal. The porous bearing is inserted into a solid housing having a circumferential groove in the middle, so as to give strength and also to prevent the escape of lubricant. Lubricant oil at low pressure (P_s) is supplied to the groove through oil – feed hole to replenish all the oil losses and to ensure that the bearing system operates under hydrodynamic lubrication condition.

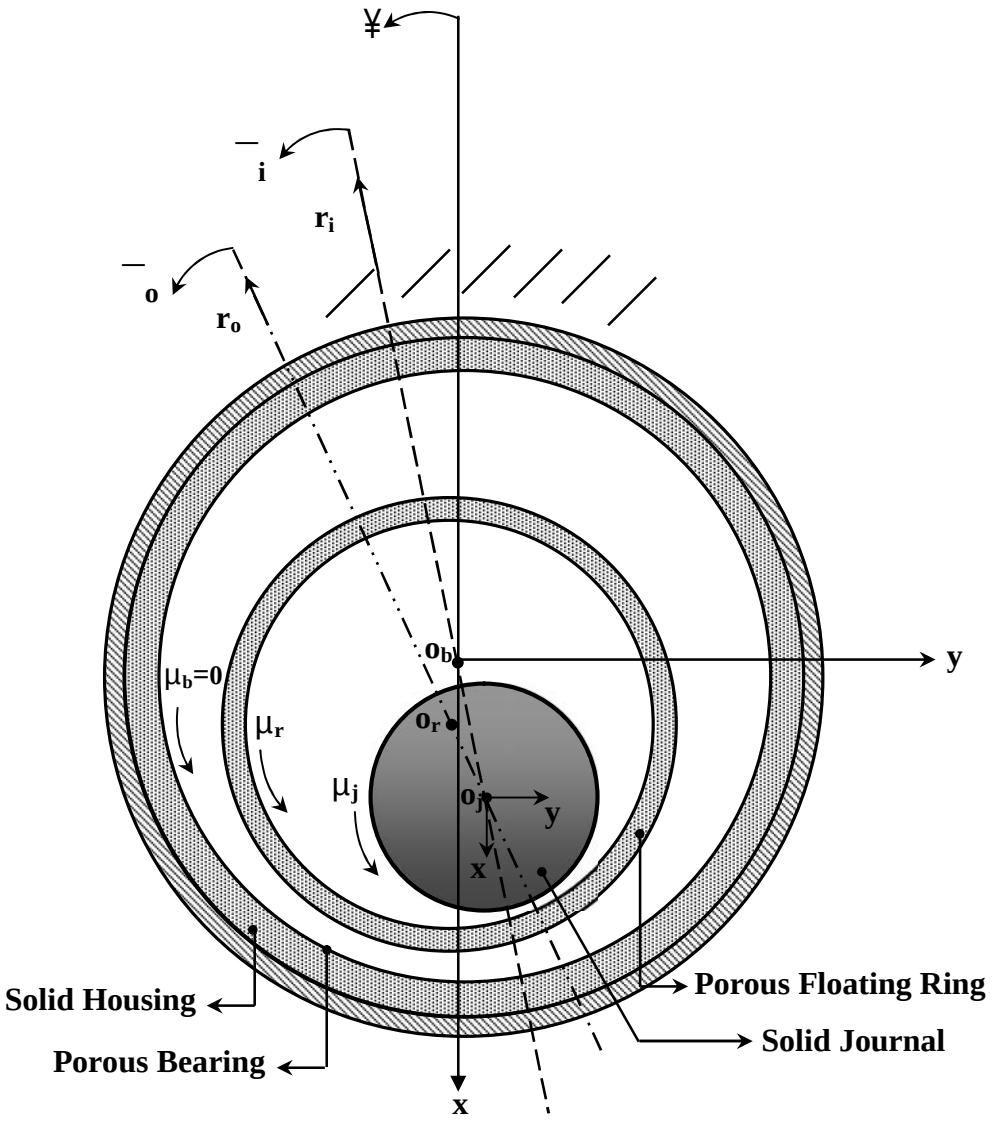

Figure (3-1), Geometry of Porous Floating Ring Journal Bearing and Coordinate System

3.3 *Coordinates System*

The two dimensional cylindrical coordinates (θ, Z) were adopted to describe the behaviour of oil films, while a three dimensional cylindrical coordinates (r,θ, Z) were used to describe the flow of oil through the porous matrix.

3.4 *Assumptions*

The following assumptions are put forward to develop the mathematical model required to solve the problem :-

1- All the assumptions used in the derivation of Reynolds' equation are valid.

2- Surface roughness effect is neglected.

3- The effect of tangential slip velocity is adopted.

4- The porous matrix is homogenous and isotropic.

5- Steady state analysis for laminar fluid flow is considered.

6- Lubricant oil at a relatively small pressure (P_s) is supplied to a groove through oil fed hole in order to ensure the existence of hydrodynamic lubrication condition.

7- The boundary lines at the inlet and trailing ends of the film extent are parallel to the axial coordinate, i.e. the values of $(\theta_1)_{ii}$ and $(\theta_2)_{ii}$ are constant in the (Z) direction.

8- The outer surface of the ring is assumed as if it press fitted in a solid housing i.e. $\frac{\partial P^{\wedge *}}{\partial r} = 0$.

3.5 *Governing Equations*

Using the assumptions mentioned before the governing equations adopted in this work can be presented as follows;

3.5.1 *Reynolds' Equation*

Starting from the Navier – Stokes and the continuity equations together with Darcy's law that expresses the flow of fluid within the porous media, the governing equation for the pressure distribution in the oil film is given by the modified Reynolds' equation including a so – called filter term and the effect of tangential slip velocity. As for constant oil viscosity, it can be written in dimensionless form as**, [7, 18];**

$$\frac{\partial}{\partial \bar{\ }}\left(h^{\wedge 3}\left(1+\text{،}_{1}\right)\frac{\partial P^{\wedge}}{\partial \bar{\ }}\right)_{ii}+\left(\frac{D_{ii}}{L}\right)^{2}\frac{\partial}{\partial Z^{\wedge}}\left(h^{\wedge 3}\left(1+\text{،}_{1}\right)\frac{\partial P^{\wedge}}{\partial Z^{\wedge}}\right)_{ii}=6\frac{\partial}{\partial \bar{\ }}\left(h^{\wedge 3}\left(1+\text{،}_{0}\right)\right)_{ii}-12\Phi_{ii}\left(\frac{\partial P^{\wedge *}}{\partial r^{\wedge}}\Big|_{r^{\wedge}=1}\right)_{jj}$$

……(3.1)

Where;

$$\left(\text{،}_{0}\right)_{ii}=\left(\frac{s}{\left(h^{\wedge}+s\right)}\right)_{ii}$$ **……(3.2)**

$$\left(\text{،}_{1}\right)_{ii}=\left(3\left(h^{\wedge}s+2\sim^{2}s^{2}\right)/\left\{h^{\wedge}\left(h^{\wedge}+s\right)\right\}\right)_{ii}$$ **……(3.3)**

$$\left(s\right)_{ii}=\left(\Phi c/R_{ii}\right)_{ii}^{1/2}/\sim$$ **……(3.4)**

$\sim$: is the slip coefficient which is a dimensionless parameter that depends on the porous material, and its value for laminar channel flow has been estimated to be 0.1, so that $\sim$ of (0.1) can be used in the present analysis as done in the previous works **[4,7,15,18,19,42].**

A full derivation of equation **(3.1)** can be found in appendix **A.**

The dimensionless oil – film thickness can be evaluated as;

$$\left(h^{\wedge}\right)_{ii} = \left(h/c\right)_{ii} = \left(1+£\cos^{-}\right)_{ii} \qquad \text{.....(3.5)}$$

The last right hand term of equation **(3.1)** is called the filter velocity which can be evaluated by using the Darcy's equation.

3.5.2 *Darcy's Equation*

The velocity components of the fluid flow in the porous media are obtained from Darcy's law which can be expressed as **[13,15];**

$$u^{*} = -\frac{k_1}{\dagger}\frac{\partial P^{*}}{\partial x} \qquad \text{.....(3.6)}$$

$$v^{*} = -\frac{k_1}{\dagger}\frac{\partial P^{*}}{\partial y} \qquad \text{.....(3.7)}$$

$$w^{*} = -\frac{k_1}{\dagger}\frac{\partial P^{*}}{\partial z} \qquad \text{.....(3.8)}$$

By substituting these velocity components into the continuity equation the following equation can be obtained as **[19]**;

$$\frac{\partial u^{*}}{\partial x} + \frac{\partial v^{*}}{\partial y} + \frac{\partial w^{*}}{\partial z} = 0 \qquad \text{.....(3.9)}$$

The governing equation of the pressure distribution inside the porous ring and the porous bearing can be obtained. This equation can be written in dimensionless form as **[7,18,42]**;

$$\frac{1}{r^{\wedge}_{jj}}\frac{\partial}{\partial r^{\wedge}}\left(r^{\wedge}\left(\frac{\partial P^{\wedge^*}}{\partial r^{\wedge}}\right)_{jj}\right)+\frac{1}{r^{\wedge^2}_{jj}}\left(\frac{\partial^2 P^{\wedge^*}}{\partial^{2-}}\right)_{jj}+\left(\frac{D_{ii}}{L}\right)^2\left(\frac{\partial^2 P^{\wedge^*}}{\partial^2 Z^{\wedge^2}}\right)_{jj}=0 \qquad \textbf{.....(3.10)}$$

3.6 *Boundary Conditions*

Many previous experimental studies **[5,6,7,18],** show that the oil film is formed over the whole bearing width in the loaded part of the bearing and the oil film region breaks up into a number of striations or steamers at both ends, extending towards the unloaded part.

In the present analysis, the boundary lines at the inlet and trialing ends of the oil films regions are assumed to be parallel to the axial coordinate, i.e. the values of $(\theta_1)_{ii}$ and $(\theta_2)_{ii}$ are constant in the Z – direction. The inlet and trailing ends of the oil films are open to the atmosphere which means that;

$$\left(P^{\wedge}\right)_{ii}=0 \quad \text{at} \quad {}^{-}=(\,{}^{-}{}_1)_{ii} \quad \text{and} \quad {}^{-}=(\,{}^{-}{}_2)_{ii} \qquad \textbf{.....(3.11)}$$

$$\left(P^{\wedge^*}\right)_{jj}=0 \ \text{at} \quad {}^{-}=(\,{}^{-}{}_1)_{ii} \quad \text{and} \quad {}^{-}=(\,{}^{-}{}_2)_{ii} \qquad \textbf{.....(3.12)}$$

where; $(\,{}^{-}{}_1)_{ii}$ and $(\,{}^{-}{}_2)_{ii}$ are determined by the following two circumferential boundary conditions derived from the momentum theorem and the balance of oil flow across the clearance gap of each oil film of the porous floating journal bearing.

Applying the momentum theorem to the oil film region, which is considered as a control volume as shown in Figure (3-2), the integral momentum equation is given by **[18];**

$$\left(M^{-}_{1}-M^{-}_{2}-M^{-}_{c}-M^{-}_{b}\right)_{ii}=\left(F_{p^{-}2}-F_{p^{-}1}+F_{2b}-F_{2j}\right)_{ii} \qquad \text{.....(3.13)}$$

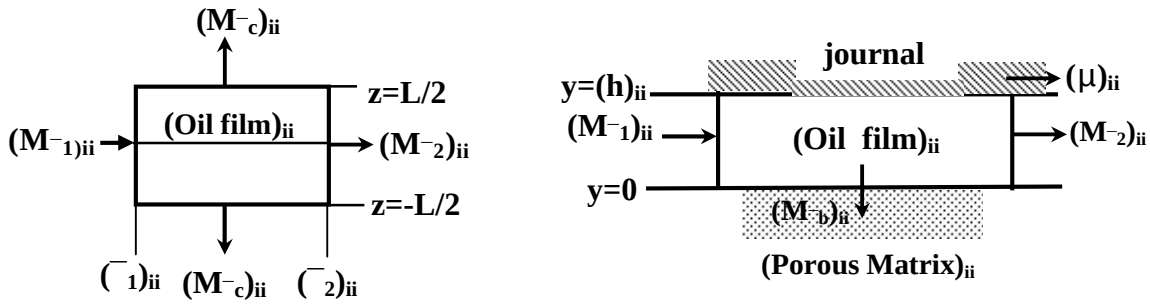

(a): Circumferential Momentum Flow Rates

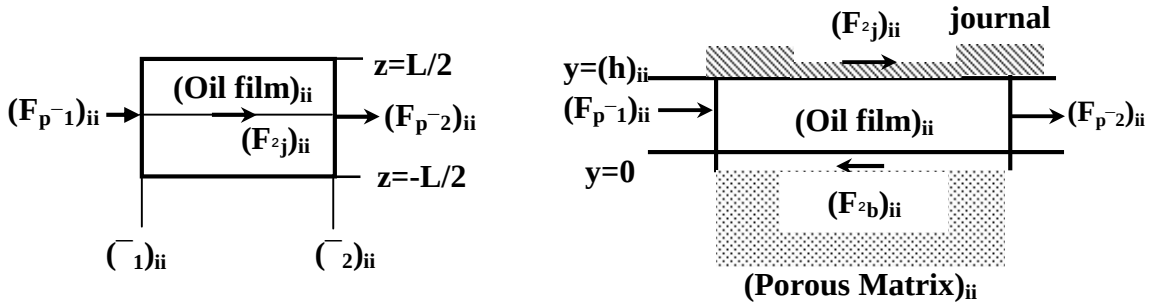

(b): External Force Components in the Circumferential Direction

Figure (3-2),Circumferential Momentum Flow Rates across the Control Surfaces(Boundaries of Oil – Film Region) and External Components in the Circumferential Direction acting on the Control Surfaces.

where;

M_1, M_2, M_c and M_b are the circumferential momentum flow rates across the control surface of the oil film, and

$F_{p_2}, F_{p_1}, F_{2_b}$ and F_{2_j} are the external forces components in the circumferential direction acting on the control surfaces of the oil film.

Since the pressure at $(\quad_1)_{ii}$ and $(\quad_2)_{ii}$ is an ambient pressure,

$$\left(F_{p_1}\right)_{ii} = 2\int_0^{L/2}\int_0^{(h_1)_{ii}} \left(P\big|_{=_1}\right)_{ii} dydz = 0 \qquad \textbf{.....(3.14)}$$

$$\left(F_{p_2}\right)_{ii} = 2\int_0^{L/2}\int_0^{(h_1)_{ii}} \left(P\big|_{=_2}\right)_{ii} dydz = 0 \qquad \textbf{.....(3.15)}$$

The shear forces on the control surfaces at y=0 and y = $(h)_{ii}$ are given by

$$\left(F_{2_b}\right)_{ii} = \left(F_{2_j}\right)_{ii} = \left(2r \int_0^{L/2}\int_{-1}^{2} \left\{ \left(\frac{h}{2r}\frac{\partial P}{\partial}\left\{1+\frac{1}{3}, 1\right\}\right)_{ii} + \left(\frac{r\mu}{h}\right)_{ii} \{1-, 0\}\right\} d dz \right)_{ii}$$

.....(3.16)

Substituting equations **(3.14)**, **(3.15)** and **(3.16)** into **(3.13),** the sum of the external forces becomes zero, i.e.

$$\left(M_1 - M_2 - M_c - M_b\right)_{ii} = 0 \qquad \textbf{.....(3.17)}$$

The momentum flow rates are given as follows **[18]**;

$$\left(M_{1}\right)_{ii} = 2\int_{0}^{L/2}\int_{0}^{(h_1)_{ii}} \circ \left[\left(u\right|_{1}\right)^{2}\Big]_{ii} dydz \qquad \text{.....(3.18)}$$

$$\left(M_{2}\right)_{ii} = 2\int_{0}^{L/2}\int_{0}^{(h_1)_{ii}} \circ \left[\left(u\right|_{2}\right)^{2}\Big]_{ii} dydZ \qquad \text{.....(3.19)}$$

$$\left(M_{c}\right)_{ii} = 2(r_{ii})\int_{1}^{2}\int_{0}^{(h)_{ii}} \circ \left[(u * u_z)\big|_{Z=L/2}\right]_{ii} dyd \qquad \text{.....(3.20)}$$

$$\left(M_{b}\right)_{ii} = 2(r_{ii})\int_{0}^{L/2}\int_{(1)_{ii}}^{(2)_{ii}} \circ \left[\left(u_{m}\right)_{ii} * \left(u_{r}^{*}\right)_{jj}\right]_{r=(r)_{ii}} d dZ \qquad \text{.....(3.21)}$$

Where ° the density of oil film and its value is is assumed to be constant. The velocity components in circumferential and axial directions in the first and second oil films are, $(u)_{ii}$ and $(u_Z)_{ii}$, while $\left(u_r^*\right)_{jj}$ is the velocity component of the oil inside the porous matrix (in the bearing and the floating ring). The different velocity components at the oil films and the porous matrix can be expressed as follows;

$$(u)_{ii} = \frac{1}{2}\left(\frac{\partial P}{r\,\partial}\right)_{ii}\left(y - h_{ii}\right)\left(y + \frac{1}{3}h_{ii}, {}_{1x}\right) + \left(\frac{r\mu}{h}\right)_{ii}\left(y(1-, {}_{0x}) + h, {}_{0x}\right)_{ii} \qquad \text{.....(3.22)}$$

$$\left(u_z\right)_{ii} = \frac{1}{2}\left(\frac{\partial P}{\partial Z}\right)_{ii}\left(y - h_{ii}\right)\left(y + \frac{1}{3}h_{ii}, {}_{1x}\right) \qquad \text{.....(3.23)}$$

$$\left(u_r^*\right)_{jj} = \frac{-k_1}{}\left(\frac{\partial P^*}{\partial r}\right)_{jj} \qquad \text{.....(3.24)}$$

In equation **(3.20)** $(u_Z)_{ii}$ at Z=L/2 takes negative value, i.e., $\left(\partial P/\partial z|_{Z=L/2}\right)_{ii} > 0$ and u_θ at Z=L/2 is assumed to be zero, since $(u_-)_{ii}$ would be zero just outside the axial end of the oil film. It yields;

$$\left(u_-|_{z=L/2}\right)_{ii} = 0 \quad \text{if} \quad \left(u_z|_{z=L/2}\right)_{ii} < 0 \qquad \left(\partial P/\partial z|_{z=L/2}\right)_{ii} > 0 \qquad \textbf{.....(3.25)}$$

The circumferential velocity component $\left(u_{-m}\right)_{ii}$ across the control surface at y=0 [bearing and floating ring surfaces] is given for both cases where the oil in the clearance gap flows into the porous matrix and flow into the clearance gap. It is expressed as;

$$\left(u_{-m}\right)_{ii} = \left(\frac{1}{h}\int_0^h u_- dy\right)_{ii}$$

$$= -\frac{1}{12\mu}\left(\frac{h^2}{r}\frac{\partial P}{\partial \theta}(1+\varepsilon_1)\right)_{ii} + \frac{(r\omega)_{ii}}{2}(1+\varepsilon_0)_{ii} \quad \text{if} \quad \left(u_r^*|_{r=r_i}\right)_{jj} \geq 0 \qquad \textbf{.....(3.26)}$$

$$\left(u_{-m}\right)_{ii} = -\frac{k_1}{\mu}\left(\frac{\partial P}{r\partial \theta}\bigg|_{r=r_i}\right)_{ii} \qquad \text{if} \quad \left(u_r^*|_{r=r_i}\right)_{jj} < 0 \qquad \textbf{.....(3.27)}$$

By substituting the above velocity components into equations **(3.18)** to **(3.21)** and normalizing each momentum flow rate by $\Omega L\left(cr\omega^2\right)_{ii}$, equation **(3.17)** can be written in dimensionless form as **[18]**;

$$\left(\hat{M}_1-\hat{M}_2-\hat{M}_c-\hat{M}_b\right)_{ii}=0 \qquad \textbf{.....(3.28)}$$

where;

$$\left(\hat{M}_1\right)_{ii}=\left(M_1\right)_{ii}/\left(c_{ii}r_{ii}^2\mu_{ii}^2L\right)=\int_0^1\left(\left(\frac{h^5}{1080}\left(\frac{\partial P}{\partial}\right)^2\left(9+15,_1+10,_1^2\right)\right)_{=1}\right)_{ii}dZ$$

$$-\int_0^1\left(\left(\frac{h^3}{36}\frac{\partial P}{\partial}\left(3+3,_0+2,_1+4,_{0,1}\right)\right)_{=1}\right)_{ii}dZ+\int_0^1\left(\left(\frac{h}{3}\left(1+,_0+,_0^2\right)\right)_{=1}\right)_{ii}dZ$$

.....(3.29)

$$\left(\hat{M}_2\right)_{ii}=\left(M_2\right)_{ii}/\left(c_{ii}r_{ii}^2\mu_{ii}^2L\right)=\int_0^1\left(\left(\frac{h^5}{1080}\left(\frac{\partial P}{\partial}\right)^2\left(9+15,_1+10,_1^2\right)\right)_{=2}\right)_{ii}dZ$$

$$-\int_0^1\left(\left(\frac{h^3}{36}\frac{\partial P}{\partial}\left(3+3,_0+2,_1+4,_{0,1}\right)\right)_{=2}\right)_{ii}dZ+\int_0^1\left(\left(\frac{h}{3}\left(1+,_0+,_0^2\right)\right)_{=2}\right)_{ii}dZ$$

.....(3.30)

$$\left(\hat{M}_c\right)_{ii}=\left(M_c\right)_{ii}/\left(c_{ii}r_{ii}^2\mu_{ii}^2L\right)=-\frac{1}{72}\left(\left(\frac{D}{L}\right)^2\int_1^2Ad\right)_{ii}$$

Where,

$$\left(A=h^3\left(3+3,_0+2,_1+4,_{0,1}\right)\left.\frac{\partial P}{\partial Z}\right|_{Z=1}\right)_{ii}\le 0 \qquad \text{if} \qquad \left(\left.\frac{\partial P}{\partial Z}\right|_{Z=1}\right)_{ii}\le 0$$

$$A = 0 \quad \text{if} \quad \left(\left. \frac{\partial P^{\wedge}}{\partial Z^{\wedge}} \right|_{Z^{\wedge}=1} \right)_{ii} > 0 \qquad \textbf{.....(3.31)}$$

$$\left(\hat{M}_{b} \right)_{ii} = \left(M_{b} \right)_{ii} / \left(\circ c_{ii} r_{ii}^{2} \mu_{ii}^{2} L \right) = \int_{0}^{1} \left(\int_{-1}^{2} B d\bar{} \right)_{ii} dZ^{\wedge}$$

$$(B)_{ii} = \left(\Phi \left\{ \frac{h^{\wedge 2}}{12} (1 + , _{1}) \frac{\partial P^{\wedge}}{\partial \bar{}} - \frac{1}{2} (1 + , _{0}) \right\} \right)_{ii} \left(\left. \frac{\partial P^{\wedge *}}{\partial r^{\wedge}} \right|_{r^{\wedge}=1} \right)_{jj} \quad \text{if} \quad \left(\left. \frac{\partial P^{\wedge *}}{\partial r^{\wedge}} \right|_{r^{\wedge}=1} \right)_{jj} \leq 0$$

$$(B)_{ii} = \left(\left(\frac{c}{r} \right) \Phi^{2} \frac{\partial P^{\wedge}}{\partial \bar{}} \right)_{ii} \left(\left. \frac{\partial P^{\wedge *}}{\partial r^{\wedge}} \right|_{r^{\wedge}=1} \right)_{jj} \quad \text{if} \quad \left(\left. \frac{\partial P^{\wedge *}}{\partial r^{\wedge}} \right|_{r^{\wedge}=1} \right)_{jj} > 0 \qquad \textbf{.....(3.32)}$$

A brief derivation of the momentum equations is given in Appendix B.

The first circumferential boundary condition for the first and second oil film pressure is given by the dimensionless integral momentum equation **(3.28).**

On the other hand, the second circumferential boundary condition is determined on the basis of the following postulate; the first is that the inflow into the bearing clearance through the porous matrix is due to the oil – feed pressure, which contributes to the developed of oil film extent. The second is that the oil leakage from the ends through the clearance gap and that into the porous matrix is due the hydrodynamic pressure generated in the film.

When the oil – film extent reaches a steady state, the flow rate across the trailing boundary line due to Poiseuilles' flow equals that due to Couettes' flow, **[7]** i.e.,

$$\left(q_{p}/q_{c}\right)_{ii}=\left(\left(\frac{(1+,1)}{6(1+,0)}h^{\wedge 2}\int_{0}^{1}\frac{\partial P^{\wedge}}{\partial}dZ^{\wedge}\right)_{=2}\right)_{ii} \qquad \textbf{……(3.33)}$$

Consequently, the locations of the inlet and trailing ends of the continuous first and second oil – films regions can be obtained as the values of $(1)_{ii}$ and $(2)_{ii}$ that simultaneous satisfy equation **(3.28)** and **(3.33).**

Knowing the values of $(1)_{ii}$ and $(2)_{ii}$ **,** the angular extent $()_{ii}$ of the first and second oil films are expressed in the form;

$$()_{ii}=(2)_{ii}-(1)_{ii} \qquad \textbf{……(3.34)}$$

The remaining boundary conditions are given as follows;

1-The axial ends of bearing are exposed to the atmosphere giving **[7,15,42];**

$$\left(P^{\wedge}\right)_{ii}=\left(P^{\wedge *}\right)_{jj}=0 \qquad \text{at} \quad Z^{\wedge}=\pm 1 \qquad \textbf{……(3.35)}$$

2- The outer surface of porous matrix consists of two parts as shown in Figure (3-3),the first is the part press – fitted inside the solid housing, where the pressure is evaluated by the condition that the permeability of the housing adjacent to the porous matrix is zero **[7,18]**;

$$\Phi=0 \;\; ; \;\; \text{at} \;\; \left(r^{\wedge}\right)_{2}\geq\left(r_{o}/r_{i}\right)_{2} \;\; \text{and} \;\; 0.5\leq\left|Z^{\wedge}\right|\leq 1 \qquad \textbf{……(3.36)}$$

The second is the part exposed to the circumferential groove in the housing, where the pressure is given by;

$$\left(P^{\wedge *}\right)_{2}=P_{s}^{\wedge}=\frac{c_{2}^{2}P_{s}}{\left(r^{2}\,\mu\right)_{2}} \quad \text{at} \quad \left(r^{\wedge}\right)_{2}=\left(r_{o}/r_{i}\right)_{2} \quad \text{and} \quad \left|Z^{\wedge}\right|\leq 0.5 \qquad \textbf{……(3.37)}$$

3- The flow is symmetrical about the mid – plan ($Z^{\wedge}$=0) for porous media and oil film regions respectively **[14,42,43]**;

$$\frac{\partial P^{\wedge *}}{\partial Z^{\wedge}}\left(\bar{\ },r^{\wedge},0\right)=0 \quad \text{and} \quad \frac{\partial P^{\wedge}}{\partial Z^{\wedge}}\left(\bar{\ },0\right)=0 \qquad \textbf{……(3.38)}$$

4- Furthermore, continuity of pressure at the interface between the porous matrix and the oil films gives **[7,18]**;

$$\left(P^{\wedge *}\right)_{jj}=\left(P^{\wedge}\right)_{ii} \text{ at } \left(r^{\wedge}\right)_{jj}=1 \ ; \ where \ ; \ r^{\wedge}=r/R_{ii} \qquad \textbf{……(3.39)}$$

3.7 *Bearing Parameters*

For the steady – state condition, modified Reynolds' equation **(3.1)** is solved simultaneously with the Darcy's equation **(3.11)** using the an improved boundary conditions [equations **(3.28)** and **(3.33)**], the solution yields the bearing dimensionless pressure fields, so, the dimensionless forces acting along and normal to the line of centers of the ring and journal can be obtained as follows **[7,43]**;

$$\left(\hat{W}_R\right)_{ii}=-\int_{0}^{\bar{1}}\int_{\bar{1}}^{\bar{2}}\left(P^{\wedge}\left(\bar{\ },z\right)_{ii}\cos\bar{\ }\right)_{ii} d\bar{\ }dz^{\wedge} \qquad \textbf{……(3.40)}$$

$$\left(\hat{W}_T\right)_{ii}=\int_{0}^{\bar{1}}\int_{\bar{1}}^{\bar{2}}\left(P^{\wedge}\left(\bar{\ },z\right)_{ii}\sin\bar{\ }\right)_{ii} d\bar{\ }dz^{\wedge} \qquad \textbf{……(3.41)}$$

The total dimensionless load is;

$$\left(\hat{W}\right)_{ii}=\sqrt{\left(\hat{W}_R\right)_{ii}^{2}+\left(\hat{W}_T\right)_{ii}^{2}} \qquad \textbf{……(3.42)}$$

The attitude angles $(\Psi)_{ii}$ and Sommerfeld numbers $(S)_{ii}$ are given by;

$$(\Psi)_{ii} = \tan^{-1}\left(W_T^{\wedge} / W_R^{\wedge}\right)_{ii} \qquad \textbf{.....(3.43)}$$

$$(S)_{ii} = 1/W_{ii} = (R_{ii} \mid \mu_{ii}) * (R/c)_{ii}^2 / (W_{ii}/L) \qquad \textbf{.....(3.44)}$$

For a Newtonian lubricant, the shear stress at the bearing, ring surfaces and the ring, journal surfaces can be evaluated as;

$$(\tau)_{ii} = \mid \frac{\partial u}{\partial y}\Big|_{h_{ii},0} \qquad \textbf{.....(3.45)}$$

The lubricant velocity field across the first and second oil film can be evaluated as **[42]**;

$$u_{ii} = \frac{1}{2\mid}\left(\frac{\partial P}{\partial x}\right)_{ii}(y - h_{ii})\left(y + \frac{1}{3}h_{ii}, {}_{1x}\right) + \frac{U_{ii}}{h_{ii}}\left(y(1 - , {}_{0x}) + h, {}_{0x}\right)_{ii} \qquad \textbf{.....(3.46)}$$

$$\frac{\partial u}{\partial y}\Big|_{h_{ii},0} = \pm\frac{1}{2\mid}\left(h\frac{\partial P}{\partial x}\right)_{ii} + \frac{1}{2\mid}\left(h\frac{, {}_1}{3}\frac{\partial P}{\partial x}\right)_{ii} + \frac{U_{ii}}{h_{ii}}(1 - , {}_0)_{ii} \qquad \textbf{.....(3.47)}$$

Substituting equation **(3.47)** into equation **(3.45)**, to get

$$(\tau)_{ii} = \pm\frac{1}{2}\left(h\frac{\partial P}{\partial x}\right)_{ii} + \frac{1}{2}\left(h\frac{, {}_1}{3}\frac{\partial P}{\partial x}\right)_{ii} + \frac{U_{ii}\mid}{h_{ii}}(1 - , {}_0)_{ii} \qquad \textbf{.....(3.48)}$$

The friction forces can be evaluated as;

$$\left(F_r^{\wedge}\right)_{ii} = \int_0^1 \int_{\left(\bar{\ }_1\right)_{ii}}^{\left(\bar{\ }_2\right)_{ii}} \left(\tau^{\wedge}\right)_{ii} d\bar{\ } dz^{\wedge} \qquad \text{.....(3.49)}$$

Substitute equation **(3.48)** into equation **(3.49)** to get **[18]**;

$$\left(F_r^{\wedge}\right)_{ii} = \int_0^1 \int_{\bar{\ }_1}^{\bar{\ }_2} \pm \left(\frac{h^{\wedge}}{2} \frac{\partial P^{\wedge}}{\partial \bar{\ }} \right)_{ii} d\bar{\ } dz^{\wedge} + \int_0^1 \int_{\bar{\ }_1}^{\bar{\ }_2} \left(\frac{h^{\wedge}}{2} \frac{\text{د } 1}{3} \frac{\partial P^{\wedge}}{\partial \bar{\ }} \right)_{ii} d\bar{\ } dz^{\wedge} + \int_0^1 \int_{\bar{\ }_1}^{\bar{\ }_2} \left(\frac{1 - \text{د } 0}{h^{\wedge}} \right)_{ii} d\bar{\ } dz^{\wedge}$$

.....(3.50)

Where;

ii=1 $\left(F_r^{\wedge}\right)_{ii} = F_{r_1}^{\wedge}$ friction force at inner surface of the ring and the negative sign of the first right term would be used.

ii= 2 $\left(F_r^{\wedge}\right)_{ii} = F_{r_2}^{\wedge}$ friction force at outer surface of the ring and the positive sign of the first right term would be used.

The friction coefficient is defined as the ratio of the friction force by the total load carried;

$$\left(\text{«}^{\wedge}\right)_{ii} = \frac{\left(F_r^{\wedge}\right)_{ii}}{\left(\hat{W}\right)_{ii}} \qquad \text{.....(3.51)}$$

if ii=1 $\left(\text{«}^{\wedge}\right)_{ii} = \text{«}_1^{\wedge}$ friction coefficient for journal –porous floating ring oil film,

and

ii= 2 $\left(\text{«}^{\wedge}\right)_{ii} = \text{«}_2^{\wedge}$ friction coefficient for porous floating ring – porous bearing oil film.

3.8 *Steady – State Performance*

The hydrodynamic action would eventually force the ring to rotate at a speed governed by bearing assembly and bearing parameters. To calculate the load carrying capacity and the frictional torque on the journal, it is necessary to find those positions of the journal and the ring centers with respect to the bearing center at which the ring is in steady state equilibrium, that is the eccentricity ratio, attitude angles for inner and outer films and the journal speed must be established. So in steady – state operating regimes at fixed journal speeds, i.e., the magnitude and the direction of inner and outer films loads must be equal, and the frictional torques acting on ring outer and inner surfaces must be equal and opposite thus **[32,33]**;

$$F_{r_1}^{\wedge} R_1 = F_{r_2}^{\wedge} R_2 \qquad \textbf{.....(3.52)}$$

By substitute equation **(3.50)** into equation **(3.52)** torques equation would be written as;

$$T_{inner}^{\wedge} = \int_0^{\bar{1}} \int_{\bar{1}}^{2} \frac{-h_1^{\wedge}}{2} \frac{\partial P_1^{\wedge}}{\partial \bar{\theta}} d\bar{\theta} dZ^{\wedge} + \int_0^{\bar{1}} \int_{\bar{1}}^{2} \frac{h_1^{\wedge}}{2} \frac{\bar{1}, 1}{3} \frac{\partial P_1^{\wedge}}{\partial \bar{\theta}} d\bar{\theta} dZ^{\wedge} + \int_0^{\bar{1}} \int_{\bar{1}}^{2} \frac{\bar{1}, 0}{h_1^{\wedge}} d\bar{\theta} dZ^{\wedge} \qquad \textbf{.....(3.53)}$$

$$T_{outer}^{\wedge} = \int_0^{\bar{1}} \int_{\bar{1}}^{2} \frac{h_2^{\wedge}}{2} \frac{\partial P_2^{\wedge}}{\partial \bar{\theta}} d\bar{\theta} dZ^{\wedge} + \int_0^{\bar{1}} \int_{\bar{1}}^{2} \frac{h_2^{\wedge}}{2} \frac{\bar{1}, 1}{3} \frac{\partial P_2^{\wedge}}{\partial \bar{\theta}} d\bar{\theta} dZ^{\wedge} + \int_0^{\bar{1}} \int_{\bar{1}}^{2} \frac{\bar{1}, 0}{h_2^{\wedge}} d\bar{\theta} dZ^{\wedge} \qquad \textbf{.....(3.54)}$$

Numerical integration using Simpson's $1/3^{rd}$ rule would be adopted to calculate the dimensionless (load carrying capacity, frictional force, frictional torque, momentum and flow rate).

By equating the dimensional torques equations the ratio of porous floating ring speed to the journal speed can be determined as follows;

$$\frac{N_r}{N_j} = \frac{T^{\wedge}_{inner}}{T^{\wedge}_{outer}} * \frac{R_1^3}{R_2^3} * \frac{c_2}{c_1} \qquad \textbf{.....(3.55)}$$

The second equilibrium condition which specifies the steady state performance of the bearing is the load balance which states that;

$$W_1^{\wedge} = W_2^{\wedge} \qquad \textbf{.....(3.56)}$$

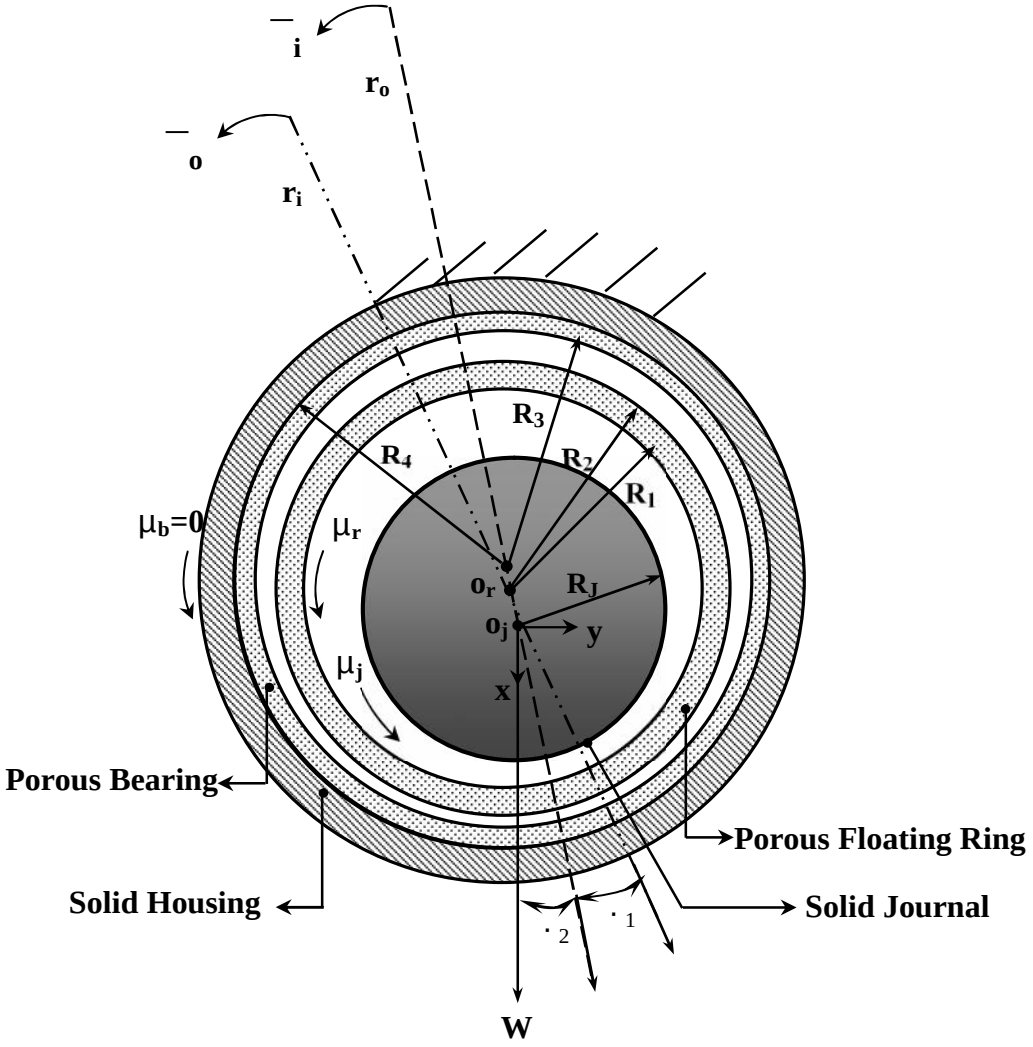

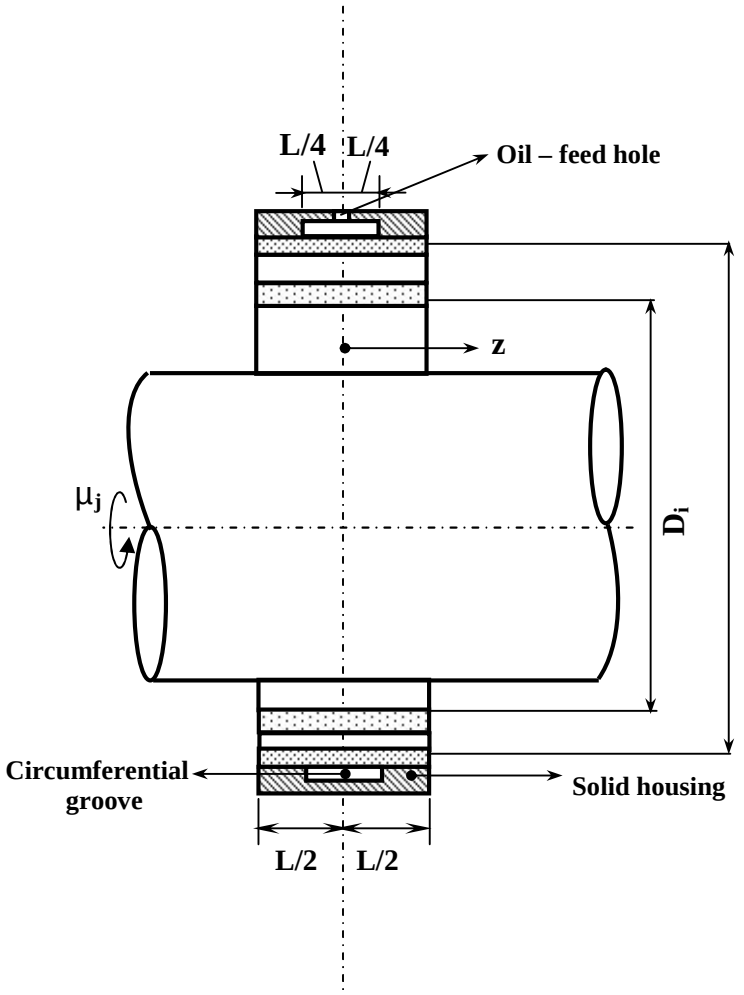

Figure (3-3), Oil film region and oil flow of porous floating ring journal bearing

CHAPTER FOUR

NUMERICAL SOLUTION

4.1 Introduction

The governing differential equations presented previously in chapter three will be solved using finite difference method. This technique was presented for steady state and isothermal conditions.

This chapter consists of constructing the grid generation, numerical solution for the governing partial differential equations, the numerical calculation algorithm and the computer program which prepared to solve the problem as will described later.

4.2 Mesh Generation

The solution of system of partial differential equations can be greatly simplified by a well – constructed grid. The dimensionless oil film pressure distribution $\left(P^{\wedge}\right)_{ii}$ and the dimensionless oil pressure distribution through the porous matrix $\left(P^{\wedge *}\right)_{jj}$ can be obtained by simultaneously solving equation (**3.1)** and **(3.10)**.

These equations are discretized yielding the mesh size of **(N_1)** in circumferential direction, **(N_2)** across the half – width of the bearing and **(N_3)** across the thickness of the porous media.

In the present analysis **180** divisions in circumferential direction (**N_1**) (100 divisions for the rupture zone **(N_{11})** and **80** divisions for the effective zone **(N_{12})**, sixteen divisions in axial direction **(N_2)** and eight divisions in radial direction **(N_3)** have been adopted.

The mesh size in circumferential direction can be defined as:

- For effective zone;

$$(\Delta^{-})_{ii} = \frac{(^{-}_{2} - ^{-}_{1})_{ii}}{80} \qquad \textbf{.....(4.1)}$$

or $$(\Delta^{-})_{ii} = \frac{(\ )_{ii}}{N_{12}} \qquad \textbf{.....(4-2)}$$

Where;

$$(\ )_{ii} = (^{-}_{2} - ^{-}_{1})_{ii} \qquad \textbf{.....(4.3)}$$

- For the rupture zone;

$$(\Delta^{-})_{ii} = \frac{360^{\circ} - (\ )_{ii}}{100} \qquad \textbf{.....(4.4)}$$

or $$(\Delta^{-})_{ii} = \frac{360^{\circ} - (\ )_{ii}}{N_{11}} \qquad \textbf{.....(4.5)}$$

Half length of the bearing and the ring has been taken into consideration due to the bearing symmetry. Therefore, the mesh size in axial direction can be defined as:

$$\Delta Z = \frac{L/2}{N_2} \qquad \text{.....(4.6)}$$

This can be normalized as follows;

$$\Delta Z^{\wedge} = \frac{\Delta Z}{L/2} \qquad \text{.....(4.7)}$$

The porous floating ring and the porous bearing can be divided radially into layers; hence the mesh size for the porous ring in radial direction can be evaluated as:

$$\Delta r = \frac{(R_2 - R_1)}{N_3} \qquad \text{.....(4.8)}$$

This can be normalized as follows:

$$\Delta r^{\wedge} = \frac{\Delta r}{R_1} \qquad \text{.....(4.9)}$$

While the mesh size on the porous bearing in radial direction can be evaluated as;

$$\Delta r = \frac{(R_4 - R_3)}{N_3} \qquad \text{.....(4.10)}$$

This can be normalized as:

$$\Delta r^{\wedge} = \frac{\Delta r}{R_3} \qquad \text{.....(4.11)}$$

The finite differences grids can be shown schematically in Figure (4-1).

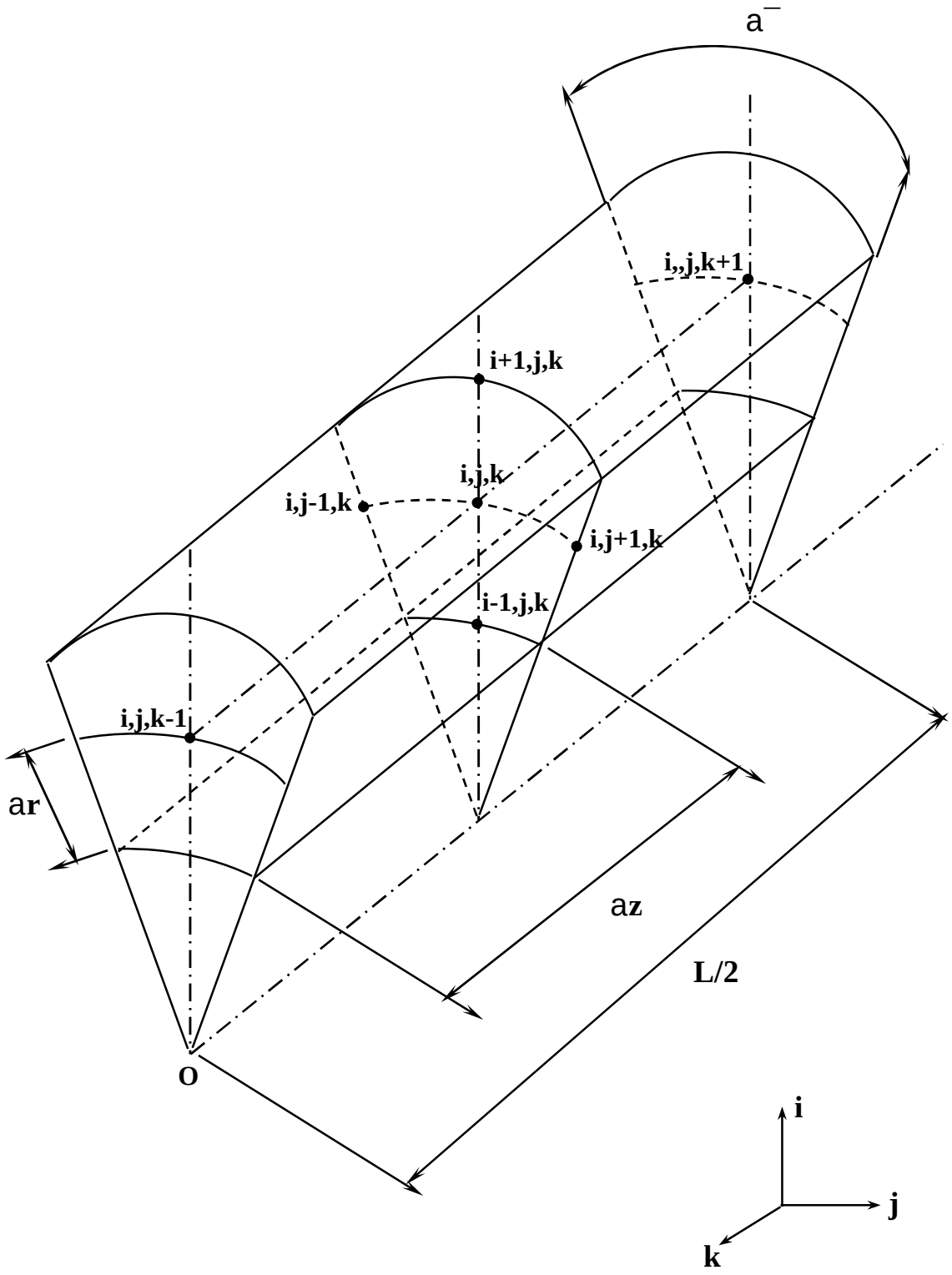

Figure (4-1a), Finite Difference Grid for Porous Layer of Floating Ring and Bearing.

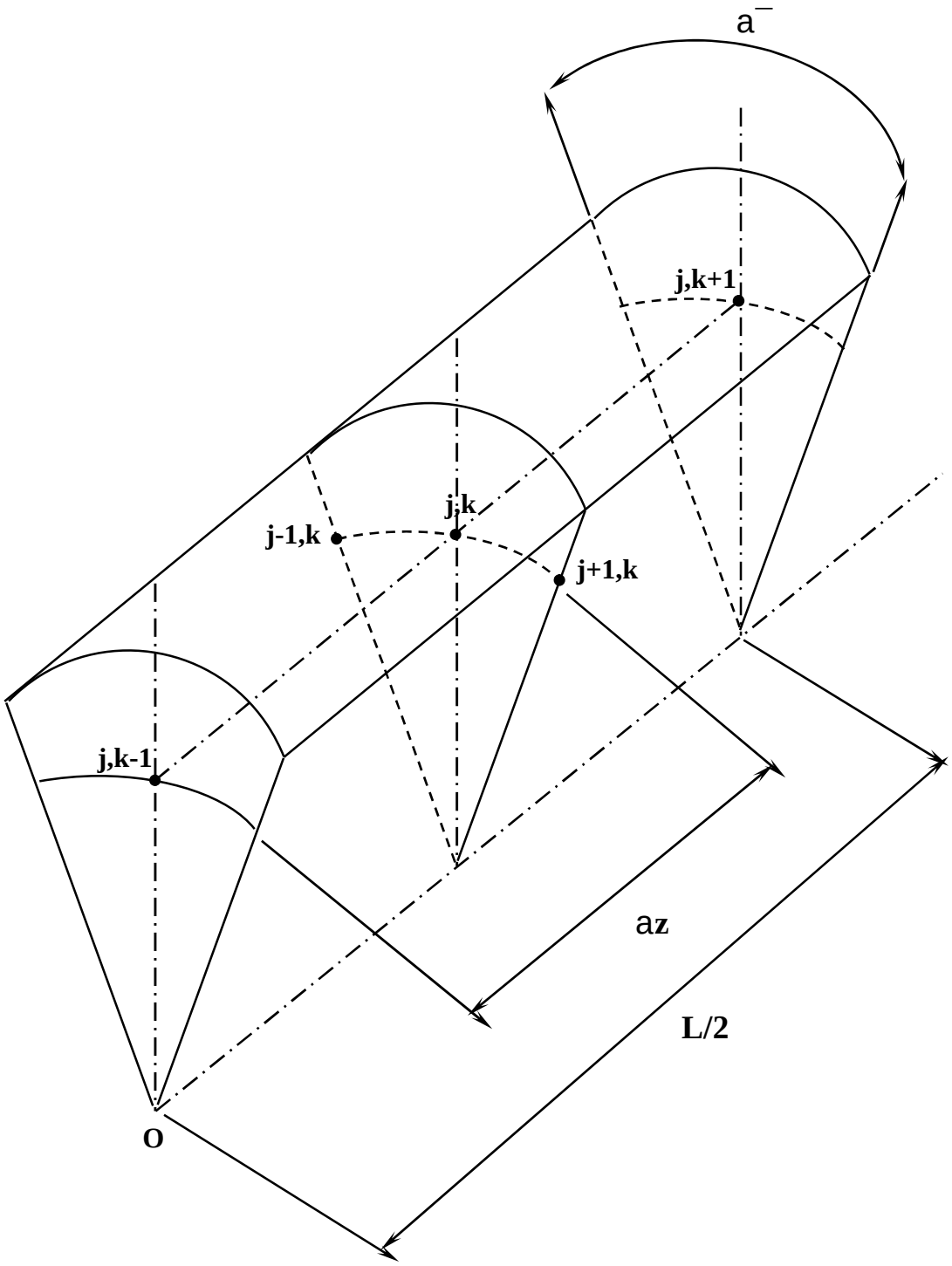

Figure (4-1b), Finite Difference Grid for the Oil Film Layer.

Figure (4-1), Mesh Generation and Finite Difference Grids.

4.3 *Discritized Form of the Governing Equations*

The numerical techniques used for solving the differential equations are based on replacing these equations by algebraic equations. In the case of popular finite difference method, this is done by replacing the derivatives by differences so that the governing equations may be written in discrete form as follows;

4.3.1 *Discritized Form of the Reynolds' Equation*

The Reynolds' equation **(3.1)** can be rewritten as follows **[42]**;

$$\frac{\partial}{\partial \bar{\theta}}\left(A\frac{\partial P^{\wedge}}{\partial \bar{\theta}}\right)_{ii}+\left(\frac{D_{ii}}{L}\right)^{2}\frac{\partial}{\partial Z^{\wedge}}\left(A\frac{\partial P^{\wedge}}{\partial Z^{\wedge}}\right)_{ii}=6\left(\frac{\partial B}{\partial \bar{\theta}}\right)_{ii}-12\Phi_{ii}\left(\frac{\partial P^{\wedge^{*}}}{\partial r^{\wedge}}\bigg|_{r^{\wedge}=1}\right)_{jj} \quad \textbf{……(4.12)}$$

Where;

$$\left(A=h^{\wedge^{3}}\left(1+\varepsilon_{1}\right)\right)_{ii} \quad \textbf{……(4.13)}$$

$$\left(B=h^{\wedge}\left(1+\varepsilon_{0}\right)\right)_{ii} \quad \textbf{……(4.14)}$$

The finite difference analog to Reynolds' equation can be written as;

$$\left.\begin{array}{l} \dfrac{A_{j+1}-A_{j-1}}{2\Delta^{-}} * \dfrac{P^{\wedge}_{j+1,k}-P^{\wedge}_{j-1,k}}{2\Delta^{-}} + A_j * \dfrac{P^{\wedge}_{j+1,k}-2P^{\wedge}_{j,k}+P^{\wedge}_{j-1,k}}{\Delta^{-2}} + \left(\dfrac{D}{L}\right)^2 * A_j * \\ \dfrac{P^{\wedge}_{j,k+1}-2P^{\wedge}_{j,k}+P^{\wedge}_{j,k-1}}{\Delta Z^{\wedge 2}} = 6 * \dfrac{B_{j+1}-B_{j-1}}{2\Delta^{-}} - 12 * \Phi * \left(\left.\dfrac{\partial P^{\wedge *}}{\partial r^{\wedge}}\right|_{r^{\wedge}=1}\right)_{jj} \end{array}\right)_{ii} \quad \textbf{.....(4.15)}$$

The above equation can be simplified by multiplying both sides by $\left(\Delta Z^{\wedge 2} * \Delta^{-2}\right)$ to get;

$$\left.\begin{array}{l} \left(A_{j+1}-A_{j-1}\right) * \left(P^{\wedge}_{j+1,k}-P^{\wedge}_{j-1,k}\right) * \left(0.25 * \Delta Z^{\wedge 2}\right) + \left(P^{\wedge}_{j+1,k}-2P^{\wedge}_{j,k}+P^{\wedge}_{j-1,k}\right) * \left(A_j * \Delta Z^{\wedge 2}\right) + \\ \left(P^{\wedge}_{j,k+1}-2P^{\wedge}_{j,k}+P^{\wedge}_{j,k-1}\right) * \left(A_j * \Delta^{-2} * \left(\dfrac{D}{L}\right)^2\right) = \left(B_{j+1}-B_{j-1}\right) * \left(3 * \Delta^{-} * \Delta Z^{\wedge 2}\right) - \\ \left(12 * \Phi * \Delta^{-2} * \Delta Z^{\wedge 2}\right) * \left(\left.\dfrac{\partial P^{\wedge *}}{\partial r^{\wedge}}\right|_{r^{\wedge}=1}\right)_{jj} \end{array}\right)_{ii}$$

.....(4.16)

which can be rearranged and rewritten as follows;

$$\left(P^{\wedge}_{j+1,k} * \left(A_{j+1}-A_{j-1}\right) * \left(0.25 * \Delta Z^{\wedge 2}\right) - P^{\wedge}_{j-1,k} * \left(A_{j+1}-A_{j-1}\right) * \left(0.25 * \Delta Z^{\wedge 2}\right) + P^{\wedge}_{j+1,K} * \left(A_j * \Delta Z^{\wedge 2}\right) + P^{\wedge}_{j-1,K} * \left(A_j * \Delta Z^{\wedge 2}\right) + \left(P^{\wedge}_{j,k+1}+P^{\wedge}_{j,k-1}\right) * \left(A_j * \Delta^{-2} * \left(\dfrac{D}{L}\right)^2\right) - \left(B_{j+1}-B_{j-1}\right) * \left(3 * \Delta^{-} * \Delta Z^{\wedge 2}\right) + \left(12 * \Phi * \Delta^{-2} * \Delta Z^{\wedge 2}\right) * \left(\left.\dfrac{\partial P^{\wedge *}}{\partial r^{\wedge}}\right|_{r^{\wedge}=1}\right)_{jj} = P^{\wedge}_{j,k} * 2 * \left(A_j * \Delta Z^{\wedge 2} + A_j * \Delta^{-2}\left(\dfrac{D}{L}\right)^2\right)_{ii}$$

.....(4.17)

The dimensionless oil film pressure can be evaluated as;

$$\left(P^{\wedge}_{j,k} = C_{1_j} * P^{\wedge}_{j+1,k} + C_{2_j} * P^{\wedge}_{j-1,k} + C_{3_j} * \left(P^{\wedge}_{j,k+1} + P^{\wedge}_{j,k-1}\right) + C_{4_j}\right)_{ii} \qquad \textbf{.....(4.18)}$$

where ;

$$\left(C_{1_j} = \frac{\left(A_j * \Delta Z^{\wedge 2}\right) + \left(A_{j+1} - A_{j-1}\right) * \left(0.25 * \Delta Z^{\wedge 2}\right)}{CC_j}\right)_{ii} \qquad \textbf{.....(4.19)}$$

$$\left(C_{2_j} = \frac{\left(A_j * \Delta Z^{\wedge 2}\right) - \left(A_{j+1} - A_{j-1}\right) * \left(0.25 * \Delta Z^{\wedge 2}\right)}{CC_j}\right)_{ii} \qquad \textbf{.....(4.20)}$$

$$\left(C_{3_j} = \frac{A_j * \Delta^{-2} * \left(\frac{D}{L}\right)^2}{CC_j}\right)_{ii} \qquad \textbf{.....(4.21)}$$

$$\left(C_{4_j} = \frac{\left(-\left(B_{j+1} - B_{j-1}\right) * \left(3 * \Delta^{-} * \Delta Z^{\wedge 2}\right) + \left(12 * \Phi * \Delta^{-2} * \Delta Z^{\wedge 2}\right) * \left(\frac{\partial P^{\wedge *}}{\partial r^{\wedge}}\Big|_{r^{\wedge}=1}\right)_{jj}\right)}{CC_j}\right)_{ii}$$

.....(4.22)

$$\left(CC_j = 2 * A_j * \left(\Delta Z^{\wedge 2} * \Delta^{-2} * \left(\frac{D}{L}\right)^2\right)\right)_{ii} \qquad \textbf{.....(4.23)}$$

$$\left(B_{j+1} = h^{\wedge}_{j+1} * \left(1 + \frac{s}{h^{\wedge}_{j+1} + s} \right) \right)_{ii} \quad \text{.....(4.24)}$$

$$\left(B_{j-1} = h^{\wedge}_{j-1} * \left(1 + \frac{s}{h^{\wedge}_{j-1} + s} \right) \right)_{ii} \quad \text{.....(4.25)}$$

$$\left(A_j = h^{\wedge 3}_{j} * \left(1 + \frac{3 * \left(h^{\wedge}_{j} * s + 2 * \sim^{2} * s^{2} \right)}{h^{\wedge}_{j} * \left(h^{\wedge}_{j} + s \right)} \right) \right)_{ii} \quad \text{.....(4.26)}$$

$$\left(A_{j+1} = h^{\wedge 3}_{j+1} * \left(1 + \frac{3 * \left(h^{\wedge}_{j+1} * s + 2 * \sim^{2} * s^{2} \right)}{h^{\wedge}_{j+1} * \left(h^{\wedge}_{j+1} + s \right)} \right) \right)_{ii} \quad \text{.....(4.27)}$$

$$\left(A_{j-1} = h^{\wedge 3}_{j-1} * \left(1 + \frac{3 * \left(h^{\wedge}_{j-1} * s + 2 * \sim^{2} * s^{2} \right)}{h^{\wedge}_{j-1} * \left(h^{\wedge}_{j-1} + s \right)} \right) \right)_{ii} \quad \text{.....(4.28)}$$

$$\left(h^{\wedge}_{j} = 1 + £ \cos\left(\vdash_{j} \right) \right)_{ii} \quad \text{.....(4.29)}$$

$$\left(h^{\wedge}_{j+1} = 1 + £ \cos\left(\vdash_{j+1} \right) \right)_{ii} \quad \text{.....(4.30)}$$

$$\left(h^{\wedge}_{j-1} = 1 + £ \cos\left(\vdash_{j-1} \right) \right)_{ii} \quad \text{.....(4.31)}$$

$$\left(,_{0} = \frac{s}{\left(h^{\wedge} + s \right)} \right)_{ii} \quad \text{.....(4.32)}$$

$$\left(,_{1} = 3\left(h^{\wedge} s + 2\sim^{2} s^{2} \right) / \left\{ h^{\wedge} \left(h^{\wedge} + s \right) \right\} \right)_{ii} \quad \text{.....(4.33)}$$

$$\left(s = \left(\Phi c / R \right)^{1/2} / \sim \right)_{ii} \quad \text{.....(4.34)}$$

4.3.2 *Discritized Form of Darcy's Equation*

To evaluate the filter velocity term at the right hand side of the Reynolds' equation the Darcy's equation **(3.10)** must be solved simultaneously with equation **(3.1)**.

The Darcy's equation **(3.10)** can be rewritten in discritized form as follows;

$$\left(\frac{P^{\wedge *}_{i+1,j,k} - 2P^{\wedge *}_{i,j,k} + P^{\wedge *}_{i-1,j,k}}{\Delta r^{\wedge 2}} + \frac{1}{r^{\wedge}} \frac{P^{\wedge *}_{i+1,j,k} - P^{\wedge *}_{i-1,j,k}}{2\Delta r^{\wedge}} + \frac{1}{r^{\wedge 2}} \frac{P^{\wedge *}_{i,j+1,k} - 2P^{\wedge *}_{i,j,k} + P^{\wedge *}_{i,j-1,k}}{\Delta^{-2}} + \right.$$

$$\left. \left(\frac{D_{ii}}{L} \right)^2 \frac{P^{\wedge *}_{i,j,k+1} - 2P^{\wedge *}_{i,j,k} + P^{\wedge *}_{i,j,k-1}}{\Delta Z^{\wedge 2}} \right)_{jj} = 0 \qquad \textbf{.....(4.35)}$$

To simplify the above equation multiply both sides by $\left(2 * r^{\wedge 2} * \Delta r^{\wedge 2} * \Delta^{-2} * \Delta Z^{\wedge 2} \right)$. Hence equation **(4.35)** can be rewritten as;

$$\left(\left(P^{\wedge *}_{i+1,j,k} + P^{\wedge *}_{i-1,j,k} \right) * \left(2 * r^{\wedge 2} \Delta^{-2} * \Delta Z^{\wedge 2} \right) + \left(P^{\wedge *}_{i+1,j,k} - P^{\wedge *}_{i-1,j,k} \right) * \left(r^{\wedge} * \Delta r^{\wedge} * \Delta^{-2} * \Delta Z^{\wedge 2} \right) + \right.$$

$$\left(P^{\wedge *}_{i,j+1,k} + P^{\wedge *}_{i,j-1,k} \right) * \left(2 * \Delta r^{\wedge 2} * \Delta Z^{\wedge 2} \right) + \left(P^{\wedge *}_{i,j,k+1} + P^{\wedge *}_{i,j,k-1} \right) * \left(2 * r^{\wedge 2} * \Delta r^{\wedge 2} * \Delta^{-2} * \left(\frac{D_{ii}}{L} \right)^2 \right) =$$

$$\left. P^{\wedge *}_{i,j,k} * 4 * \left\{ \left(r^{\wedge 2} * \Delta^{-2} * \Delta Z^{\wedge 2} \right) + \left(\Delta r^{\wedge 2} * \Delta Z^{\wedge 2} \right) + \left(r^{\wedge 2} * \Delta r^{\wedge 2} * \Delta^{-2} * \left(\frac{D_{ii}}{L} \right)^2 \right) \right\} \right)_{jj}$$

.....(4.36)

The dimensionless oil pressure inside the porous matrix can be calculated as;

$$\left(P^{\wedge *}_{i,j,k} = S_{1_j} * \left(P^{\wedge *}_{i+1,j,k} + P^{\wedge *}_{i-1,j,k} \right) + S_{2_j} * \left(P^{\wedge *}_{i+1,j,k} - P^{\wedge *}_{i-1,j,k} \right) + S_{3_j} * \left(P^{\wedge *}_{i,j+1,k} + P^{\wedge *}_{i,j-1,k} \right) + \right.$$

$$\left. S_{4_j} * \left(P^{\wedge *}_{i,j,k+1} + P^{\wedge *}_{i,j,k-1} \right) \right)_{jj} \qquad \text{.....(4.37)}$$

where;

$$\left(S_{1_j} = \frac{2 * r^{\wedge 2} * \Delta^{-2} * \Delta Z^{\wedge 2}}{SS_j} \right)_{jj} \qquad \text{.....(4.38)}$$

$$\left(S_{2_j} = \frac{r^{\wedge} * \Delta r^{\wedge} * \Delta^{-2} * \Delta Z^{\wedge 2}}{SS_j} \right)_{jj} \qquad \text{.....(4.39)}$$

$$\left(S_{3_j} = \frac{2 * \Delta r^{\wedge 2} * \Delta Z^{\wedge 2}}{SS_j} \right)_{jj} \qquad \text{.....(4.40)}$$

$$\left(S_{4_j} = \frac{2 * r^{\wedge 2} * \Delta r^{\wedge 2} * \Delta^{-2} * \left(\frac{D_{ii}}{L} \right)^2}{SS_j} \right)_{jj} \qquad \text{.....(4.41)}$$

$$\left(SS_j = 4 * \left\{ \left(r^{\wedge 2} * \Delta^{-2} * \Delta Z^{\wedge 2} \right) + \left(\Delta r^{\wedge 2} * \Delta Z^{\wedge 2} \right) + \left(r^{\wedge 2} * \Delta r^{\wedge 2} * \Delta^{-2} * \left(\frac{D_{ii}}{L} \right)^2 \right) \right\} \right)_{jj}$$

.....(3.42)

The points at which the above equations fail to describe the pressure include the points at the inner surface of the bearing and the ring, and the starting and the end points in the θ-direction of pressure distribution inside porous matrix. These points are treated as critical points. Suitable modifications of the above equation adopted at these points are as follows;

1- At the inner surface of the porous bearing and the ring (i.e. I=1), a forward central difference in radial direction was adopted, so that the pressure equation was modifies as follows;

$$\left(P^{\wedge *}_{i,j,k} = S_{1_j} * \left(P^{\wedge *}_{i+2,j,k} - 2 * P^{\wedge *}_{i+1,j,k} \right) + S_{2_j} * \left(P^{\wedge *}_{i+1,j,k} \right) + S_{3_j} * \left(P^{\wedge *}_{i,j+1,k} + P^{\wedge *}_{i,j-1,k} \right) + \right.$$

$$\left. S_{4_j} * \left(P^{\wedge *}_{i,j,k+1} + P^{\wedge *}_{i,j,k-1} \right) \right)_{jj} \qquad \textbf{.....(4.43)}$$

where;

$$\left(S_{1_j} = \frac{r^{\wedge 2} * \Delta^{-2} * \Delta Z^{\wedge 2}}{SS_j} \right)_{jj} \qquad \textbf{.....(4.44)}$$

$$\left(S_{2_j} = \frac{r^{\wedge} * \Delta r^{\wedge} * \Delta^{-2} * \Delta Z^{\wedge 2}}{SS_j} \right)_{jj} \qquad \textbf{.....(4.45)}$$

$$\left(S_{3_j} = \frac{\Delta r^{\wedge 2} * \Delta Z^{\wedge 2}}{SS_j} \right)_{jj} \qquad \textbf{.....(4.46)}$$

$$\left(S_{4_j} = \frac{r^{\wedge 2} * \Delta r^{\wedge 2} * \Delta^{-2} * \left(\frac{D_{ii}}{L} \right)^2}{SS_j} \right)_{jj} \qquad \textbf{.....(4.47)}$$

$$\left(SS_j = \left(-r^{\wedge 2} * \Delta^{-2} * \Delta Z^{\wedge 2} \right) + \left(r^{\wedge} * \Delta r^{\wedge} * \Delta^{-2} * \Delta Z^{\wedge 2} \right) + \left(2 * \Delta r^{\wedge 2} * \Delta Z^{\wedge 2} \right) + 2 * r^{\wedge 2} * \Delta r^{\wedge 2} * \Delta^{-2} * \left(\frac{D_{ii}}{L} \right)^2 \right)_{jj}$$

……(4.48)

2- At the starting point (in theta direction) for the pressure equation of the porous bearing and the ring (i.e. j = 1), a forward central difference in θ-direction has been adopted, so that the pressure equation in this point can be written as;

$$\left(P^{\wedge *}_{i,j,k} = S_{1_j} * \left(P^{\wedge *}_{i+1,j,k} \right) + S_{2_j} * \left(P^{\wedge *}_{i-1,j,k} \right) + S_{3_j} * \left(P^{\wedge *}_{i,j+2,k} \right) + S_{4_j} * \left(P^{\wedge *}_{i,j+1,k} \right) + S_{5_j} * \left(P^{\wedge *}_{i,j,k+1} + P^{\wedge *}_{i,j,k-1} \right) \right)_{jj}$$

……(4.49)

$$\left(S_{1_j} = \frac{2 * r^{\wedge 2} * \Delta^{-2} * \Delta Z^{\wedge 2} + r^{\wedge} * \Delta r^{\wedge} * \Delta^{-2} * \Delta Z^{\wedge 2}}{SS_j} \right)_{jj}$$

……(4.50)

$$\left(S_{2_j} = \frac{2 * r^{\wedge 2} * \Delta^{-2} * \Delta Z^{\wedge 2} - r^{\wedge} * \Delta r^{\wedge} * \Delta^{-2} * \Delta Z^{\wedge 2}}{SS_j} \right)_{jj}$$

……(4.51)

$$\left(S_{3_j} = \frac{2 * \Delta r^{\wedge 2} * \Delta Z^{\wedge 2}}{SS_j} \right)_{jj}$$

……(4.52)

$$\left(S_{4_j} = \frac{-4 * \Delta r^{\wedge 2} * \Delta Z^{\wedge 2}}{SS_j} \right)_{jj}$$

……(4.53)

$$\left(S_{5_j} = \frac{2 * r^{\wedge 2} * \Delta r^{\wedge 2} * \Delta^{-2} * \left(\frac{D_{ii}}{L} \right)^2}{SS_j} \right)_{jj} \qquad \textbf{.....(4.54)}$$

$$\left(SS_j = 4 * \left(r^{\wedge 2} * \Delta^{-2} * \Delta Z^{\wedge 2} \right) - \left(0.5 * \Delta r^{\wedge 2} * \Delta Z^{\wedge 2} \right) + \left(r^{\wedge 2} * \Delta r^{\wedge 2} * \Delta^{-2} * \left(\frac{D_{ii}}{L} \right)^2 \right) \right)_{jj}$$

.....(4.55)

3- The end point (in theta direction) for the pressure equation of the porous bearing and the ring (i.e. when j = N_1+1), a backward central difference in θ-direction had been adopted, so that the pressure equation in this point can be written as;

$$\left(P_{i,j,k}^{\wedge *} = S_{1_j} * \left(P_{i+1,j,k}^{\wedge *} \right) + S_{2_j} * \left(P_{i-1,j,k}^{\wedge *} \right) + S_{3_j} * \left(P_{i,N_1-1,k}^{\wedge *} \right) + S_{4_j} * \left(P_{i,N_1,k}^{\wedge *} \right) + \right.$$

$$\left. S_{5_j} * \left(P_{i,j,k+1}^{\wedge *} + P_{i,j,k-1}^{\wedge *} \right) \right)_{jj} \qquad \textbf{.....(4.56)}$$

where,

$S_{1_j}, S_{2_j}, S_{3_j}, S_{4_j}, S_{5_j}$ are defined as in equation **(4.50)** to **(4.55).**

4.4 *Convergence Criteria*

The following convergence criteria are used to stop the loops of iteration when solving the pressure through the oil film and the porous matrix.

1- To stop loop of iteration when solving the equation which governs the oil pressure inside the porous matrix, the following convergence criterion may be used;

$$\left(\frac{\sum\sum\sum \left| P_{i,j,k}^{\wedge *(n+1)} - P_{i,j,k}^{\wedge *(n)} \right|}{\sum\sum\sum \left| P_{i,j,k}^{\wedge *(n)} \right|} < £_{P^{\wedge *}} \right)_{jj} \qquad \text{.....(4.57)}$$

while, the following convergence criterion is used to stop the loop of iteration when solving the equation which govern the pressure through the oil films.

$$\left(\frac{\sum\sum \left| P_{j,k}^{\wedge (n+1)} - P_{j,k}^{\wedge (n)} \right|}{\sum\sum \left| P_{j,k}^{\wedge (n)} \right|} < £_{P^{\wedge}} \right)_{ii} \qquad \text{.....(4.58)}$$

2- The loop iterations used to obtain the location of the leading edge line of the oil – film region, are stopped when the following convergence criterion is satisfied:

$$\left(\left| \underline{M}_1^{\wedge} - \underline{M}_2^{\wedge} - \underline{M}_c^{\wedge} - \underline{M}_b^{\wedge} \right| / \left| \underline{M}_1^{\wedge} \right| < £_{M^{\wedge}} \right)_{ii} \qquad \text{.....(4.59)}$$

Similarly the loop of iterations used to obtain the location of the trailing boundary line for the oil – film regions is stopped when the following convergence criterion is satisfied;

$$\left(\left|q_p / q_c\right|\right)_{ii} = \left(\left|\left(\frac{(1+,1)}{6(1+,0)} h^{\wedge 2} \int_0^1 \frac{\partial P^{\wedge}}{\partial} dz^{\wedge}\right)_{= 2}\right| < £_{q^{\wedge}}\right)_{ii} \qquad \textbf{.....(4.60)}$$

3- To ensure the steady state performance of the bearing, the following equilibrium conditions must be satisfied;

- torque equilibrium :

$$\left|T_{inner} - T_{outer}\right| < £_{T^{\wedge}} \qquad \textbf{.....(4.61)}$$

- load equilibrium :

$$\left|W_1^{\wedge} - W_2^{\wedge}\right| < £_{W^{\wedge}} \qquad \textbf{.....(4.62)}$$

Always (n) and (n+1) used in above equations denote two consecutive iterations and the points i, j, k represent the grid number in radial, circumferential, and axial directions respectively.

The iteration is continued until the above inequalities are satisfied simultaneously. The values of (1E-5) , (1E-5) , (1E-3) , (1E-3) , (1E-3) and (1E-3) are used for $£_{P^{\wedge *}}$, $£_{P^{\wedge}}$, $£_{M^{\wedge}}$, $£_{q^{\wedge}}$, $£_{T^{\wedge}}$ and $£_{W^{\wedge}}$ respectively.

4.5 *Computation Algorithm*

The numerical calculation described in the previous articles can be transformed into a computational algorithm, as follows;
Choose material, geometry, computation zone dimensions and then,

1- Choose a value for the journal – ring eccentricity ratio.

2- Assume a value for the ring – bearing eccentricity ratio.

3- Guess a value for θ_1 and θ_2.

4- Perform the mesh generation of the porous layer at the bearing and the ring in (r , θ , z) directions.

5- Perform the mesh generation for the ring – bearing oil film in (θ, z) directions.

6- Calculate the pressure distribution of the oil inside the porous matrix ($P^{\wedge *}$) by solving Darcy's' equation **(4.37), (4.43)** and **(4.49)**. Test the convergence using the convergence criterion **(4.57)**.

7- Calculate the pressure distribution through the oil film ($P^{\wedge}$) use the iterative procedure with Gauss Seidel method and under relaxation factor by solving equation **(4.18)** .Test the convergence using the convergence criterion **(4.58)**.

8- Apply the boundary condition for the leading edge; use the momentum equations **(3.29)** to **(3.32).** Test the convergence with the convergence criterion **(4.59).**

- ❖ If not converged modify the value of the θ_1 and return to step (4).
- ❖ If converged the algorithm moves to the next step.

9- Apply the boundary condition for trailing edge; use the flow rate equation **(3.33)**. Test the convergence with convergence criterion **(4.60)**

- ❖ If no converged, modify the value of θ_2 and return to step (4).
- ❖ If converged fixed the value of θ_2 and move to the next step of the algorithm.

10- Calculate the load carrying capacity of the ring – bearing oil film using equation **(3.42).**

11- Calculate the frictional torque at the outer surface of the ring using equation **(3.54)**.

12- Repeat the above procedure with journal – ring oil film, and calculate the load carrying capacity of the journal – ring oil film, also, evaluate the frictional torque at the inner surface of the ring using equation **(3.53)**.

13- If $\left(\left|W_1^{\wedge} - W_2^{\wedge}\right| < 10^{-3}\right)_{ii}$ and $\left(\left|T_{inner}^{\wedge} - T_{outer}^{\wedge}\right| < 10^{-3}\right)_{ii}$ then move to the next step. Otherwise modify the value of ε_2 and return to step (3).

14- Calculate the value of N_r and N_r/N_j using the equation **(3.55)**.

15- Print out the results.

4.6 *Computer Program*

A suitable computer program was prepared and written in (FORTRAN – 90) language, to solve governing equations which govern the performance of the porous floating ring journal bearing. The flow chart and the structure chart of the computer program can be shown in Figure (4-2) and appendix C respectively.

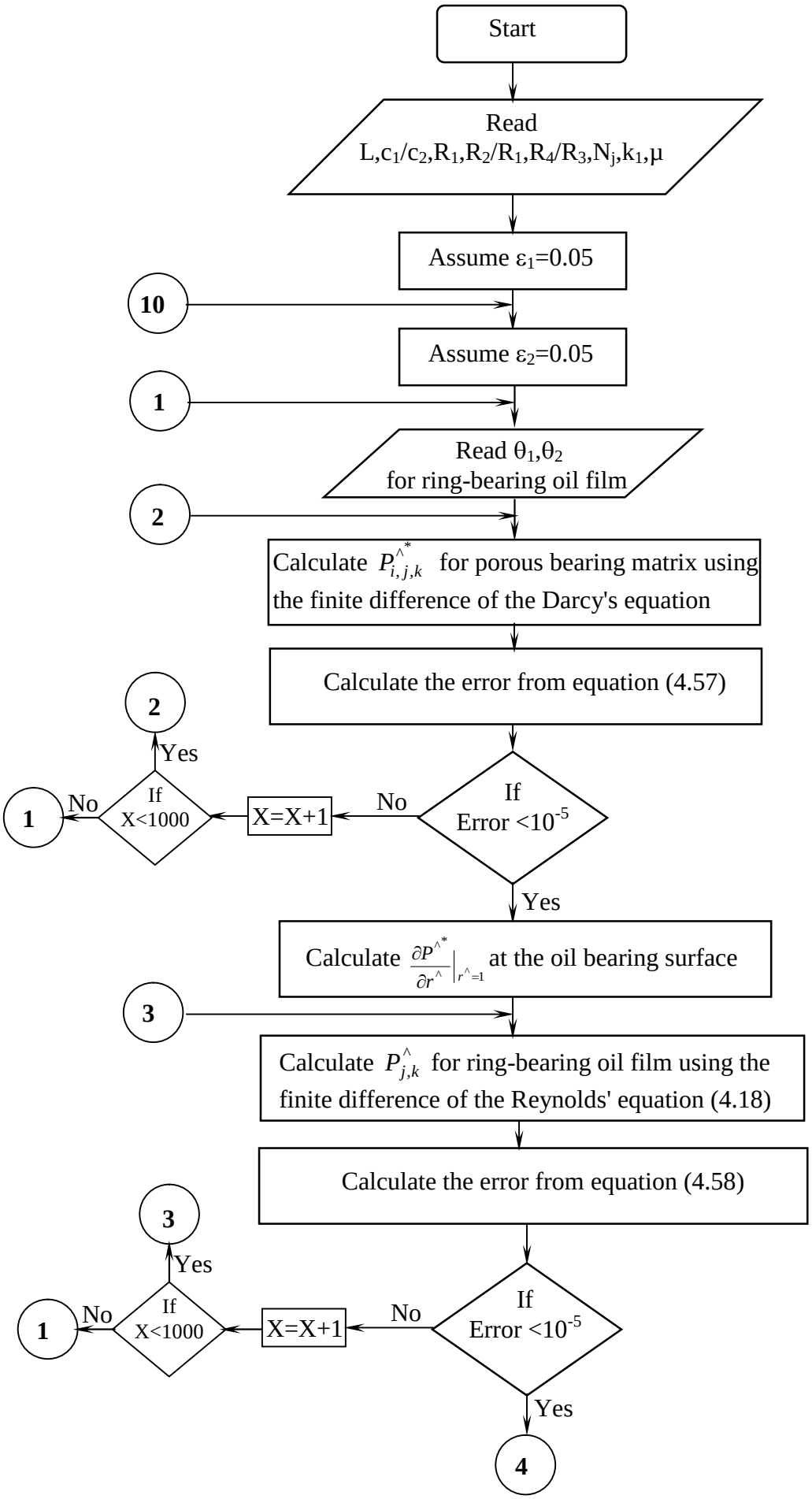

Figure (4-2), Flow Chart of Computer Program " continued"

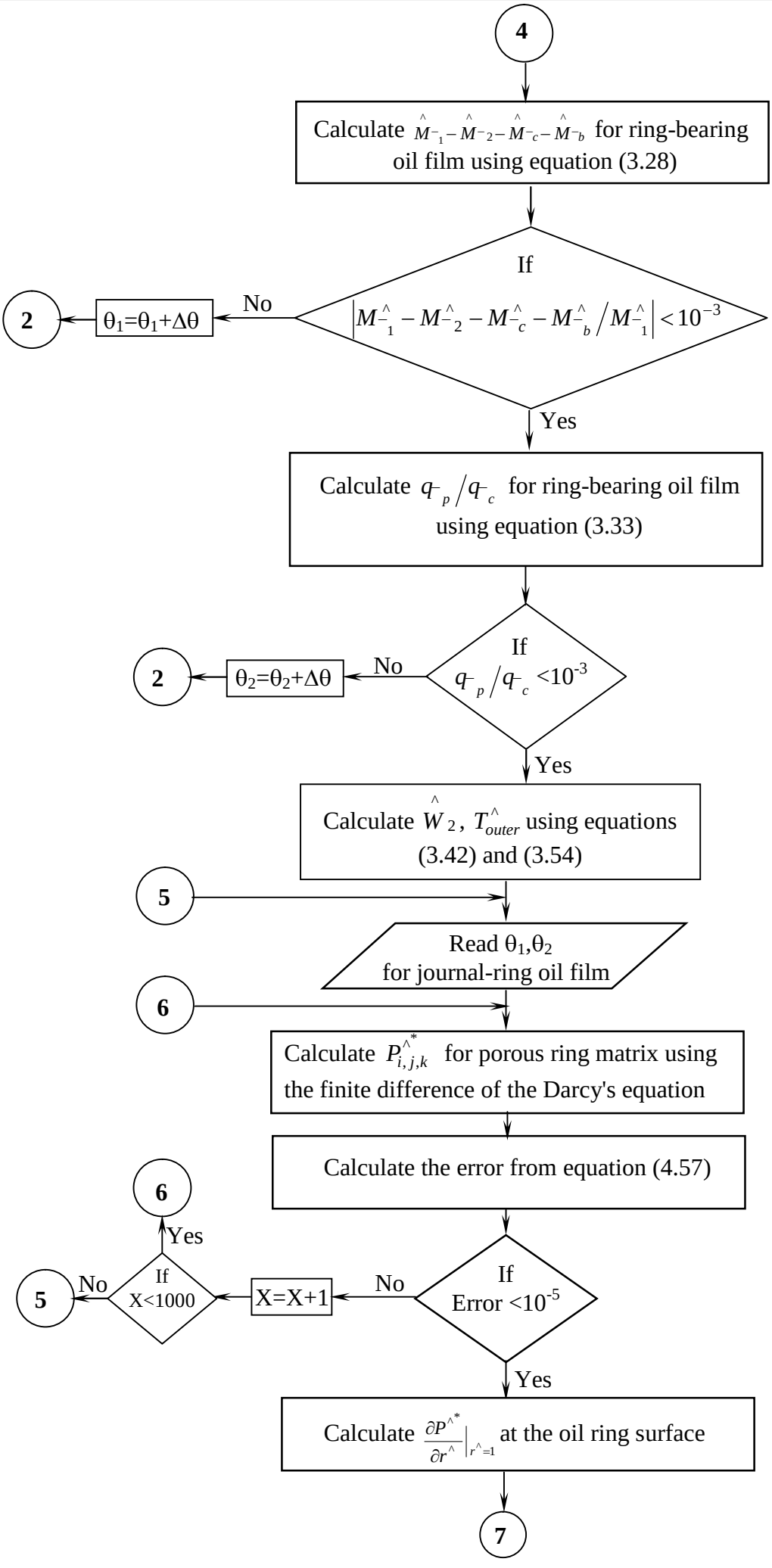
4
Calculate $\hat{M}_{-1}-\hat{M}_{-2}-\hat{M}_{-c}-\hat{M}_{-b}$ for ring-bearing oil film using equation (3.28)
If
$\left|M_{-1}^{\wedge}-M_{-2}^{\wedge}-M_{-c}^{\wedge}-M_{-b}^{\wedge}\right/M_{-1}^{\wedge}\left|<10^{-3}\right.$
No
θ1=θ1+Δθ
2
Yes
Calculate q_{-p}/q_{-c} for ring-bearing oil film using equation (3.33)
If
q_{-p}/q_{-c} <10-3
No
θ2=θ2+Δθ
2
Yes
Calculate $\hat{W}_2$, $T_{outer}^{\wedge}$ using equations (3.42) and (3.54)
5
Read θ1,θ2 for journal-ring oil film
6
Calculate $P_{i,j,k}^{\wedge *}$ for porous ring matrix using the finite difference of the Darcy's equation
Calculate the error from equation (4.57)
If
Error <10-5
No
X=X+1
If
X<1000
No
5
Yes
6
Yes
Calculate $\frac{\partial P^{\wedge *}}{\partial r^{\wedge}}\Big|_{r^{\wedge}=1}$ at the oil ring surface
7

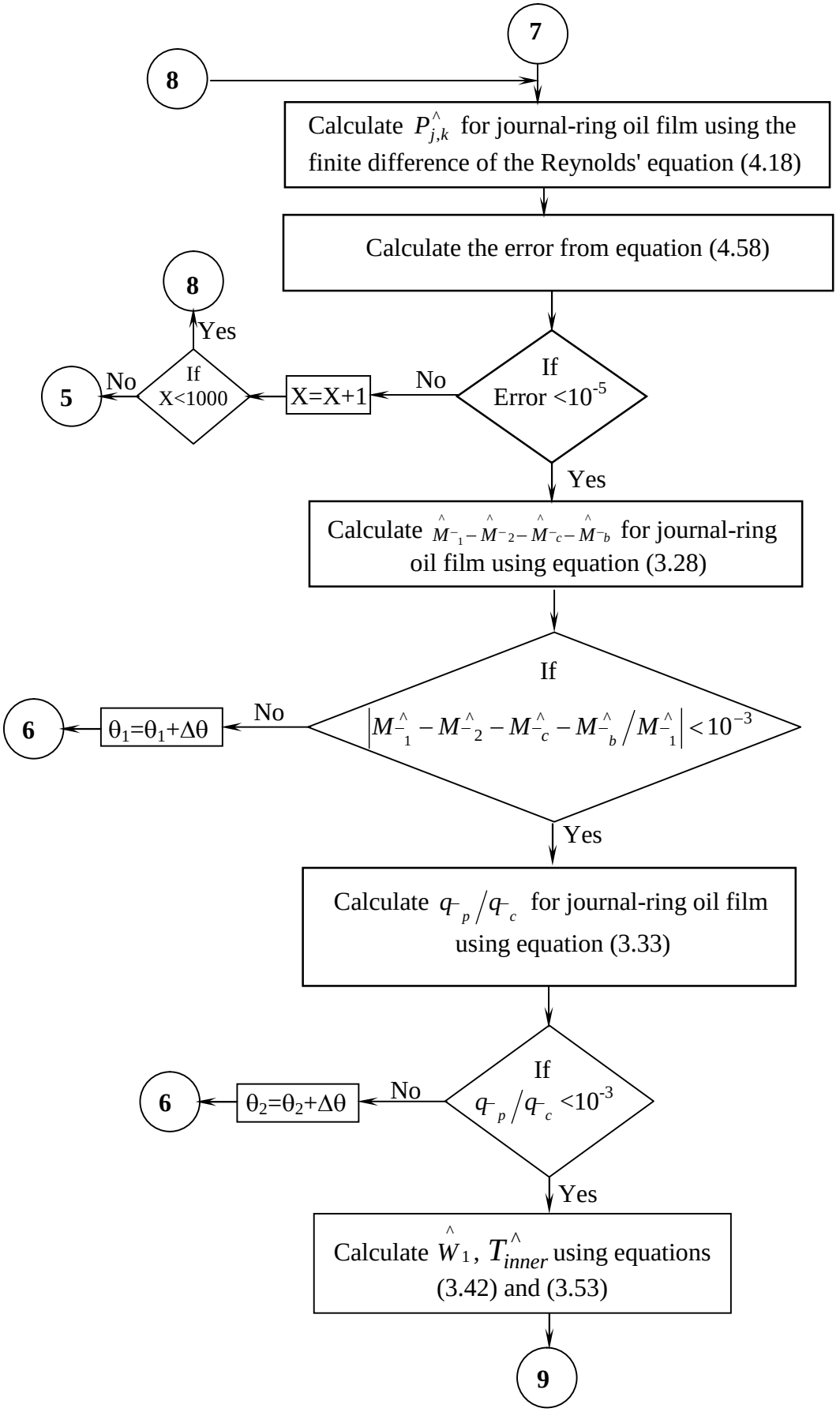
7
8
Calculate $P_{j,k}^{\wedge}$ for journal-ring oil film using the finite difference of the Reynolds' equation (4.18)
Calculate the error from equation (4.58)
8
Yes
If Error <10^-5
No
X=X+1
If X<1000
No
5
Yes
Calculate $\hat{M}_1 - \hat{M}_2 - \hat{M}_c - \hat{M}_b$ for journal-ring oil film using equation (3.28)
If $\left|M_1^{\wedge} - M_2^{\wedge} - M_c^{\wedge} - M_b^{\wedge} / M_1^{\wedge}\right| < 10^{-3}$
No
$\theta_1=\theta_1+\Delta\theta$
6
Yes
Calculate q_p / q_c for journal-ring oil film using equation (3.33)
If q_p / q_c <10^-3
No
$\theta_2=\theta_2+\Delta\theta$
6
Yes
Calculate $\hat{W}_1$, $T_{inner}^{\wedge}$ using equations (3.42) and (3.53)
9

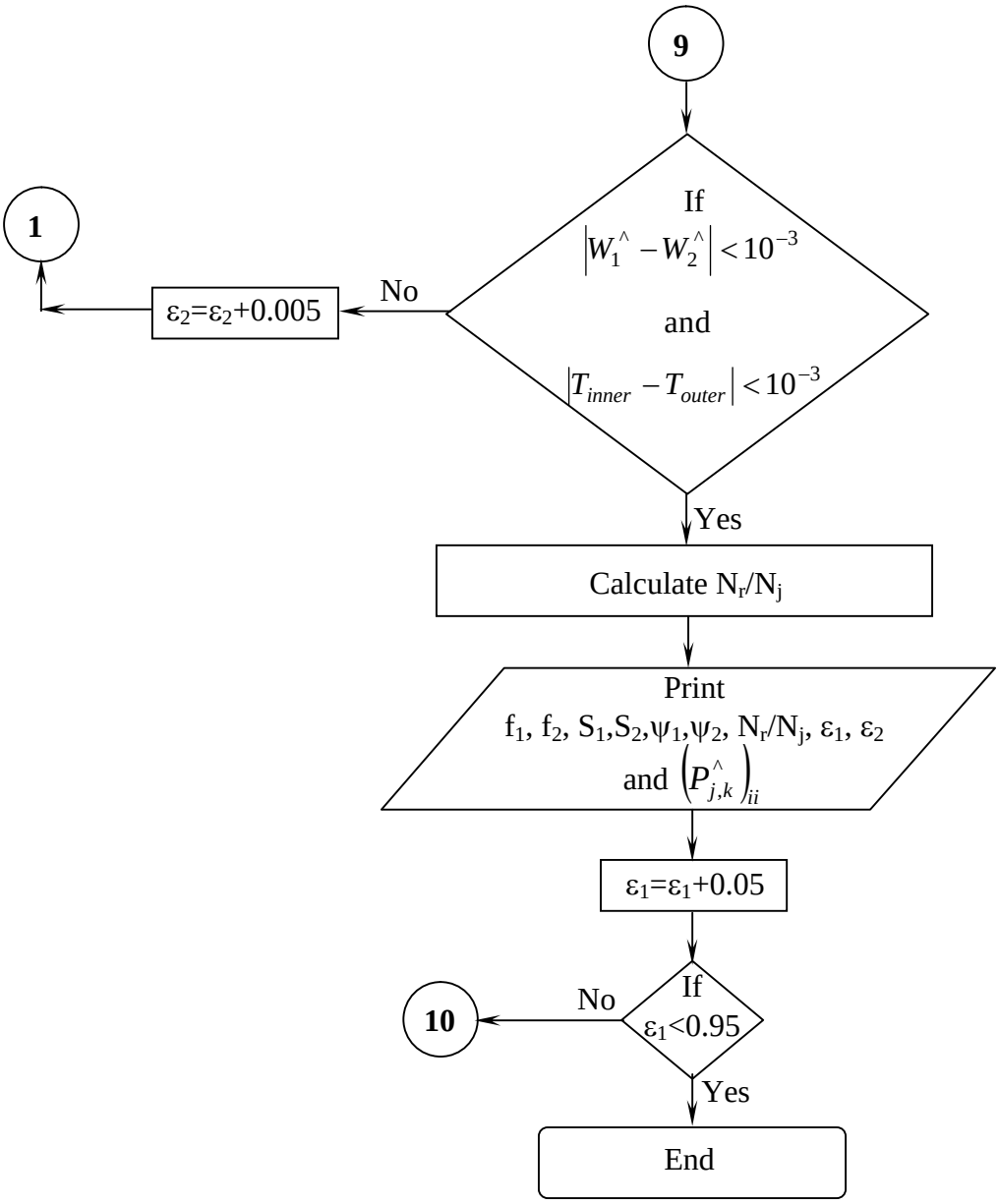
9
If
$\left|W_1^{\wedge} - W_2^{\wedge}\right| < 10^{-3}$
and
$\left|T_{inner} - T_{outer}\right| < 10^{-3}$
No
1
$\varepsilon_2=\varepsilon_2+0.005$
Yes
Calculate N_r/N_j
Print
f_1, f_2, S_1,S_2,ψ_1,ψ_2, N_r/N_j, ε_1, ε_2
and $\left(P_{j,k}^{\wedge}\right)_{ii}$
$\varepsilon_1=\varepsilon_1+0.05$
If
$\varepsilon_1<0.95$
No
10
Yes
End

4.7 *Verification of Computer Program*

The solution of the porous floating ring journal bearing merely consists of the parallel solution of two ordinary porous journal bearings via the mobility method **[32]**. These problems are coupled through equations **(3.28)** and **(3.33).**

Since there is no available information about the performance of the porous floating ring journal bearing, then the computer program mentioned before had been tested by comparing the results obtained from the solution of porous journal bearing obtained by Kaneko et, al., 1997, [18] with that obtained from the computer program prepared for this study as shown in Figures (4-3a), (4-3b), (4-3c), (4-4a) and (4-4b).

It seems that there is a good agreement between the results obtained by Kaneko et, al., 1997, [18] and that obtained by this study.

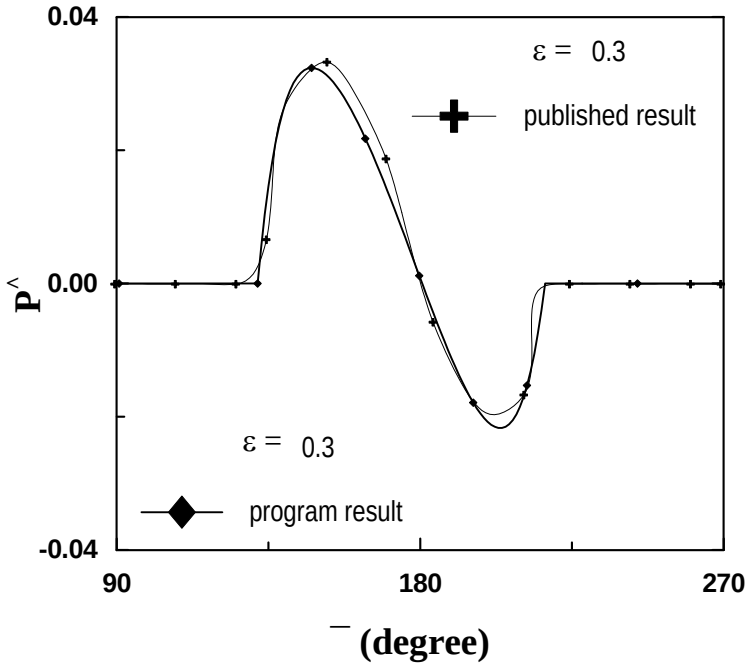

Figure (4-3a)

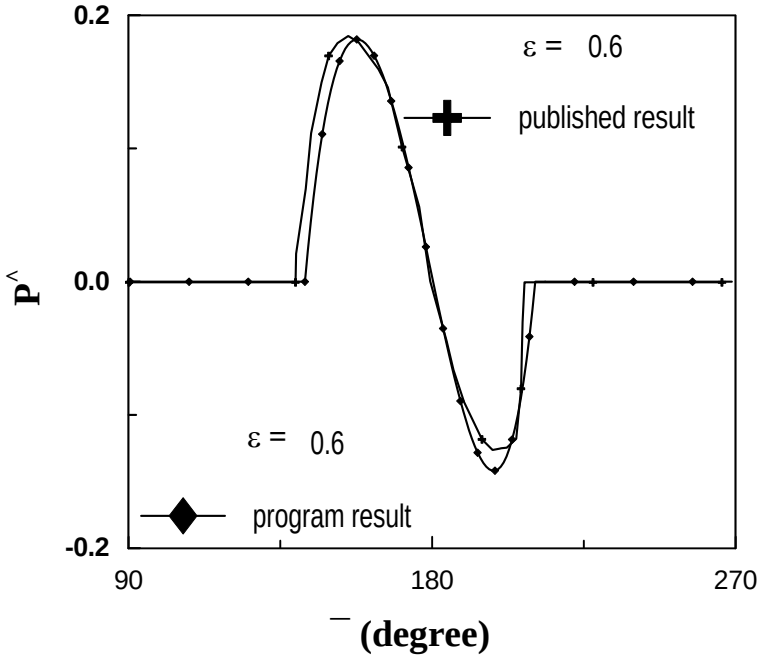

Figure (4-3b)

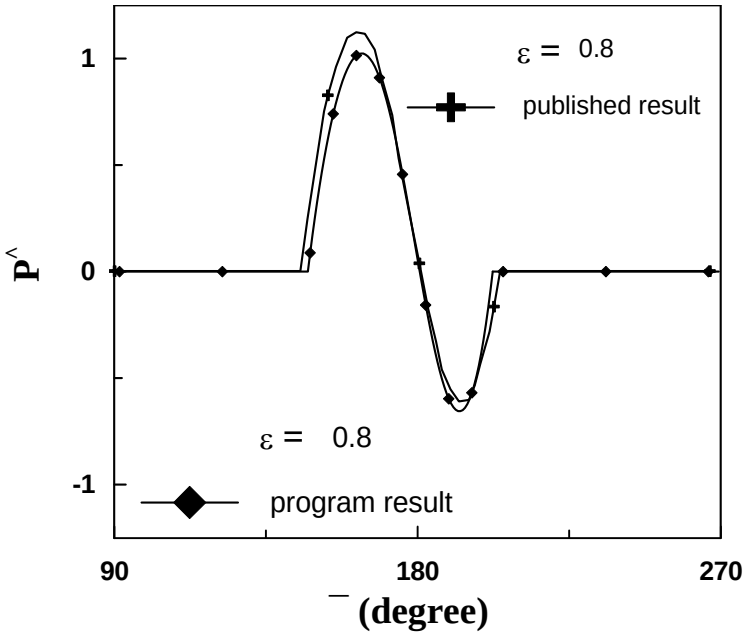

Figure (4-3c)

Figure (4-3), Comparison Between Experimental Published Results [18] with the Results obtained in the Present Work for Pressure Distribution at $P^{\wedge}_S = 0.1$.

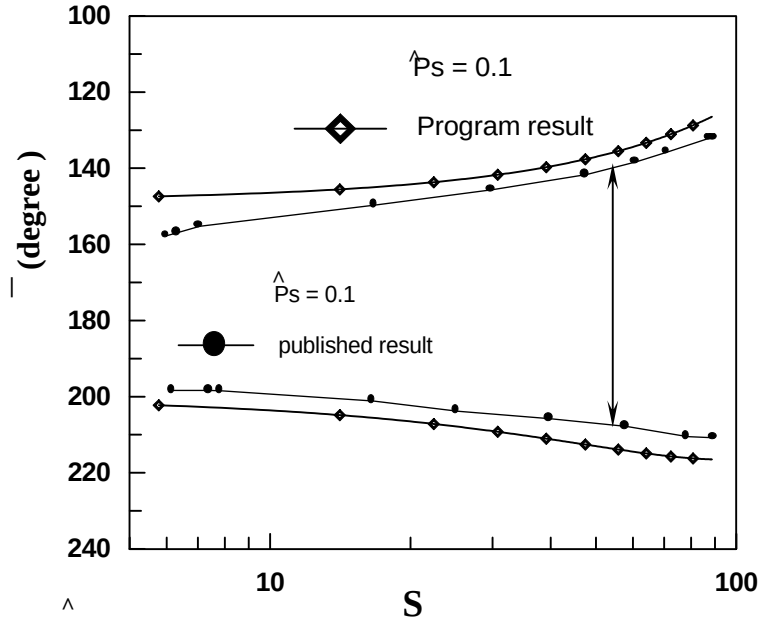

Figure (4-4a)

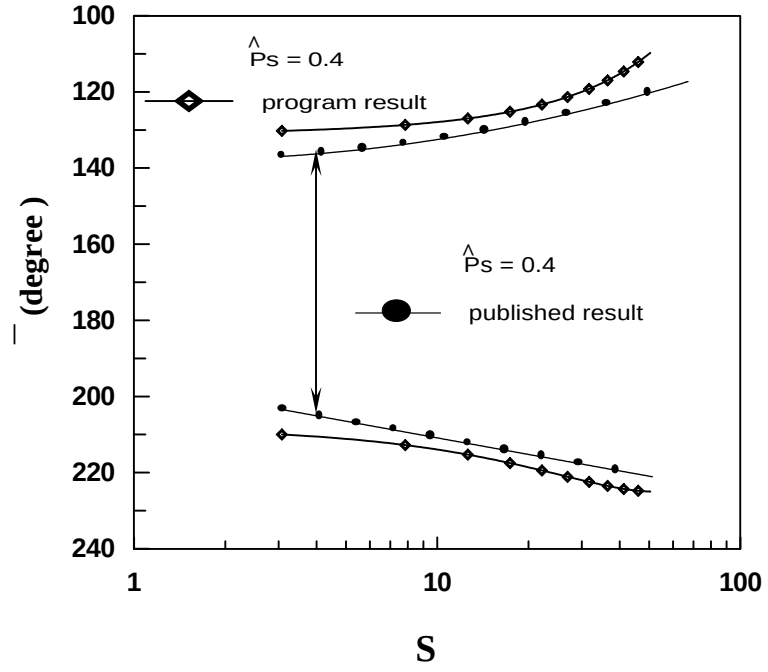

Figure (4-4b)

Figure (4-4), Comparison Between Published Results [18] with the Results obtained in the Present Work for Oil – Film Extent.

CHAPTER FIVE

RESULTS AND DISCUSSION

The results presented in this chapter represents the effect of different operating parameters on the steady state performance of porous floating ring journal bearing. A finite length bearing working under isothermal condition had been adopted by this work. The effect of different parameters, namely, supply pressure, clearance ratio, radii ratio, and permeability and eccentricity ratio on the performance of the bearing are studied and cleared in a form of graphs as shown below.

The effect of the bearing and ring permeabilities on the pressure distribution build up in ring – bearing and journal – ring oil film is presented in Figures (5-1) and (5-2). Both figures show that the oil pressure increases with increasing the values of the permeability of the porous materials. This can be postulated to the increases of the oil flow out of the permeable surfaces as the permeability of the porous material increases. This seems to be the same behavior of the porous bearing, as reported by some workers **[7].**

Figures (5-3) to (5-6) show the effect of the ring – bearing eccentricity ratio and the journal – ring eccentricity ratio on the oil pressure build up in both films.These figures show that the oil pressure increases with increasing the values of the eccentricity ratios, as expected. Both ends of the oil curves, at which the oil – films pressure becomes zero, correspond to the locations of the inlet and trailing ends of the continuous film regions (θ_1 and θ_2).

Using the improved boundary conditions in this study yields negative oil – film pressures in the region before the trailing end.

The effect of the supply pressure on the pressure distribution of the journal – ring and ring – bearing oil films is represented in Figures (5-7) to (5-10). All these figures show that, increasing the supply pressure yields a higher peak pressure in the positive oil film pressure in both oil films and a higher oil films extent. This can be proposed to the higher oil flow out of the porous material with increasing the values of the supply pressure.

The effect of clearance ratio on the oil film pressure of both oil films can be shown by Figures (5-11) to (5-13). These figures show that the oil extent increases with increasing the values of the clearance ratio. Also, they show that the peak of pressure increases with increasing the values of the clearance ratio. This is due to the increase in the oil – film extent.

Under the same working conditions the peak of the oil film pressure increases as the radii ratio decreases as shown in Figures (5-14) to (5-16). Also, it can be shown from these figures that the peak of oil film pressure increases with increasing the value of the eccentricity ratio. This can be explained by knowing that the ring speed becomes higher for rings of lower radii ratios.

The relation between the ring – bearing eccentricity ratio (ε_2) and the journal – ring eccentricity ratio (ε_1) for a bearing with different values of ring and bearing permeabilities is presented in Figure (5-17). These figure shows that the journal – ring eccentricity ratio is greater than the ring – bearing eccentricity ratio for the porous material permeability (1.9E-13 m^2), while for the permeability lower than (8.98E-14 m^2), the journal – ring eccentricity ratio becomes lower than the ring – bearing eccentricity ratio,

this is true in order to maintain the two regions, journal – ring and ring – bearing hydrodynamically lubricated.

The effect of clearance ratio on the relation between the ring – bearing eccentricity ratio (ε_2) and the journal – ring eccentricity ratio (ε_1) is presented in Figure (5-18). It can be shown from this figure that for higher clearance, namely $c_1/c_2 > 1.75$ the ring – bearing eccentricity ratio become lower than the journal – ring eccentricity ratio, while for $c_1/c_2 < 1.6$ the ring – bearing eccentricity ratio becomes greater than the journal – ring eccentricity ratio, this is true in order to maintain the equilibrium conditions of the bearing and to ensure that the bearing hydrodynamically lubricated.

The correlation between the ring – bearing and the journal – ring eccentricity ratios is affected by the radii ratio as shown in Figure (5-19). It is clear that the ring – bearing eccentricity ratio becomes lower than the journal – ring eccentricity ratio for a bearing with a ring of radii ratio is less than (1.25) while, the ring – bearing eccentricity ratio become greater than the journal – ring eccentricity ratio for a ring with a radii ratio grater than (1.25). This is true to maintain the steady state performance of the bearing. Also the ring speed becomes greater as the radii ratio decreases which make (ε_1) greater than (ε_2) in this case.

In all of the above cases, the limit value of the ring – bearing and the journal – ring eccentricity ratios are equal to unity which indicates that failure in any lubricant film will account to failure in the other, producing metal to metal contact condition.

The speed ratio N_r/N_j , which is the ratio of the rotational speed of the ring to that of the journal is plotted against Sommerfeld number as shown in figures (5-20), (5-21) and (5-22). For a specified value of Sommerfeld

number the speed ratio increases as the clearance ratio decreases, indicating that the increase in ring rotational speed becomes higher as the ring becomes closer to the journal (See Figure (5-20)). Also, the oil flow from the clearance gap becomes larger with increasing the clearance which increases the oil film extent. Figure (5-20) also, shows that the speed ratio increases with increasing the values of Sommerfeld number which indicates the dependences of the induced ring speed on the frictional forces acting on the inner and outer ring surfaces. The ring speed is greatly enhanced by the ring dimensions as shown in Figure (5-21). It is clear from this figure that for a given Sommerfeld number the speed ratio increases with decreasing values of radii ratio, i.e. for lighter ring. Also, this figure indicates that the speed ratio increases with increasing values of the Sommerfeld number which indicates the depends of the induced ring speed on the applied load. The supply pressure seems to have lower effect on the speed ratio as shown in Figure (5-22). It can be shown from this figure that slight increase in speed ratio with decreasing the values of the supply pressure is due to the increase in friction force applied to the both sides of the ring in this case.

The effect of different operating parameters on the oil – film extent can be shown in Figures (5-23) to (5-30). These figures show the variation of oil film extent with Sommerfeld number. In all these figures the curves in the range $\theta < 180$ deg. correspond to the inlet end of the film extent (θ_1) while those in the range $\theta > 180$ deg. correspond to the trailing end (θ_2).

The effect of permeability of the porous material on the oil – film extent can be shown in Figure (5-23). It is clear from this figure that the oil film extent increases with increasing the values of the permeability of the porous matrix since the oil flow from the porous matrix would generally be higher for large values of permeability. Also, it can be shown from this

figure that the oil extent increases with increasing the values of Sommerfeld number, this is due to the decrease of the oil leakage into the porous matrix because of the reduction in the magnitude of the hydrodynamic pressure generated in the film. The same thing can be said about Figure (5-24); which shows that the oil – film extent increases for higher values of ring permeability.

The effect of the oil supply pressure on the oil – film extent can be shown in figures (5-25) and (5-26). The oil – film extent increases with increasing values of supply pressure, since the oil flow into the clearance gap increases in this case. Furthermore, increasing Sommerfeld number mainly decreases the oil leakage into the porous matrix due to the reduction in the magnitude of hydrodynamic pressure generated in the oil film, hence the oil film extent increases.

Also, the oil – film extent increases with increasing values of clearance ratio as shown in Figures (5-27) and (5-28). For a given eccentricity ratio, higher oil flow through the clearance is obtained in this case. The oil – film extent increases with the Sommerfeld number as explained before.

The effect of the ring dimension on the development of oil extent can be shown in Figures (5-29) and (5-30). The higher values of the radii ratio of the ring are the lower oil – film extent. The narrow oil gap causes a small oil flow through the clearance gap which leads to lower values of oil – film extent.

Figures (5-31) and (5-32) represent the variation of friction coefficient with the Sommerfeld number. These figures show that the friction coefficient increases with higher values of permeability of the porous ring

and the bearing. Also, it can be shown from these figures that the value of the Sommerfeld number which gives the minimum friction decreases with decreasing the values of the permeabilities. This is attributable to the fact that decease in permeability allows the system to operate under hydrodynamic lubrication conditions.

The effect of supply pressure on the coefficient of friction for both oil films can be shown in figures (5-33) and (5-34). Referring to these figures, it is clear that the values of Sommerfeld number which gives the minimum friction decreases with increasing the values of the supply pressure. This is due to the fact that the angular oil – film extent increases with increasing the values of the supply pressure which allows the system to work under the hydrodynamic lubrication condition. The same thing can be said about the effect of clearance ratio on the friction coefficient as shown in Figures (5-35) and (5-36). These figures show that the coefficient of friction decreases with increasing the values of clearance ratio since the higher values of clearance ratio allow the bearing to work under the hydrodynamic lubrication condition as shown before.

The effect of the ring dimensions on friction coefficient can be shown in figures (5-37) and (5-38). These figures show that the minimum value of Sommerfeld number which give the minimum value of the coefficient of friction decreases with decreasing the values of radii ratio. This can be explained by referring to Figure (5-30) which shows that the bearing works under the hydrodynamic lubrication condition for the rings have lower values of the radii ratio.

Figures (5-39) to (5-44) represent the variation of the coefficient of friction with different values of the eccentricity ratio under different

parameters mentioned before. Again it can be shown from these figures that the minimum value of the coefficient of friction occurred at higher eccentricity ratio when the system works under the hydrodynamic lubrication condition.

The effect of permeability parameter on the attitude angle can be shown in Figures (5-45) and (5-46). It is clear that the attitude angle increases with increasing the values of the permeability parameter when the bearing works under the same conditions. This is owing to an increase in the amount of the oil supplied to the clearance of the bearing through the porous matrix.

The same effect can be obtained when the bearing works under different supply pressure as shown in Figures (5-47) and (5-48). It can be shown from these figures that the attitude angle increases with increasing the values of the supply pressure. This is attributed to the fact that the oil – film extent increases with increasing the values of the supply pressure which allows the bearing to work under the hydrodynamic lubrication condition. This suggests that the effect of the permeability parameter is qualitatively corresponds to those of the supply pressure as obtained in reference **[7]**.

The attitude angle also increases with increasing the values of the clearance ratio of the bearing as shown in Figure (5-49) since the increase of the clearance causes larger oil – film extent as previously shown. The effect of the ring dimension on the attitude angle can be shown in Figure (5-50). This figure shows that the attitude angle increases with decreasing values of the radii ratio of the ring. This is attributed to the fact that the oil – film extent increases with decreasing the radii ratio as has been shown before.

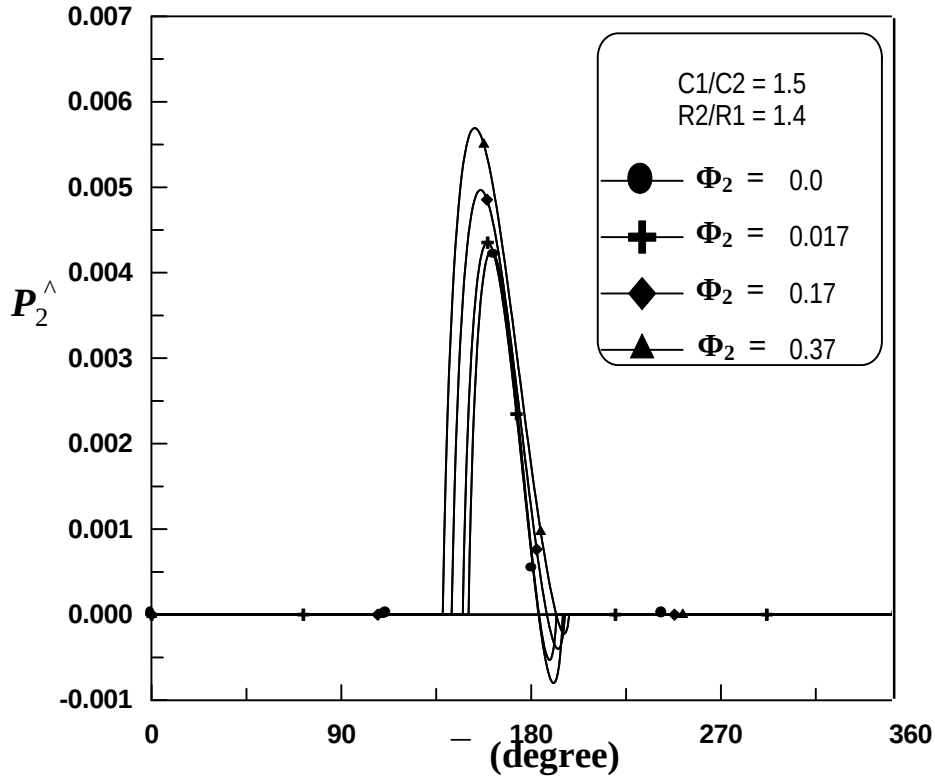

Figure (5-1), Computed Results for Circumferential Pressure Distribution in Ring – Bearing Clearance Gap for Various Values of Permeability Parameter ;($P^{\wedge}_s$ = 0.05, ε_2 = 0.3)

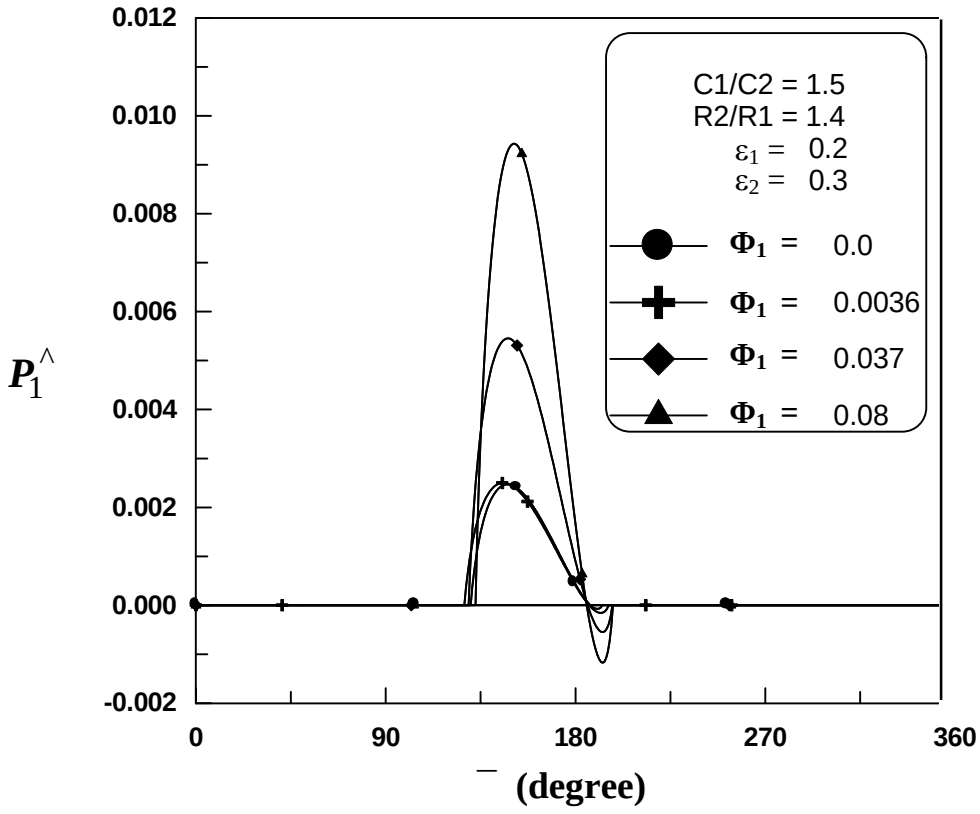

Figure (5-2), Computed Results for Circumferential Pressure Distribution in Journal – Ring Clearance Gap for Various Values of Permeability Parameter ; ($P^{\wedge}_s$ = 0.05)

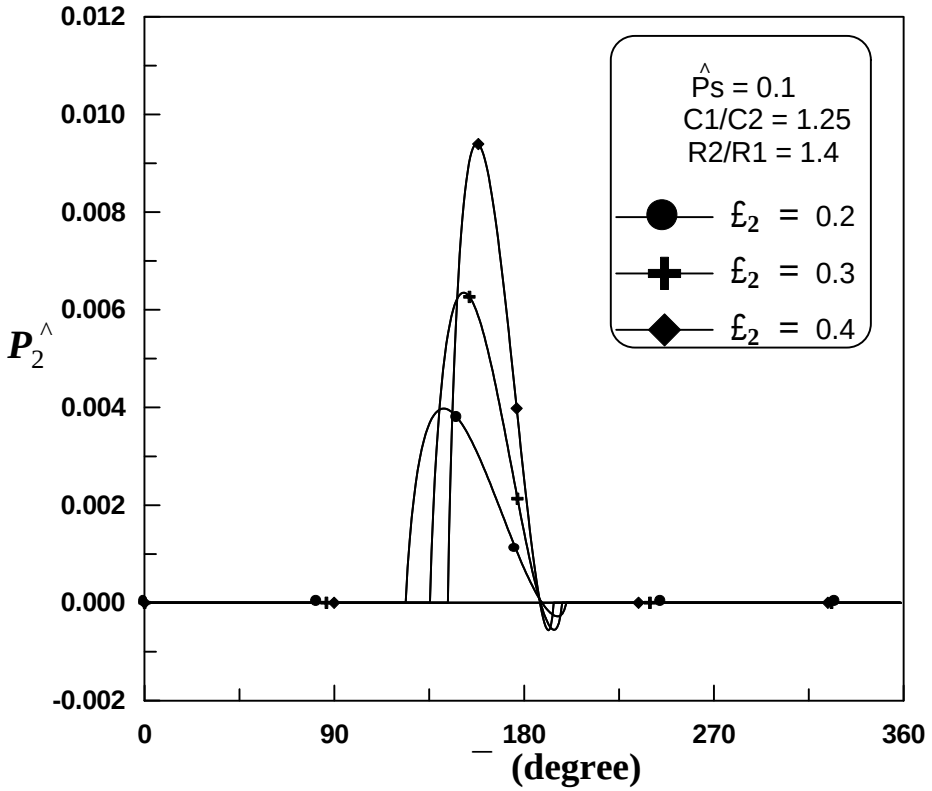

Figure (5- 3), Computed Results for Circumferential Pressure Distribution in Ring – Bearing Clearance Gap for Various Values of Ring Eccentricity Ratio.

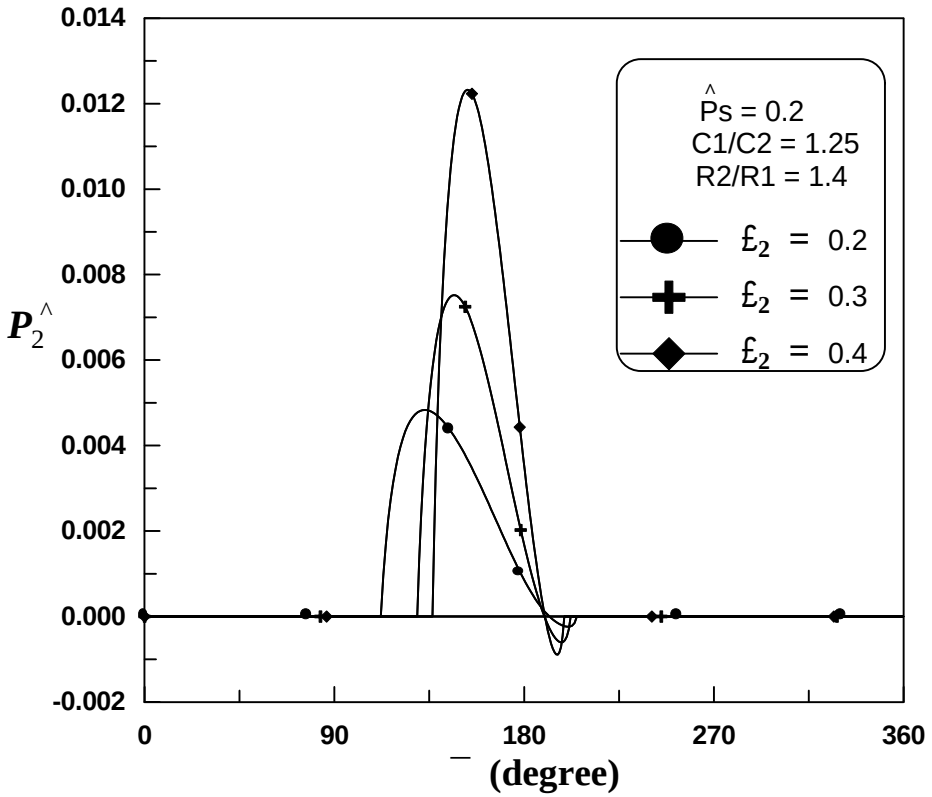

Figure (5-4),Computed Results for Circumferential Pressure Distribution in Ring – Bearing Clearance Gap for Various Values of Ring Eccentricity Ratio.

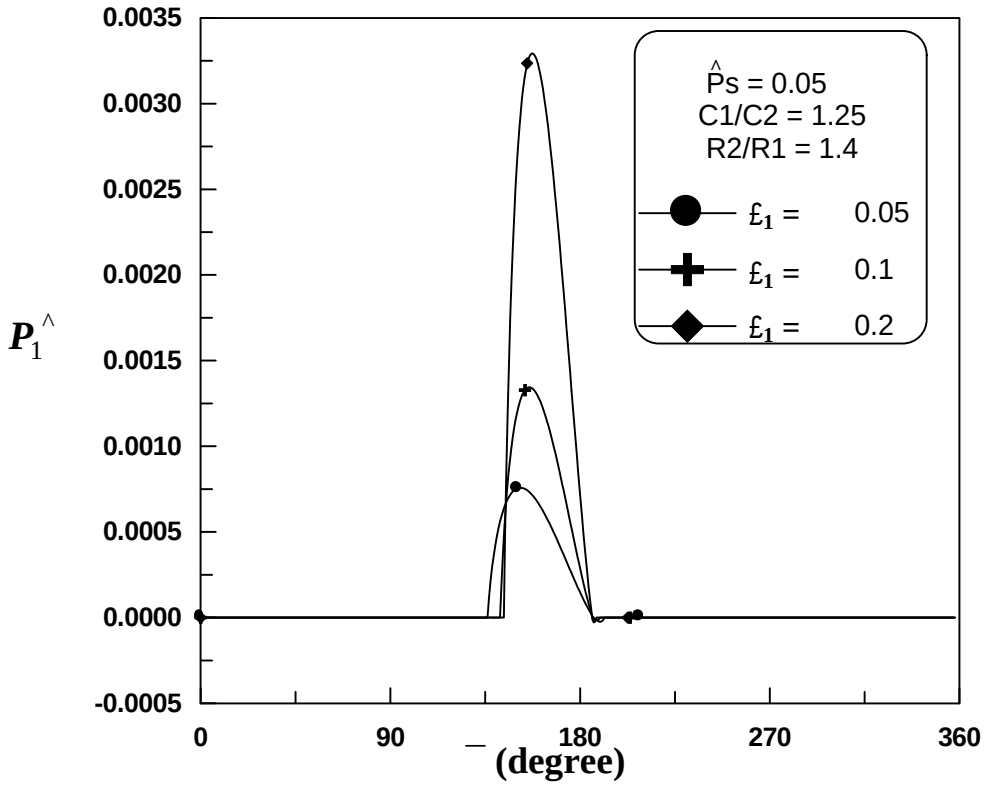

Figure (5-5), Circumferential Pressure Distribution in Journal – Ring Clearance Gap for Different Values of Journal Eccentricity Ratio.

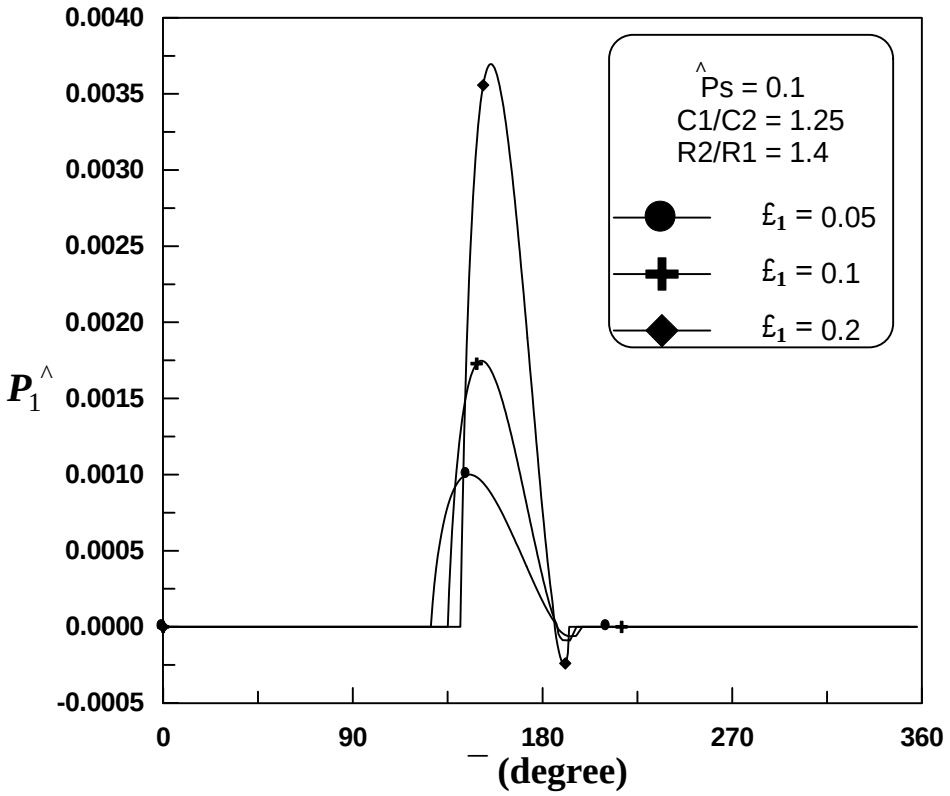

Figure (5-6), Circumferential Pressure Distribution in Journal – Ring Clearance Gap for Different Values of Journal Eccentricity Ratio.

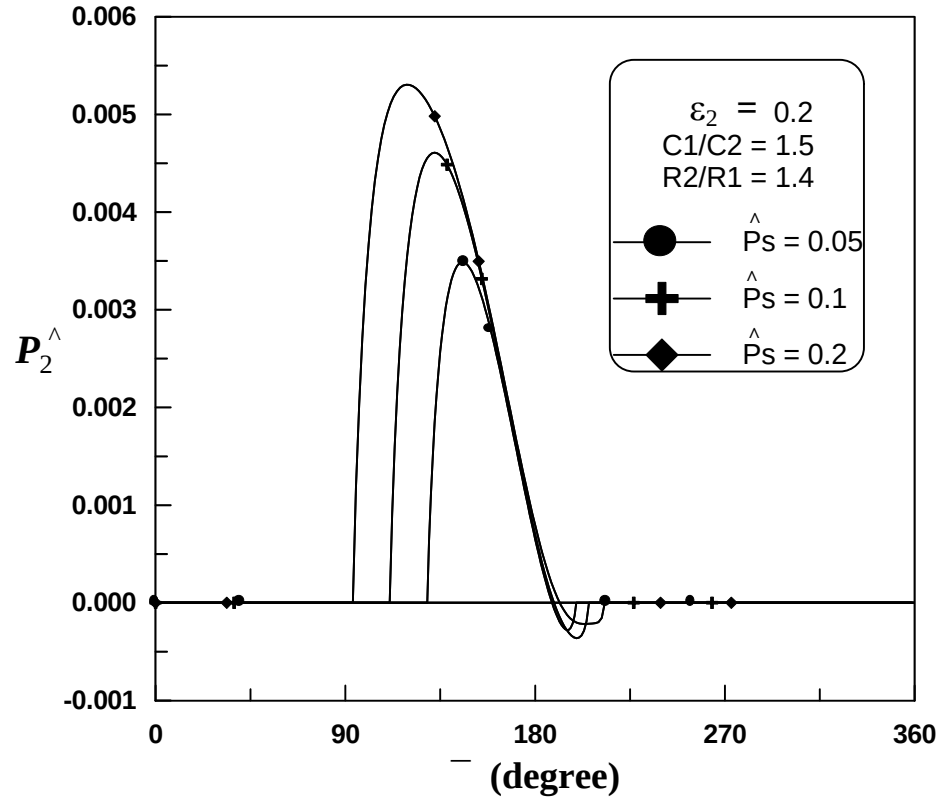

Figure (5-7),Computed Results for Circumferential Pressure Distribution in Ring - Bearing Clearance Gap for Various Values of Dimensionless Oil – Feed Pressure.

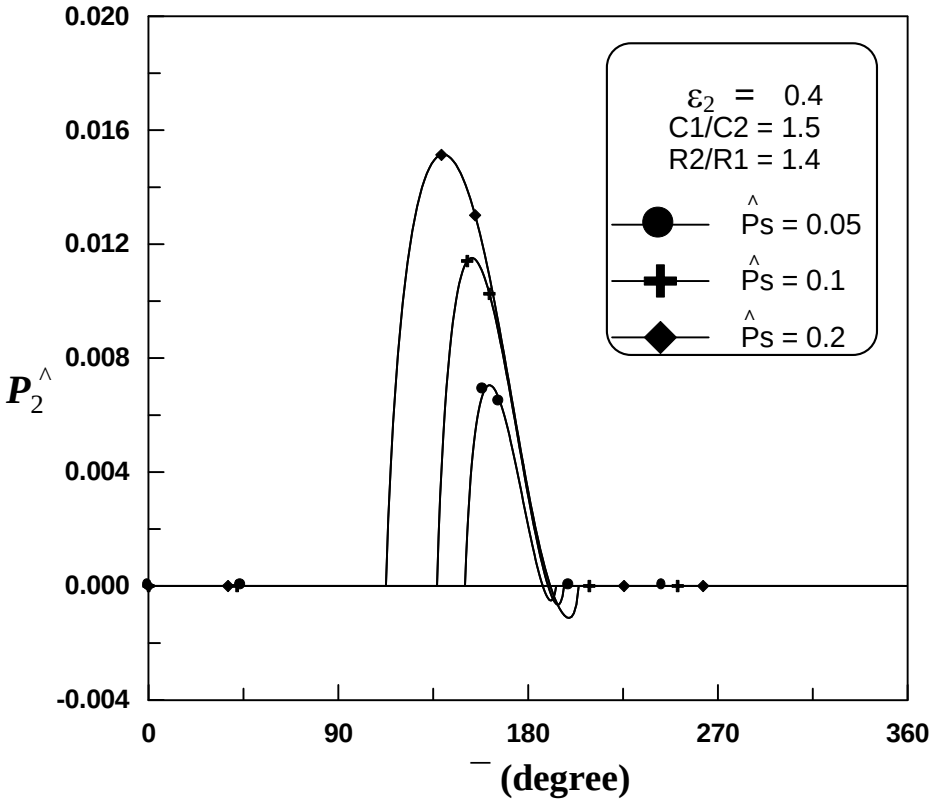

Figure (5-8),Computed Results for Circumferential Pressure Distribution in Ring - Bearing Clearance Gap for Various Values of Dimensionless Oil – Feed Pressure.

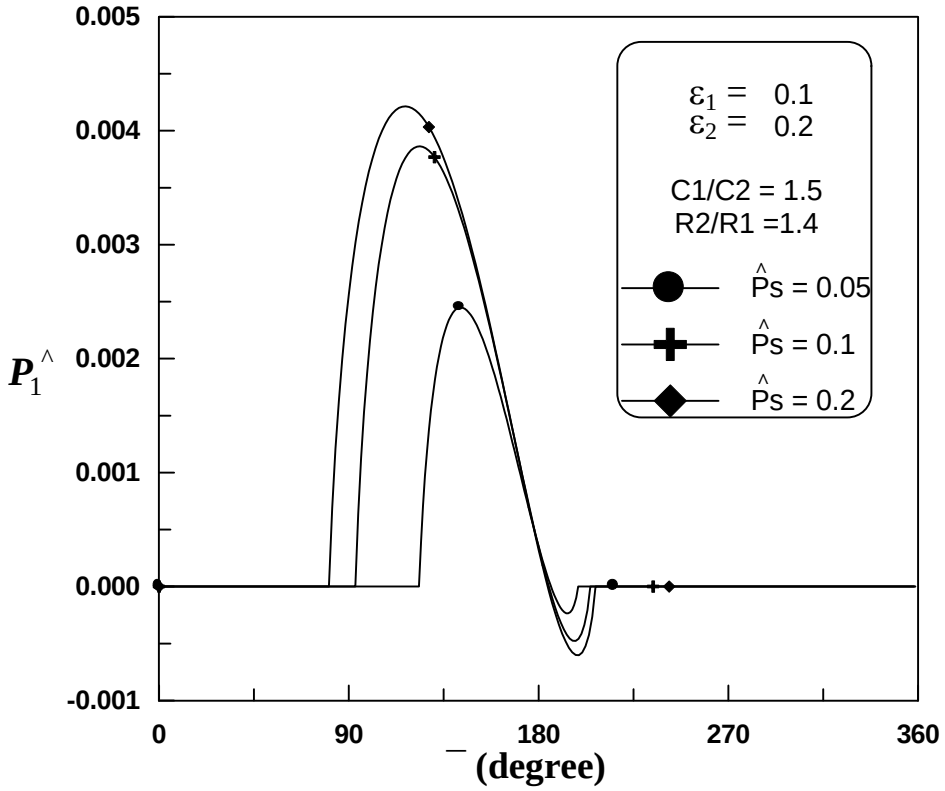

Figure (5-9), Circumferential Pressure Distribution in Journal – Ring Clearance Gap for Various Values of Dimensionless Oil – Feed Pressure.

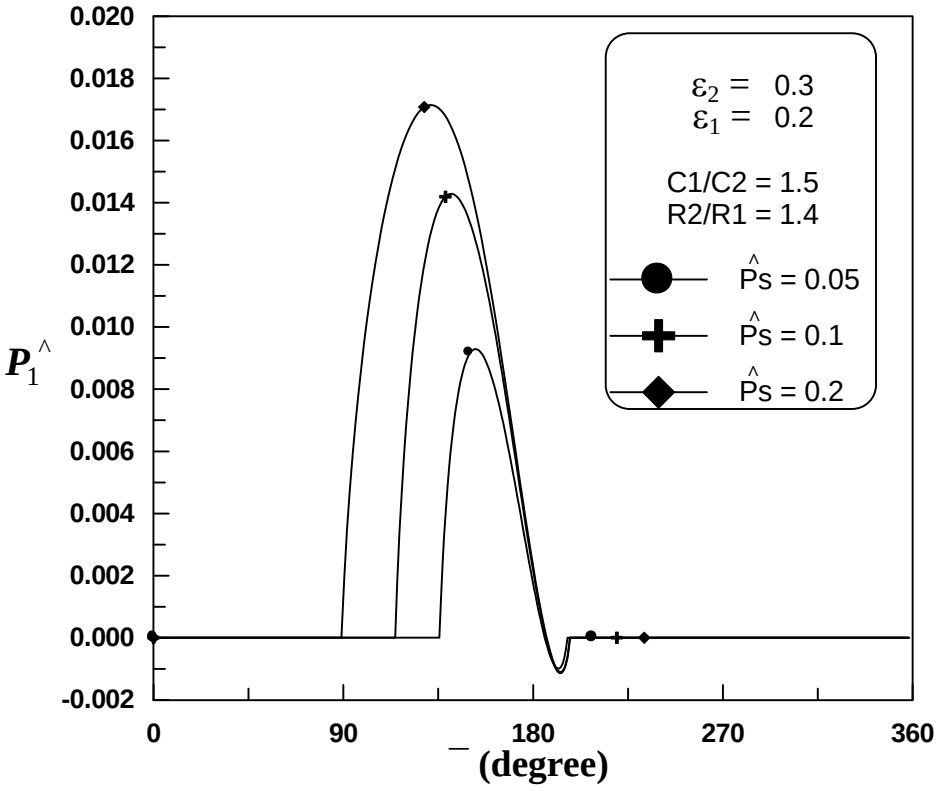

Figure (5-10), Circumferential Pressure Distribution in Journal – Ring Clearance Gap for Various Values of Dimensionless Oil – Feed Pressure.

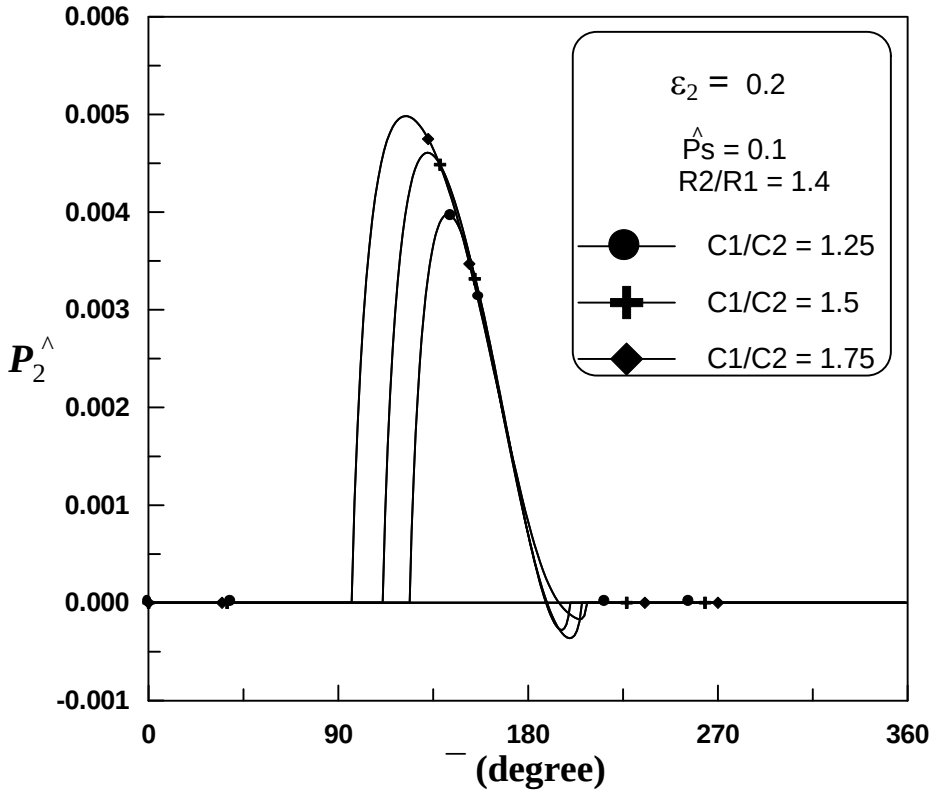

Figure (5-11), Circumferential Pressure Distribution in Ring – Bearing Clearance Gap for Various Values of Clearance Ratios.

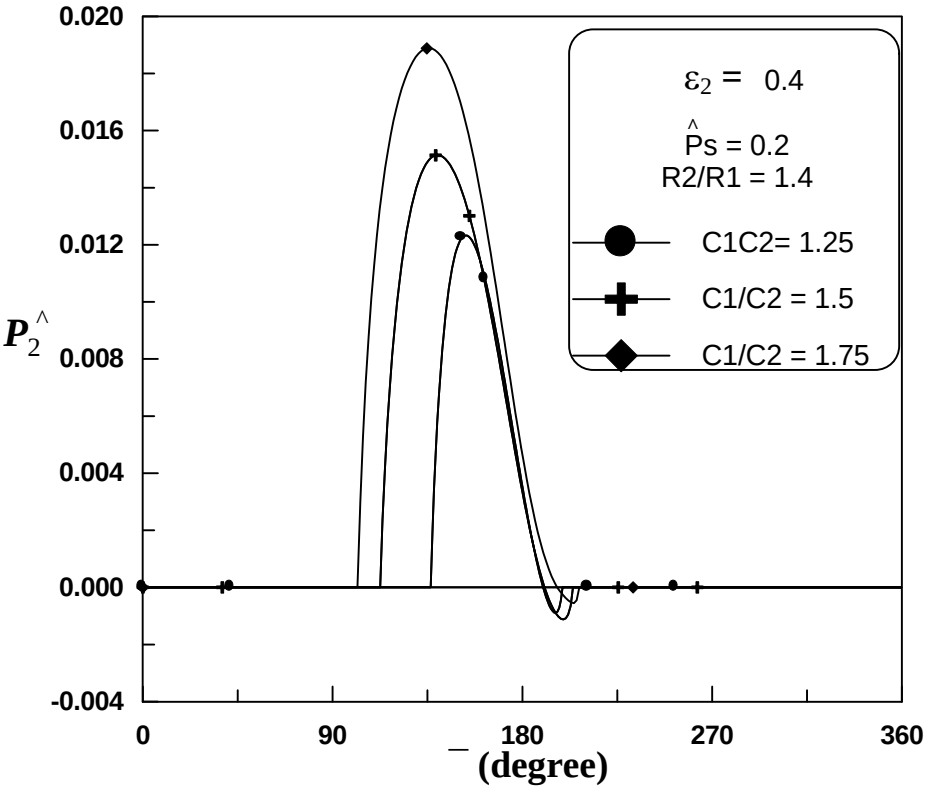

Figure (5-12), Circumferential Pressure Distribution in Ring – Bearing Clearance Gap for Various Values of Clearance Ratios.

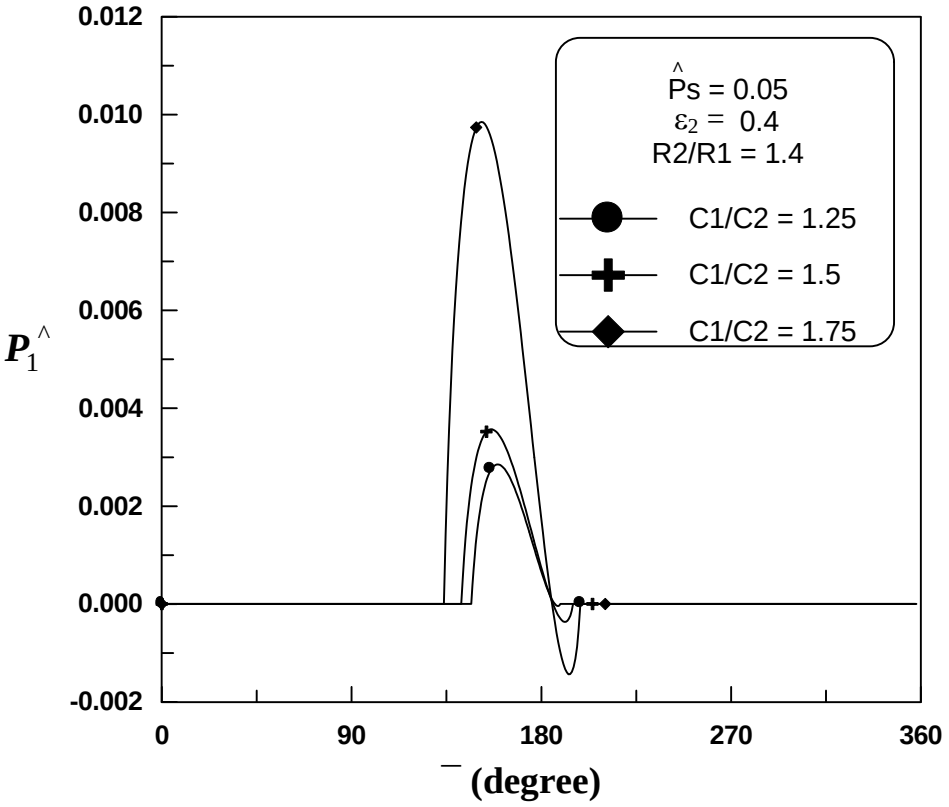

Figure (5-13), Circumferential Pressure Distribution in Journal – Ring Clearance Gap for Various Values of Clearance Ratios.

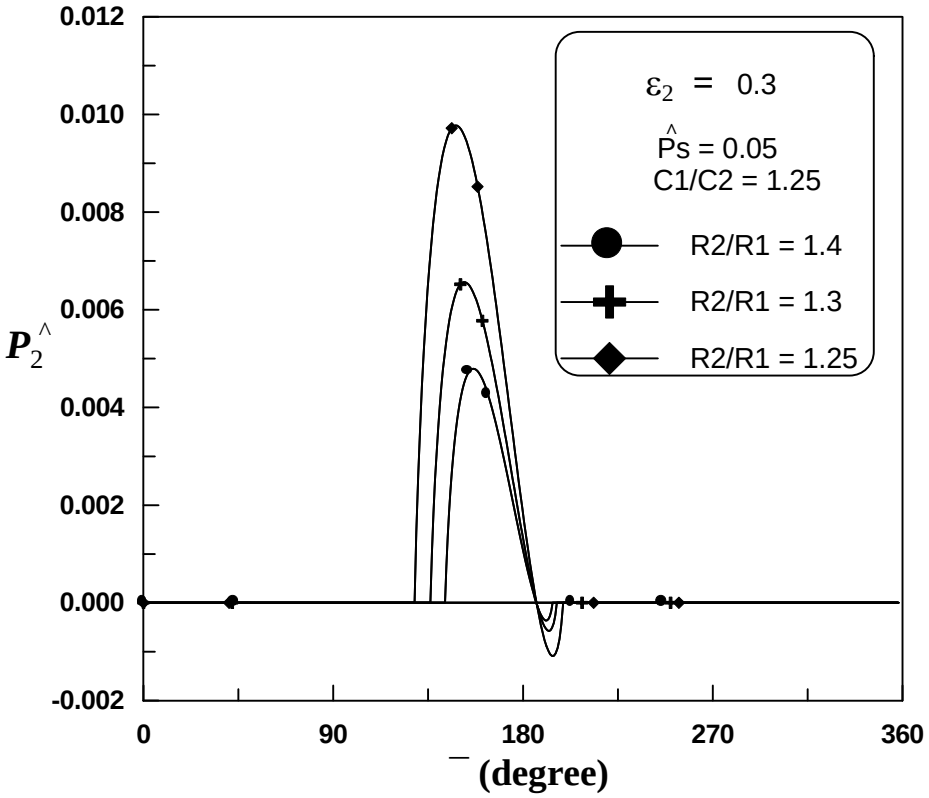

Figure (5-14), Circumferential Pressure Distribution in Ring – Bearing Clearance Gap for Different Values of Radii Ratios.

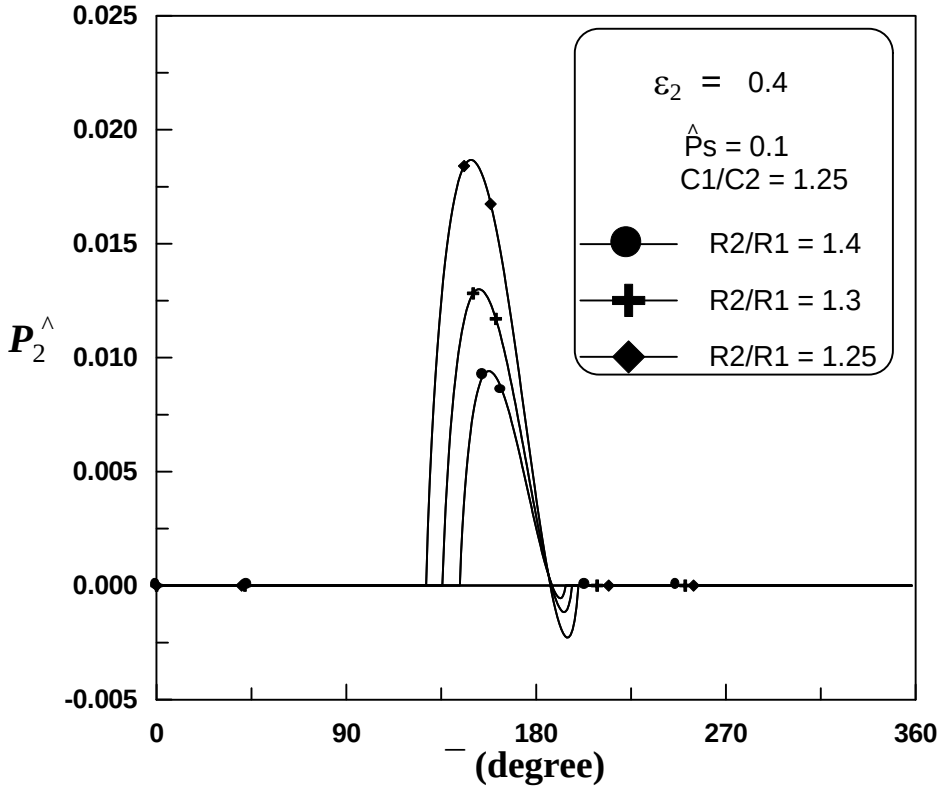

Figure (5-15), Circumferential Pressure Distribution in Ring – Bearing Clearance Gap for Different Values of Radii Ratios.

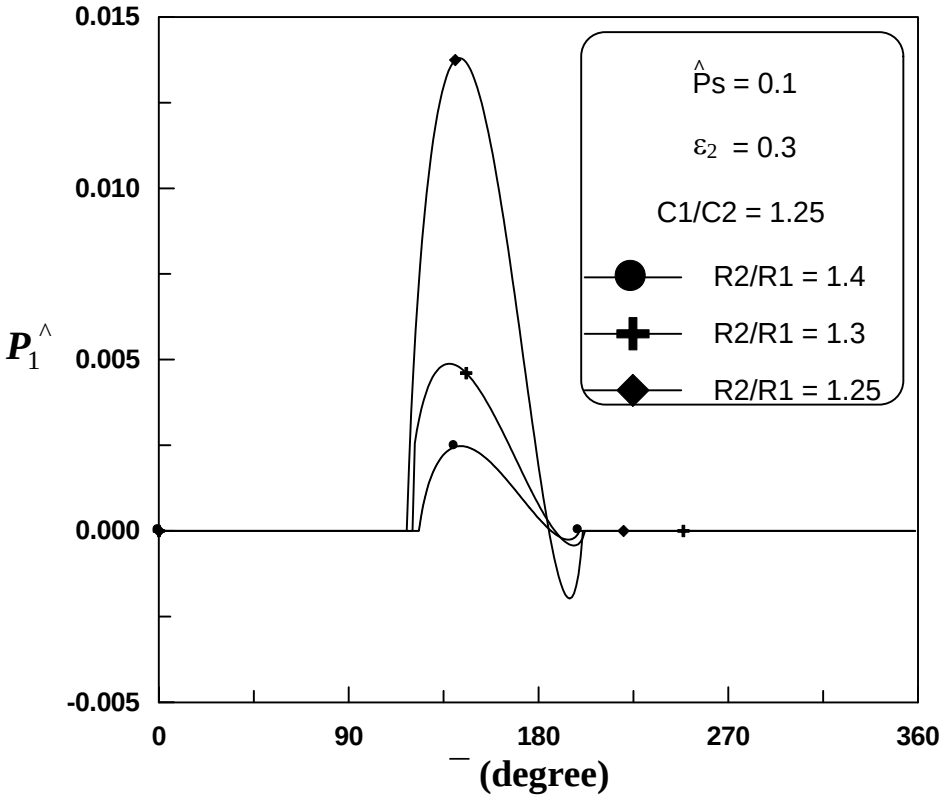

Figure (5-16), Circumferential Pressure Distribution in Journal – Ring Clearance Gap for Various Values of Radii Ratios.

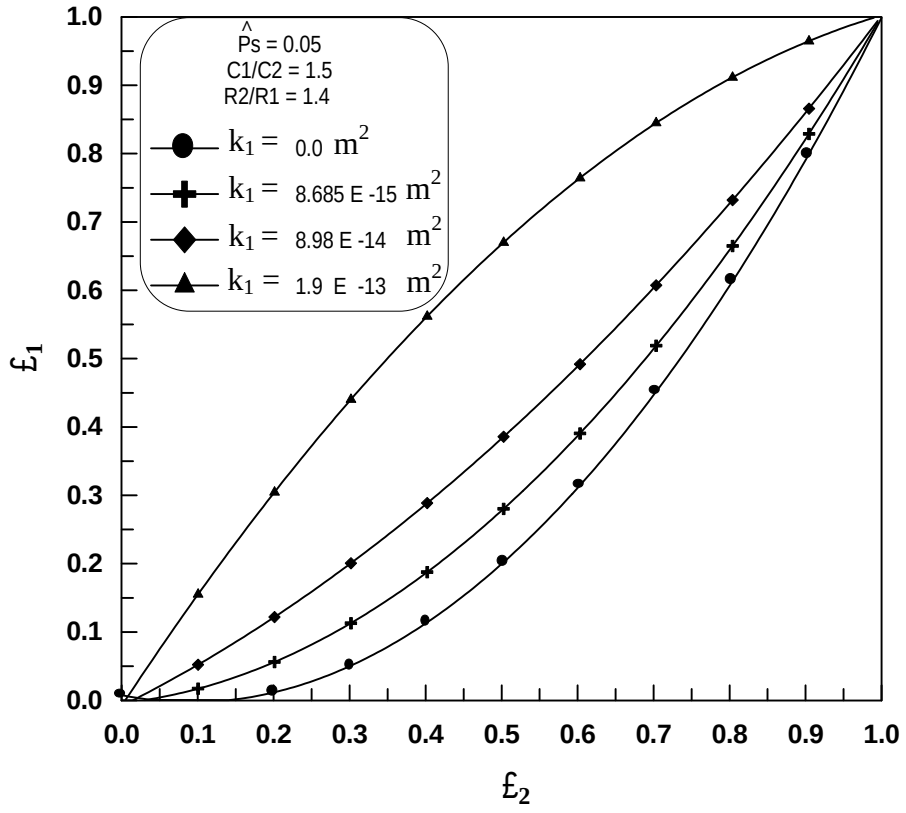

Figure (5-17),Correlation Between Journal Eccentricity Ratio **($£_1$)** and Ring Eccentricity Ratio **($£_2$)** for Various Values of Permeability.

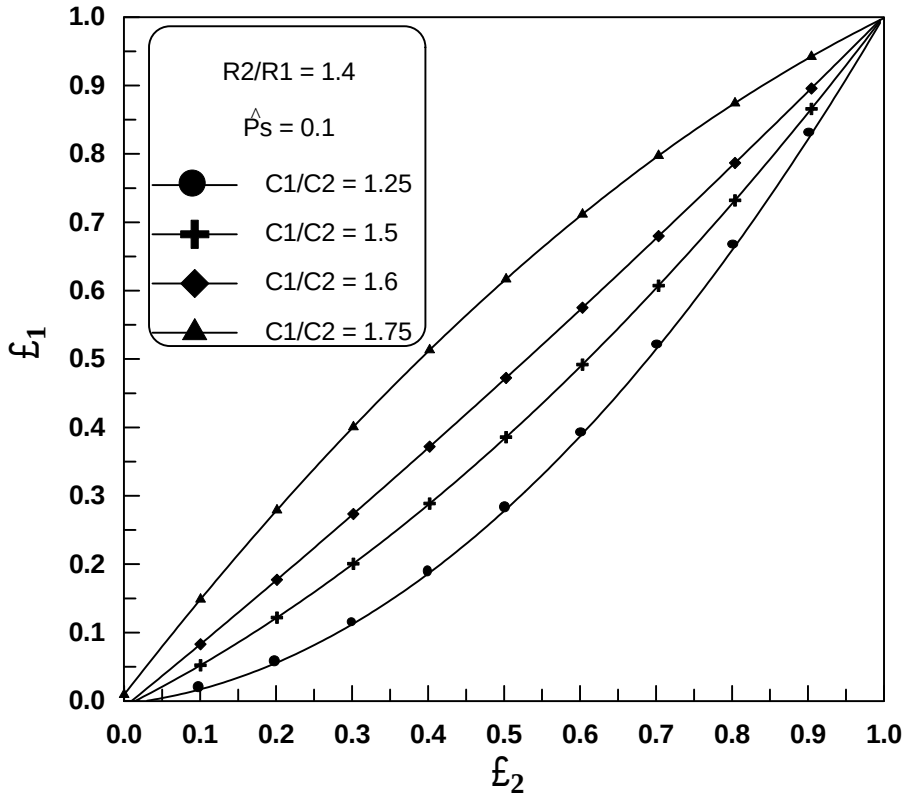

Figure (5-18), Correlation Between Journal Eccentricity Ratio **($£_1$)** and Ring Eccentricity Ratio **($£_2$)** for Various Values of Clearance Ratio.

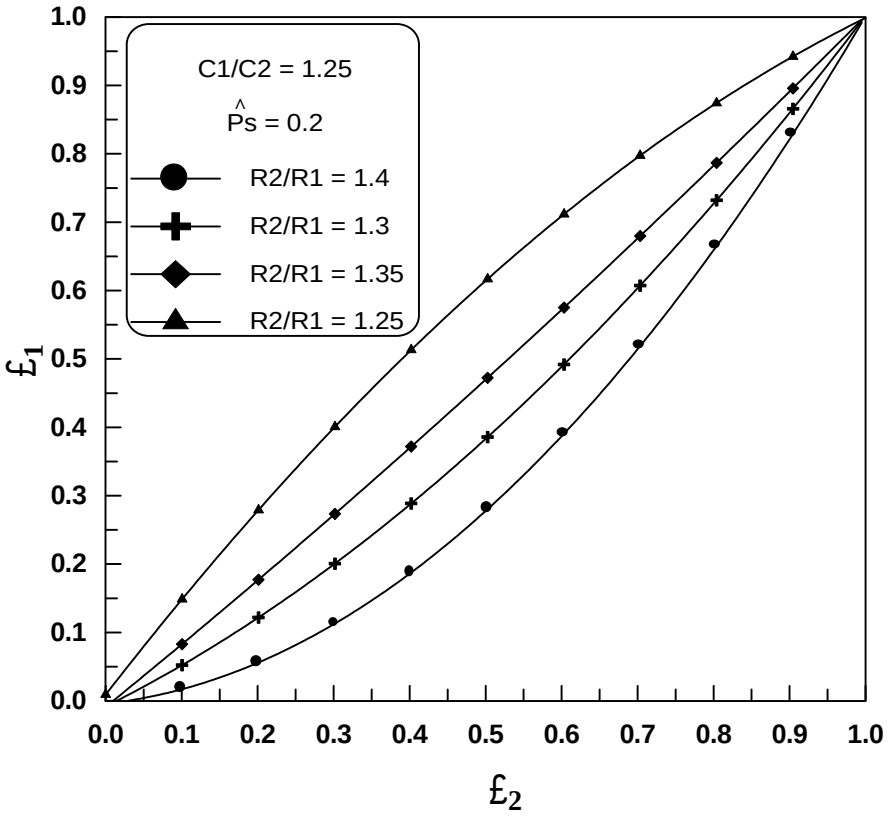

Figure (5-19), Correlation Between Journal Eccentricity Ratio **($£_1$)** and Ring Eccentricity Ratio **($£_2$)** for Various Values of Radii Ratio.

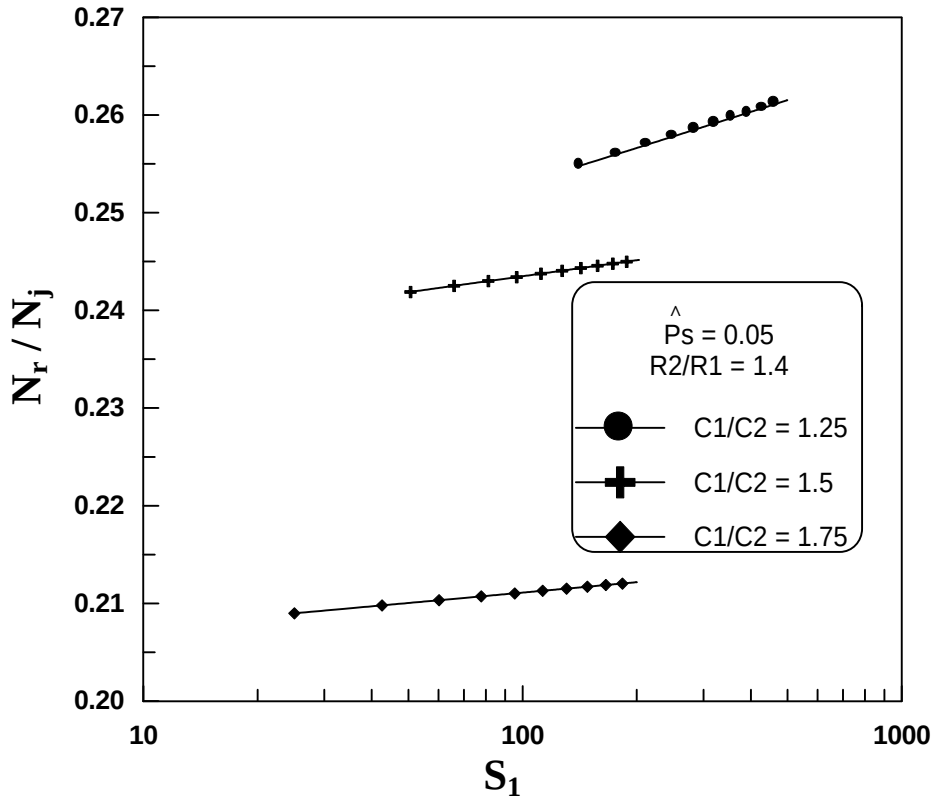

Figure (5-20), Computed Results Sommerfeld Number Versus Ring to Journal Speed Ratio for Various Values of Clearance Ratios.

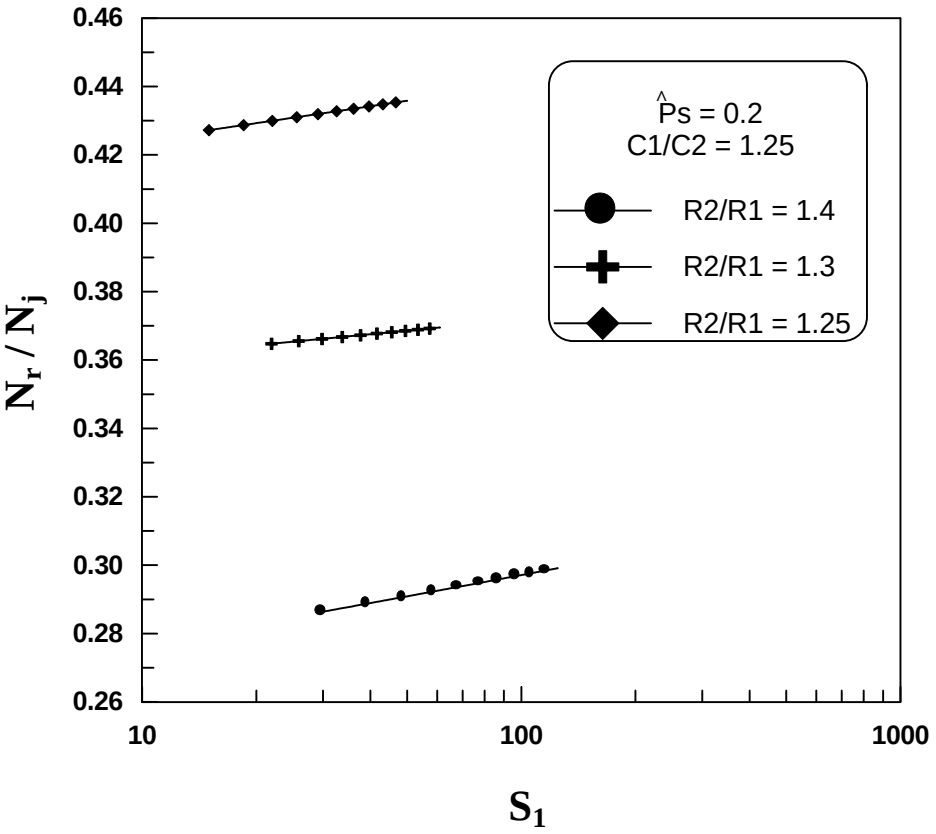

Figure (5-21), Computed Results Sommerfeld Number Versus Ring to Journal Speed Ratio for Various Values of Radii Ratios.

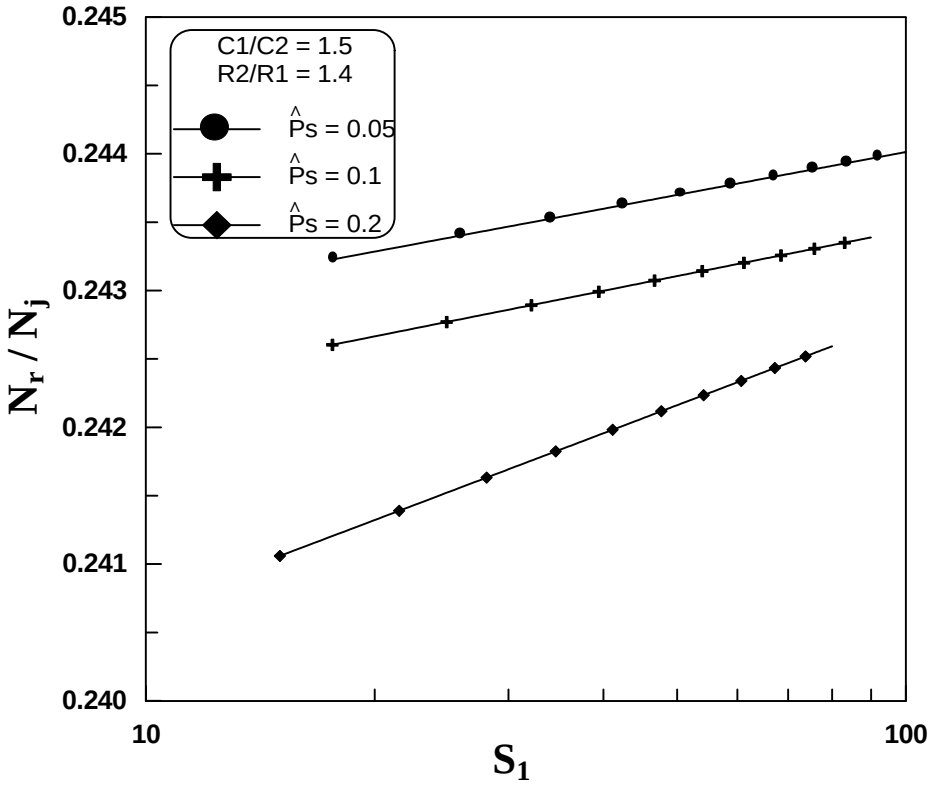

Figure (5-22), Computed Results Sommerfeld Number Versus Ring to Journal Speed Ratio for Various Values of Dimensionless Oil – Feed Pressure.

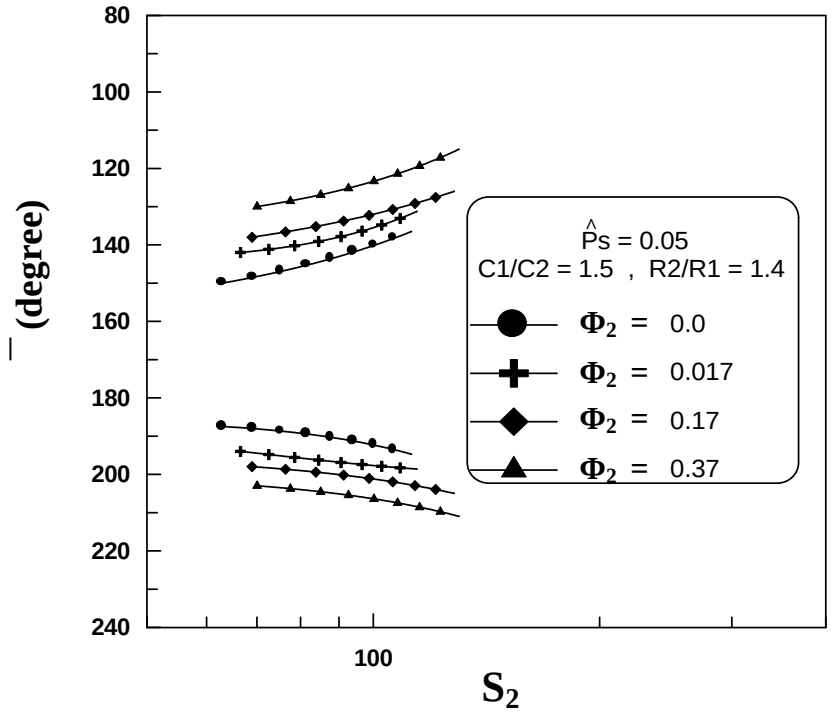

Figure (5-23), Computed Results for Outer Oil – Film Extent Versus Sommerfeld Number for Various Values of permeability parameter.

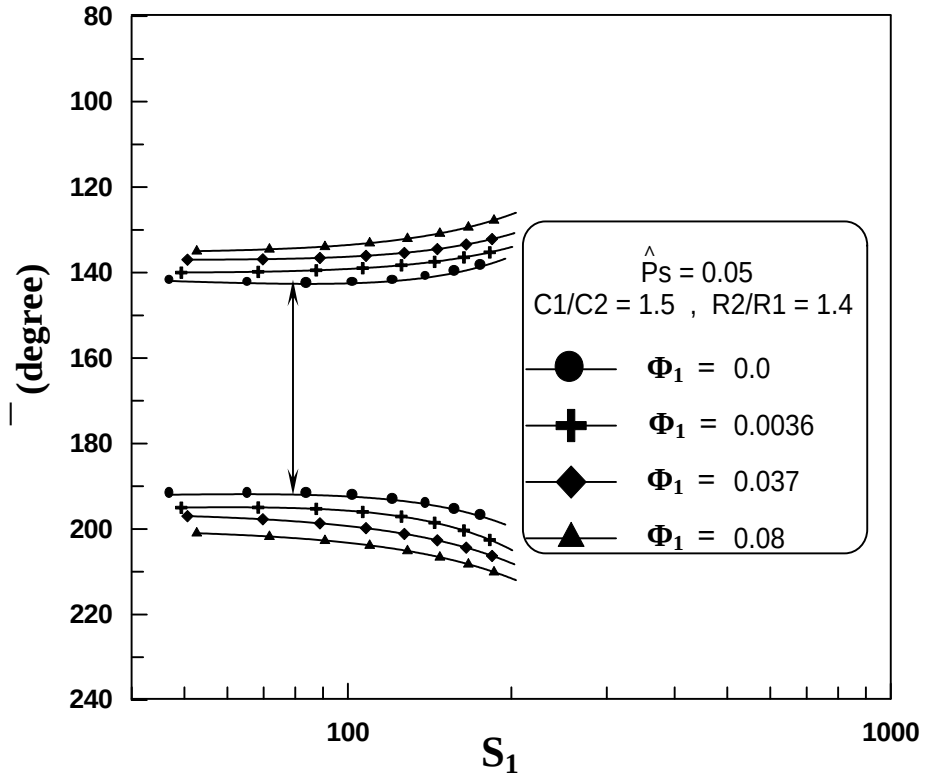

Figure (5-24), Computed Results for Inner Oil – Film Extent Versus Sommerfeld Number for Various Values of permeability parameter.

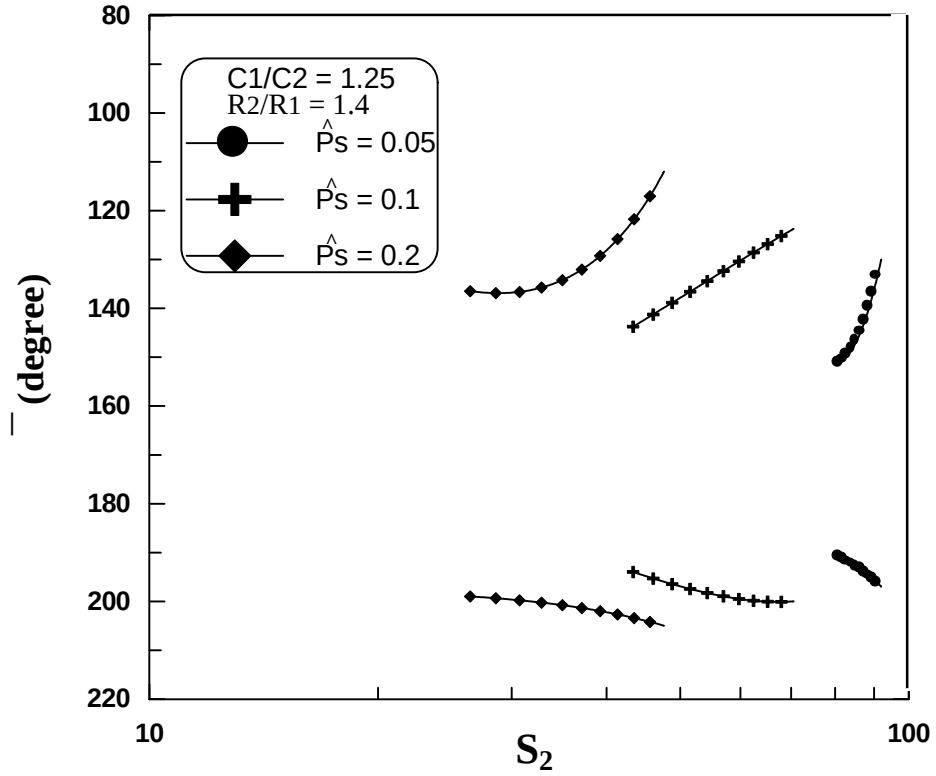

Figure (5-25), Computed Results for Outer Oil – Film Extent Versus Sommerfeld Number for Various Values of Dimensionless Oil – Feed Pressure.

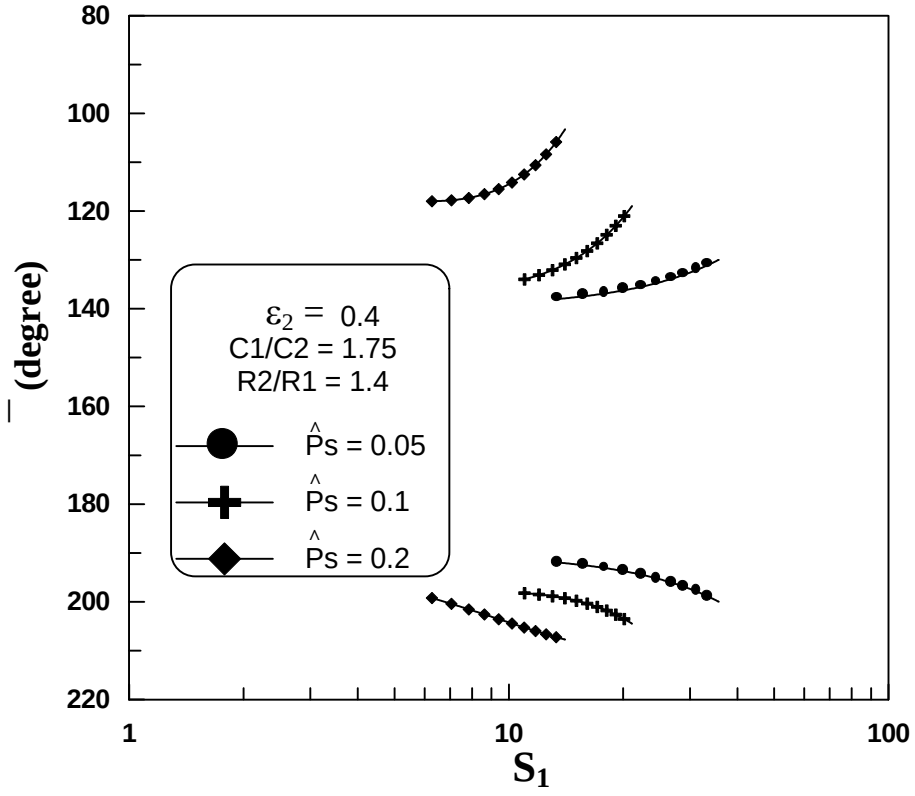

Figure (5-26), Computed Results for Inner Oil – Film Extent Versus Sommerfeld Number for Various Values of Dimensionless Oil – Feed Pressure.

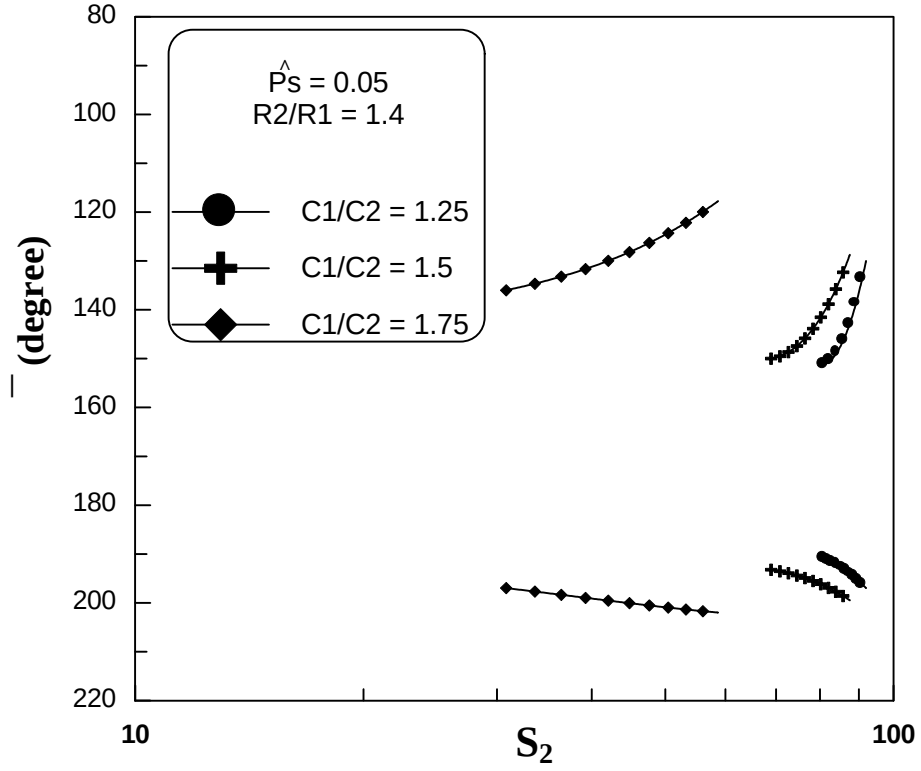

Figure (5-27), Computed Results for Outer Oil – Film Extent Versus Sommerfeld Number for Various Values of Clearance Ratios.

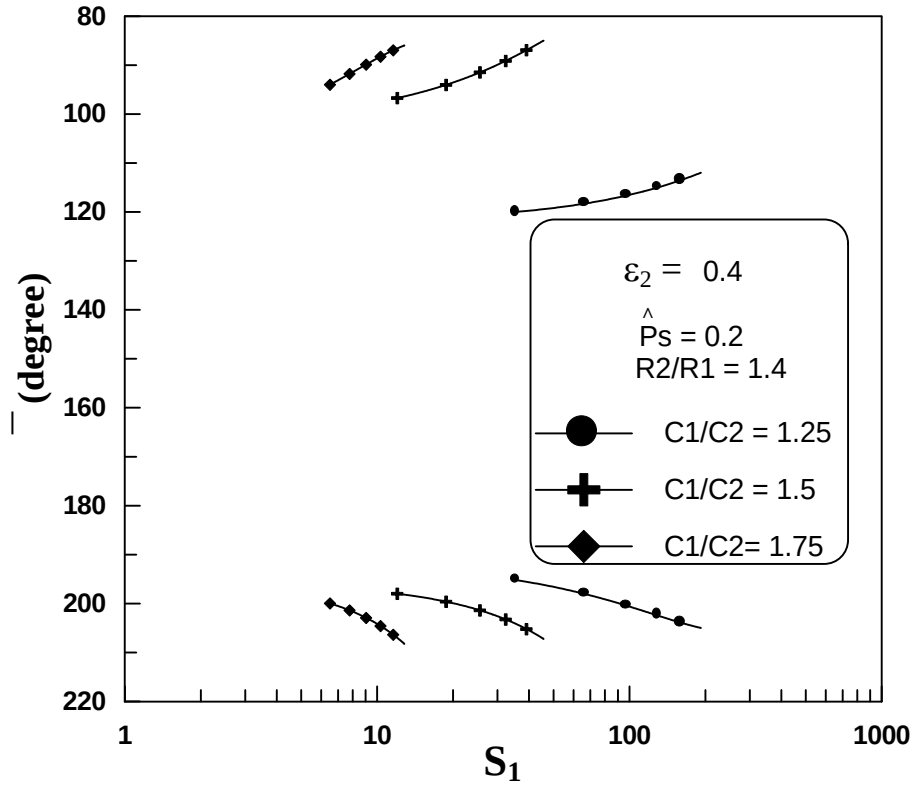

Figure (5-28), Computed Results for Inner Oil – Film Extent Versus Sommerfeld Number for Various Values of Clearance Ratios .

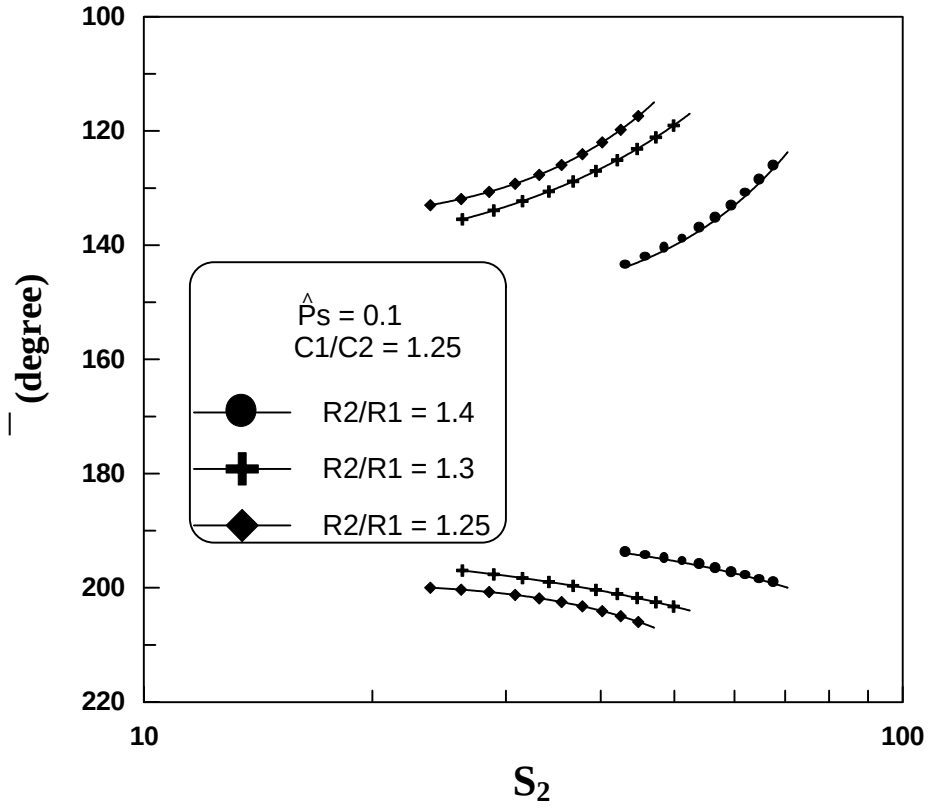

Figure (5-29), Computed Results for Outer Oil – Film Extent Versus Sommerfeld Number for Various Values of Radii Ratios.

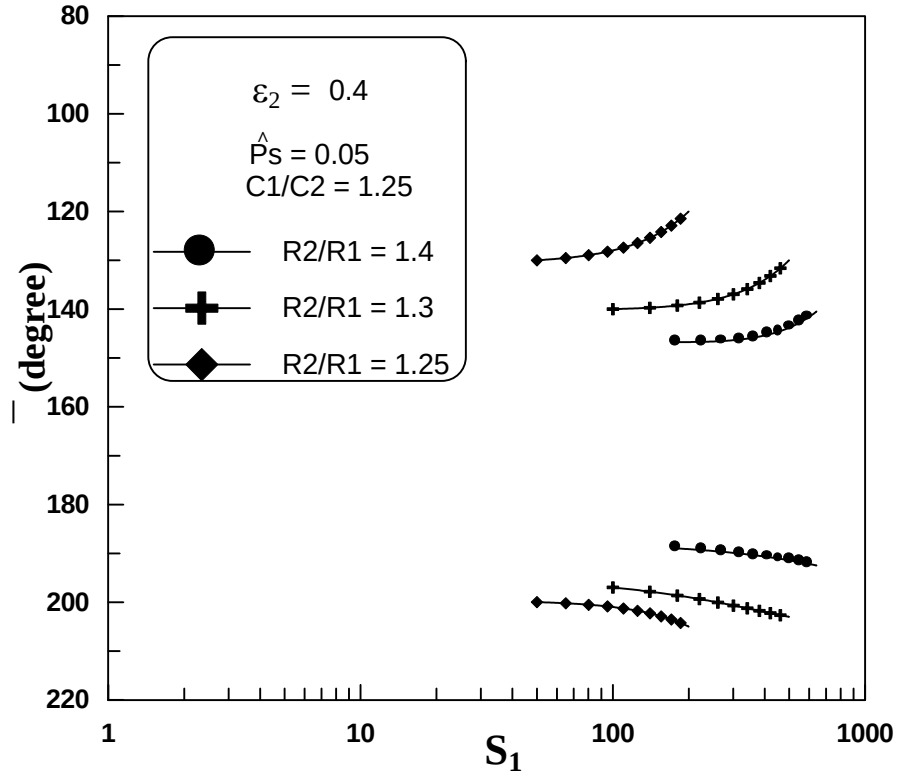

Figure (5-30), Computed Results for Inner Oil – Film Extent Versus Sommerfeld Number for Various Values of Radii Ratios.

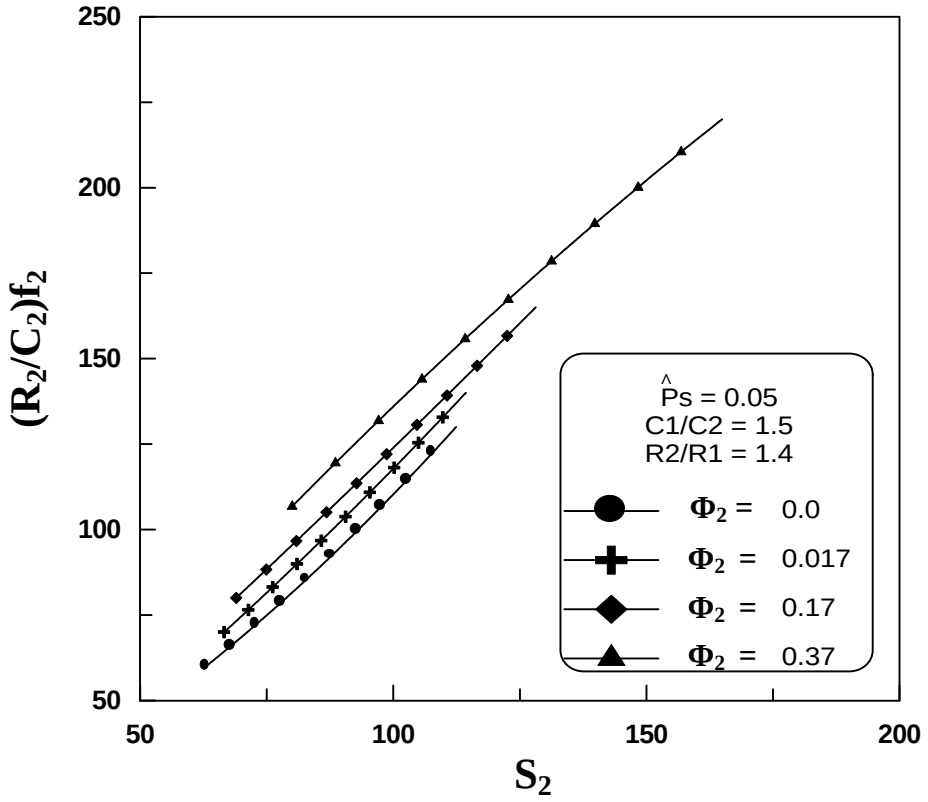

Figure (5-31), Friction Coefficient of Outer Oil – Film Versus Sommerfeld Number for Various Values of Permeability Parameter.

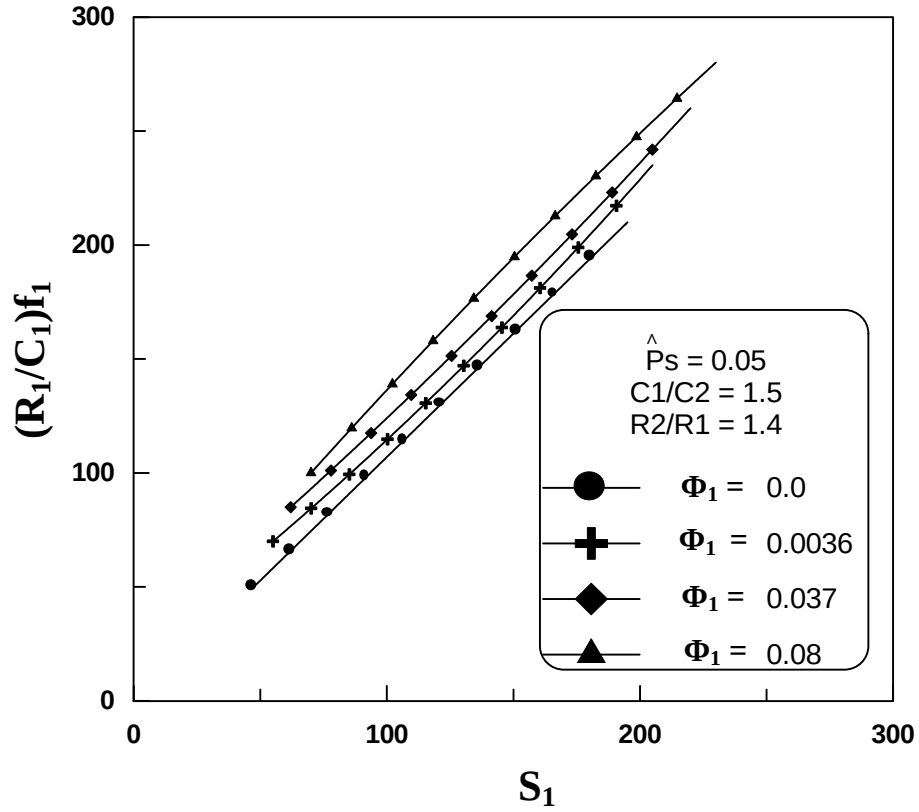

Figure (5-32), Friction Coefficient of Inner Oil – Film Versus Sommerfeld Number for Various Values of Permeability Parameter.

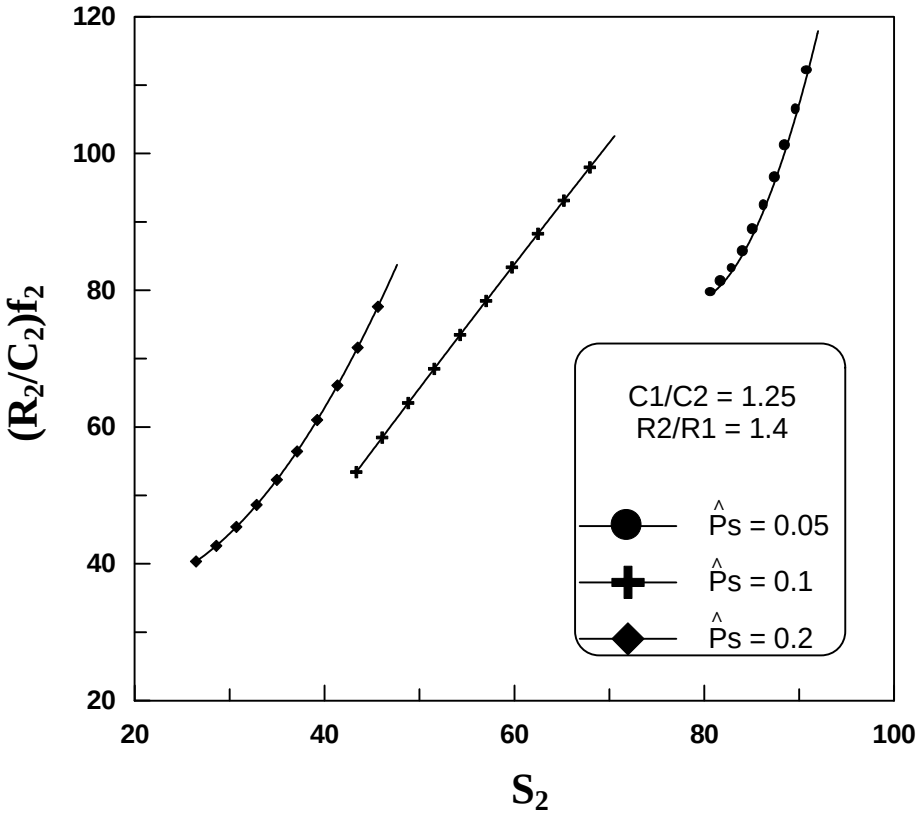

Figure (5-33), Friction Coefficient of Outer Oil – Film Versus Sommerfeld Number for Various Values of Dimensionless Oil – Feed Pressure.

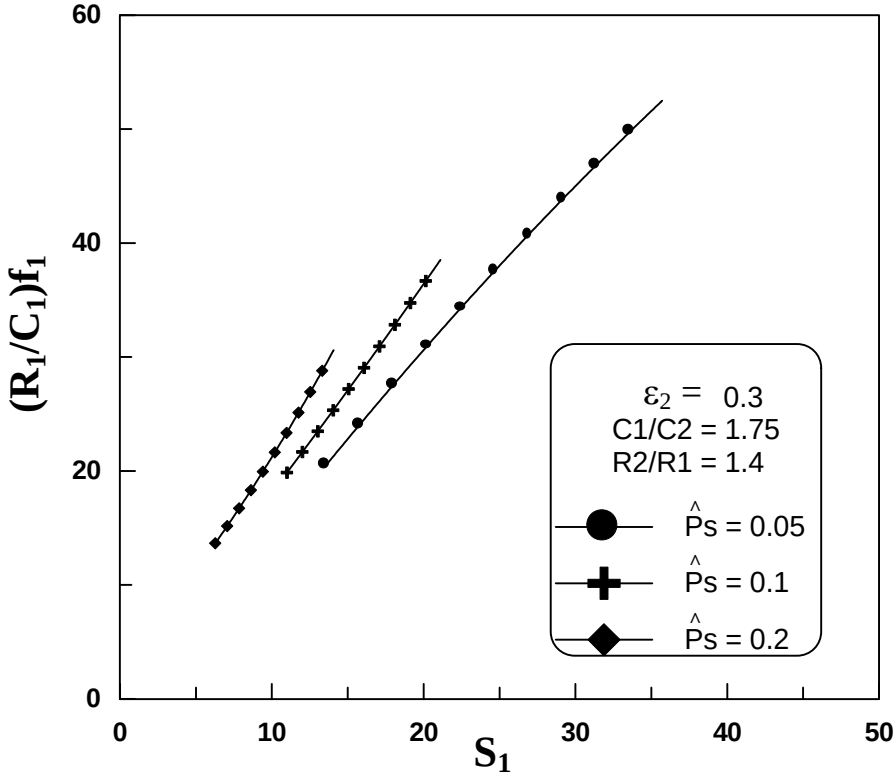

Figure (5-34), Friction Coefficient of Inner Oil – Film Versus Sommerfeld Number for Various Values of Dimensionless Oil – Feed Pressure.

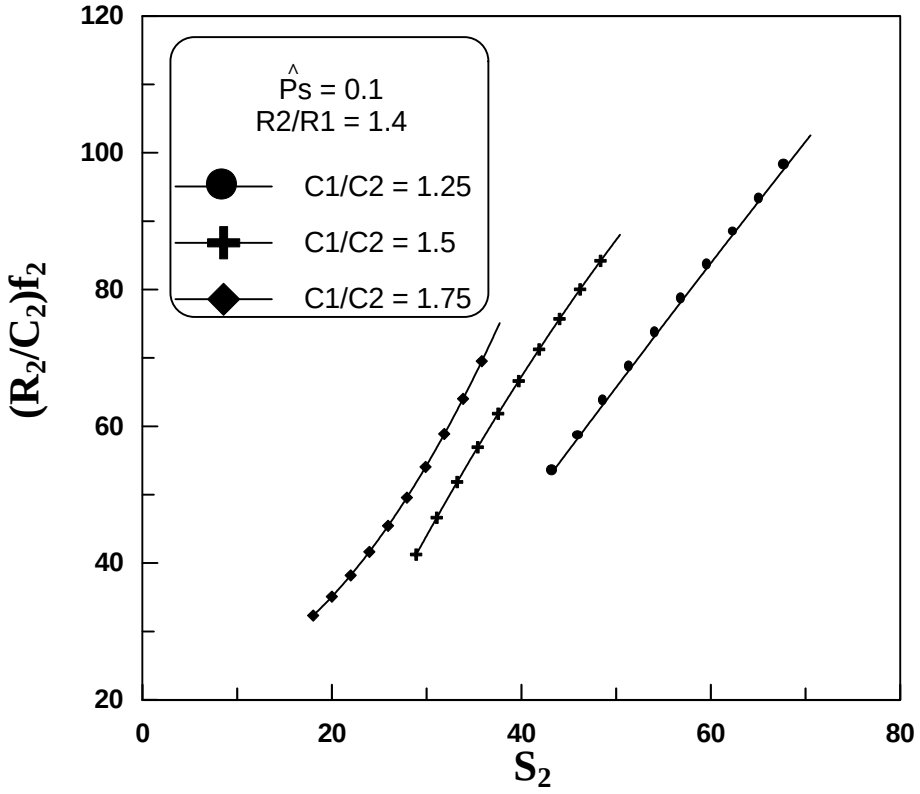

Figure (5-35), Friction Coefficient of Outer Oil – Film Versus Sommerfeld Number for Various Values of Clearance Ratios.

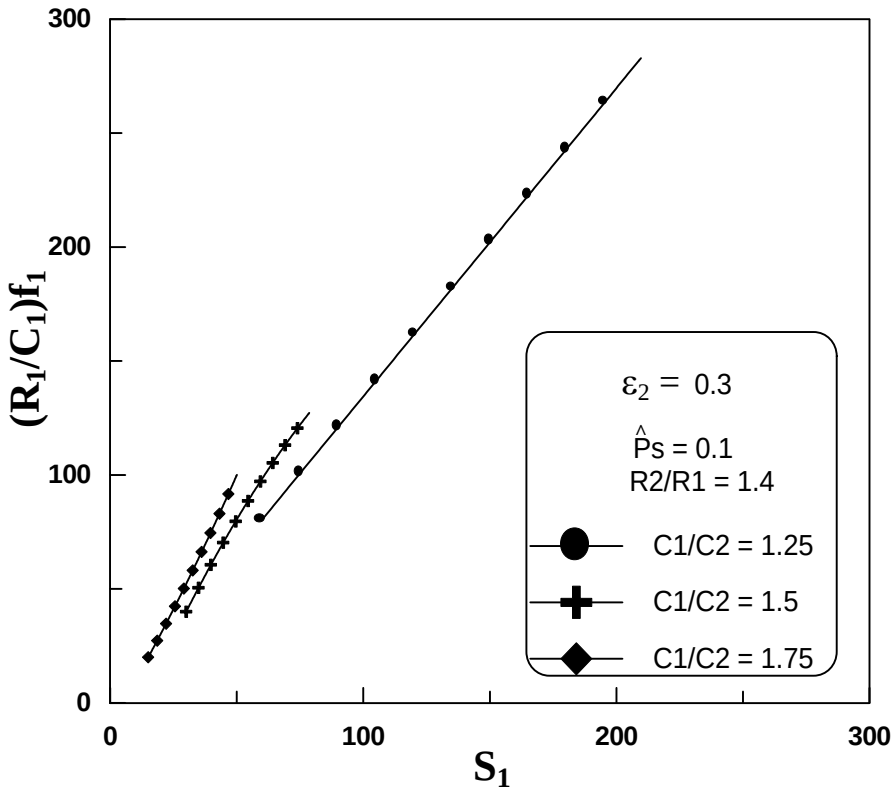

Figure (5-36), Friction Coefficient of Inner Oil – Film Versus Sommerfeld Number for Various Values of Clearance Ratios.

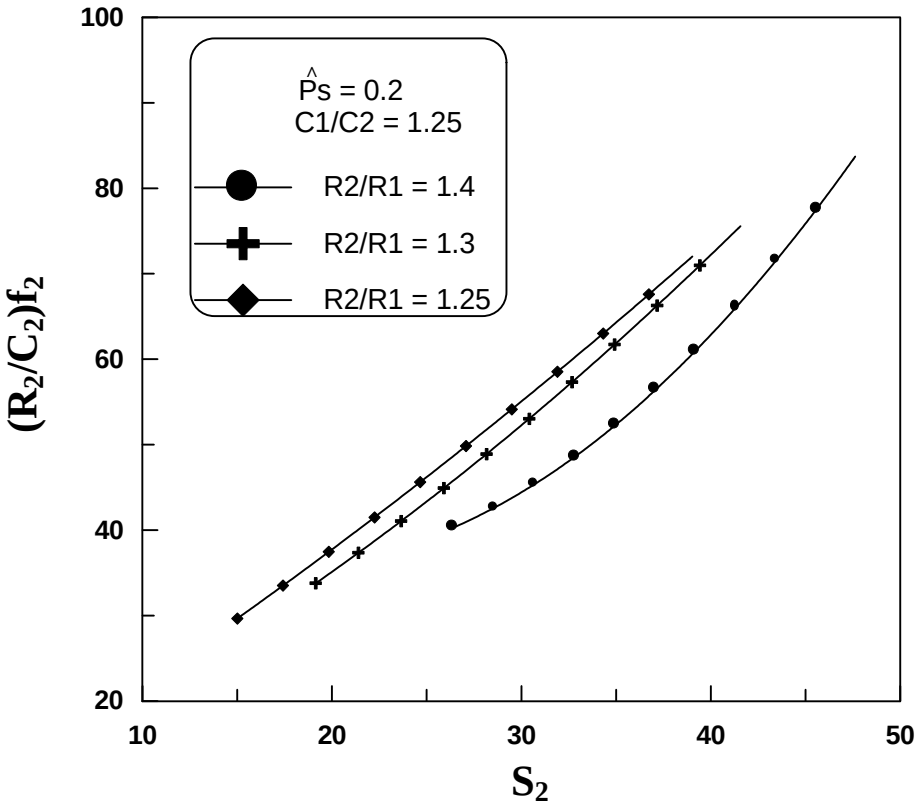

Figure (5-37), Friction Coefficient of Outer Oil – Film Versus Sommerfeld Number for Various Values of Radii Ratios.

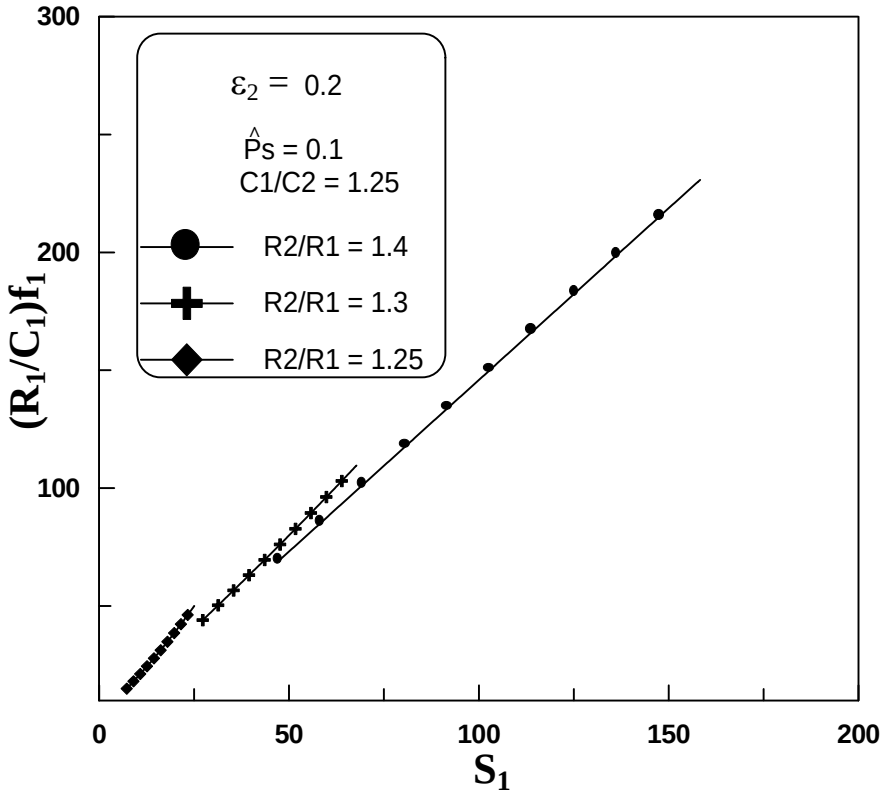

Figure (5-38), Friction Coefficient of Inner Oil – Film Versus Sommerfeld Number for Various Values of Radii Ratios.

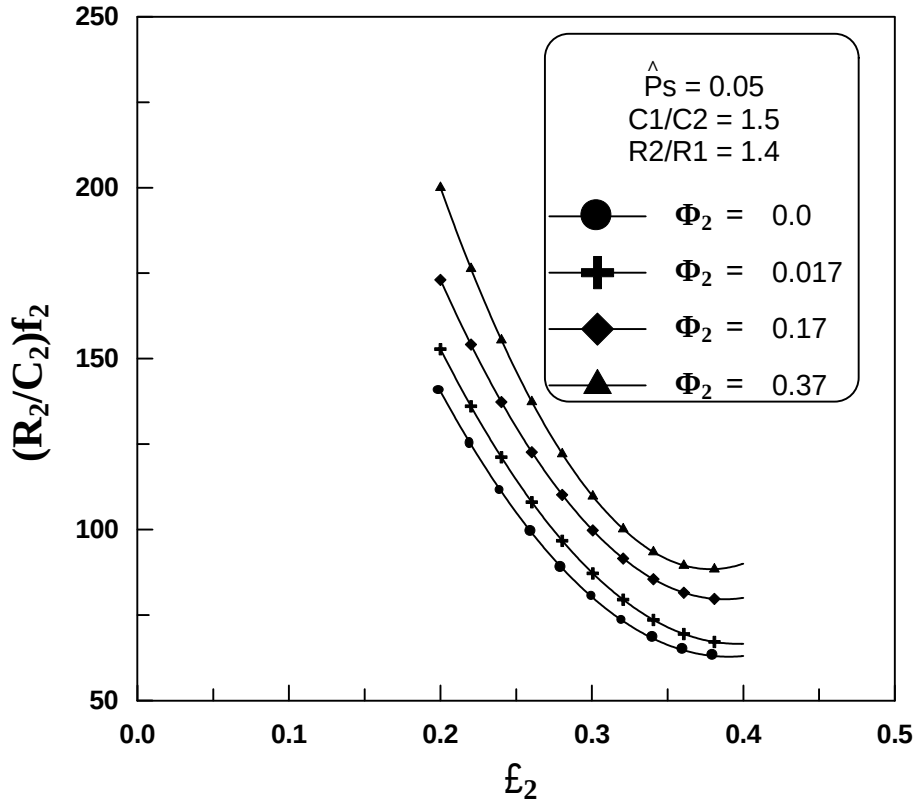

Figure (5-39), Friction Coefficient for Ring – Bearing Oil – Film Versus Eccentricity Ratio for Various Values of Permeability Parameter.

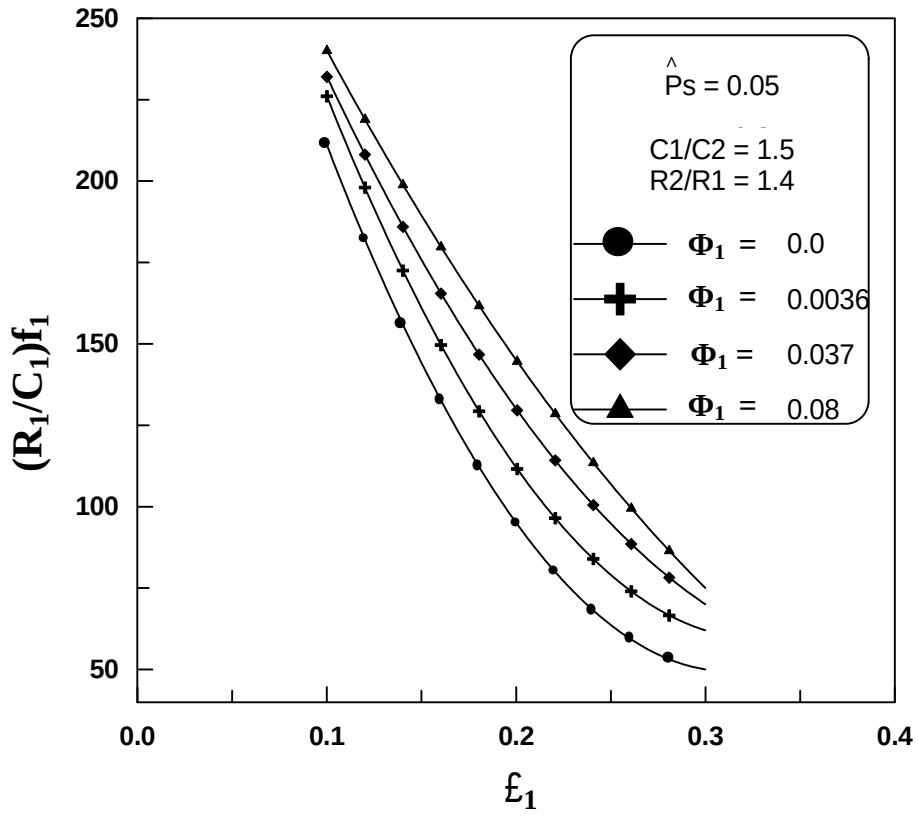

Figure (5-40), Friction Coefficient for Journal – Ring Oil – Film Versus Eccentricity Ratio for Various Values of Permeability Parameter.

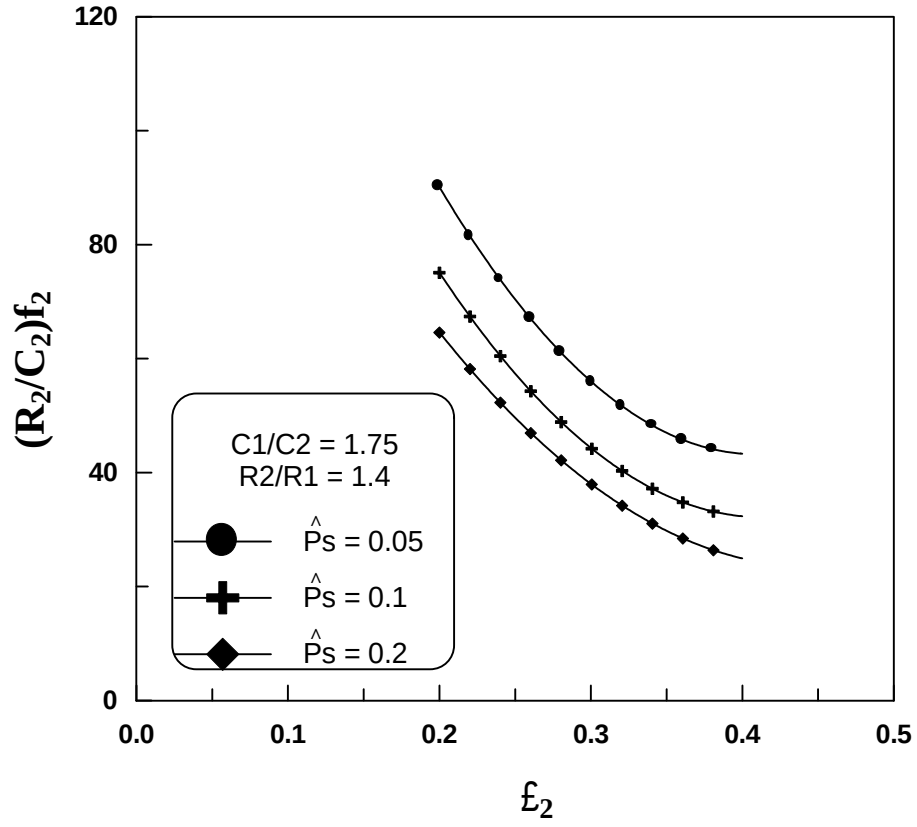

Figure (5-41), Friction Coefficient for Ring – Bearing Oil – Film Versus Eccentricity Ratio for Various Values of Dimensionless Oil – Feed Pressure.

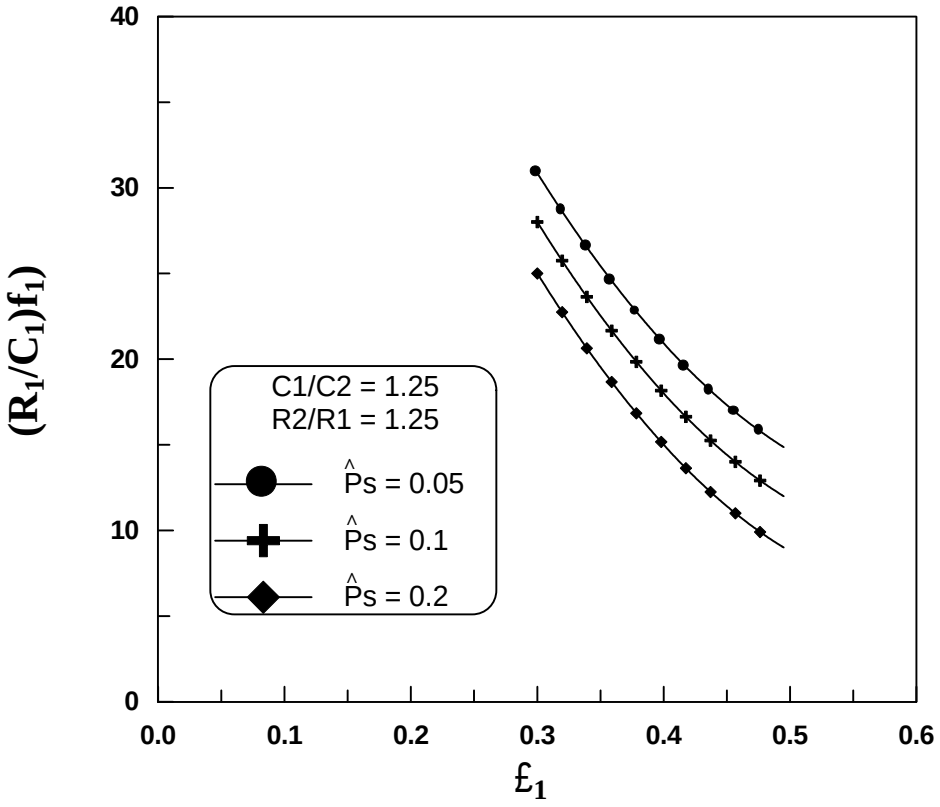

Figure (5-42), Friction Coefficient for Journal – Ring Oil – Film Versus Eccentricity Ratio for Various Values of Dimensionless Oil – Feed Pressure.

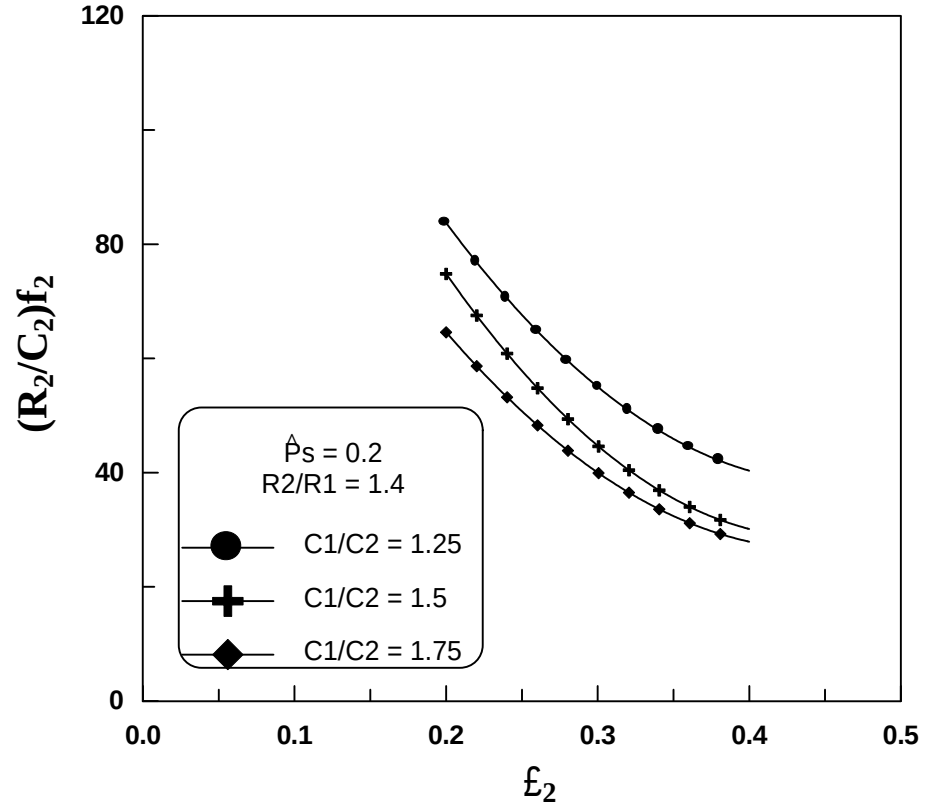

Figure (5-43), Friction Coefficient for Ring – Bearing Oil – Film Versus Eccentricity Ratio for Various Values of Clearance Ratio.

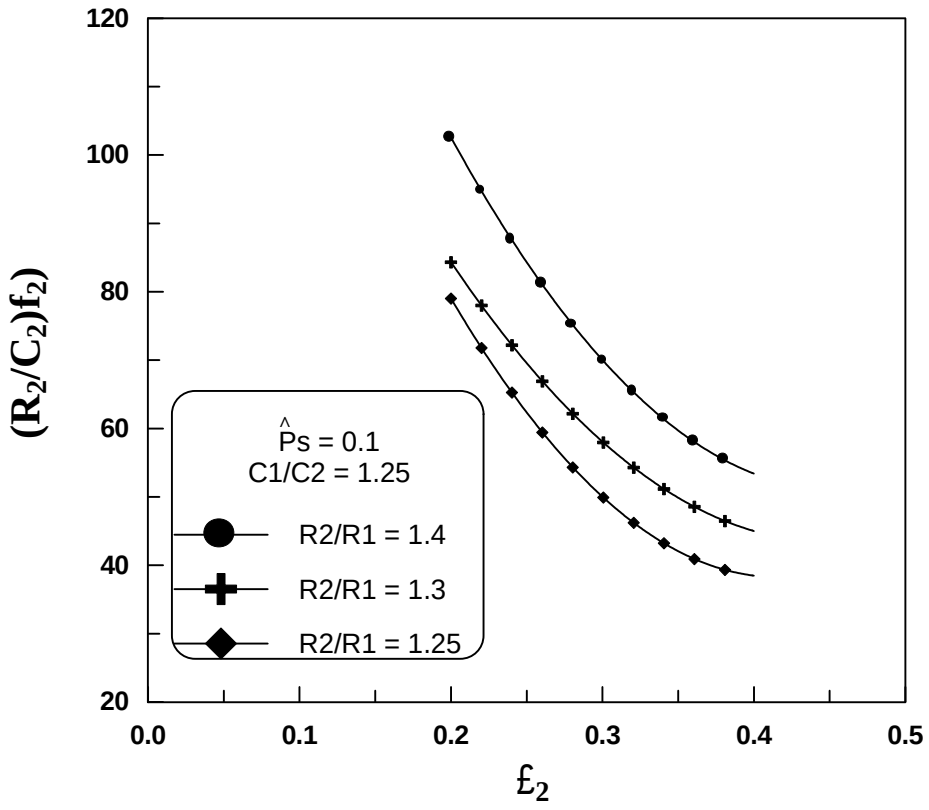

Figure (5-44), Friction Coefficient for Ring – Bearing Oil – Film Versus Eccentricity Ratio for Various Values of Radii Ratio.

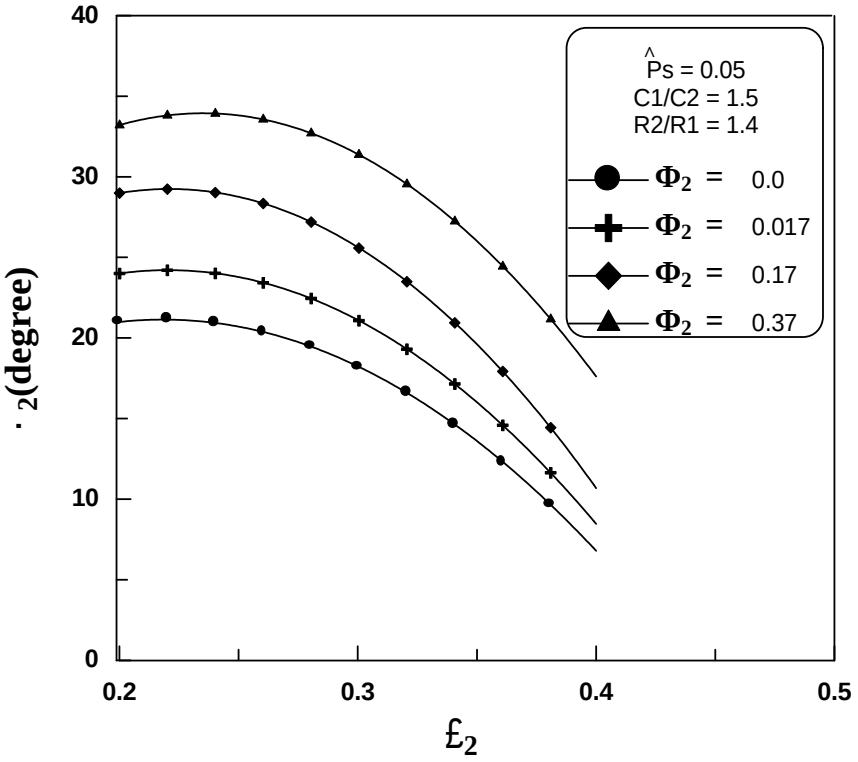

Figure (5-45), Attitude Angle for Ring – Bearing Oil – Film Versus Eccentricity Ratio for Various Values of Permeability Parameter.

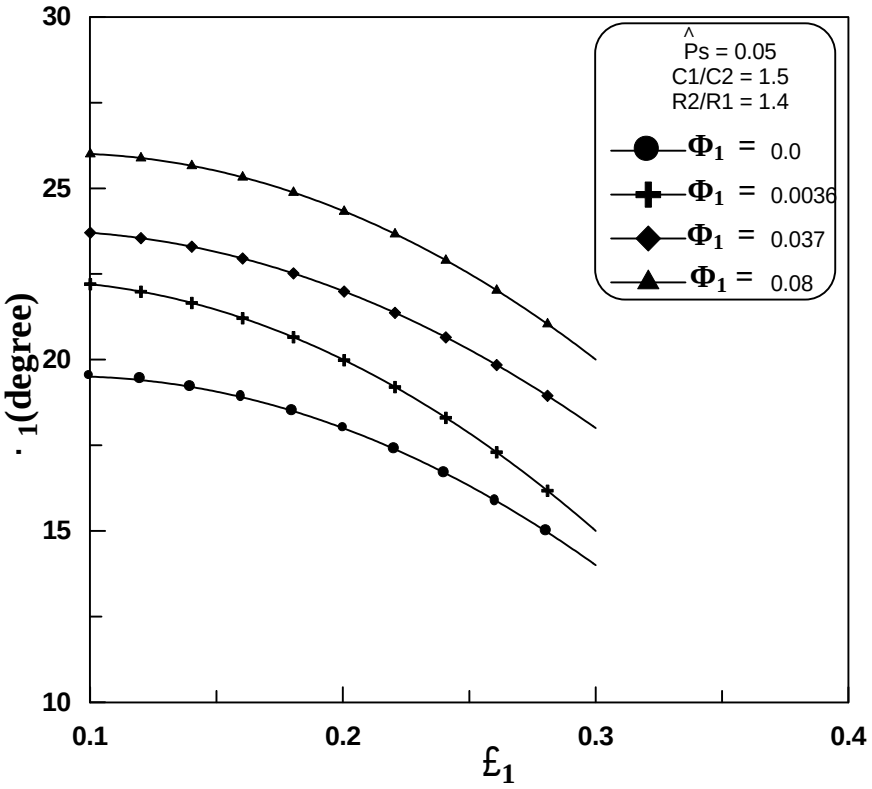

Figure (5-46), Attitude Angle for Journal - Ring Oil – Film Versus Eccentricity Ratio for Various Values of Permeability Parameter.

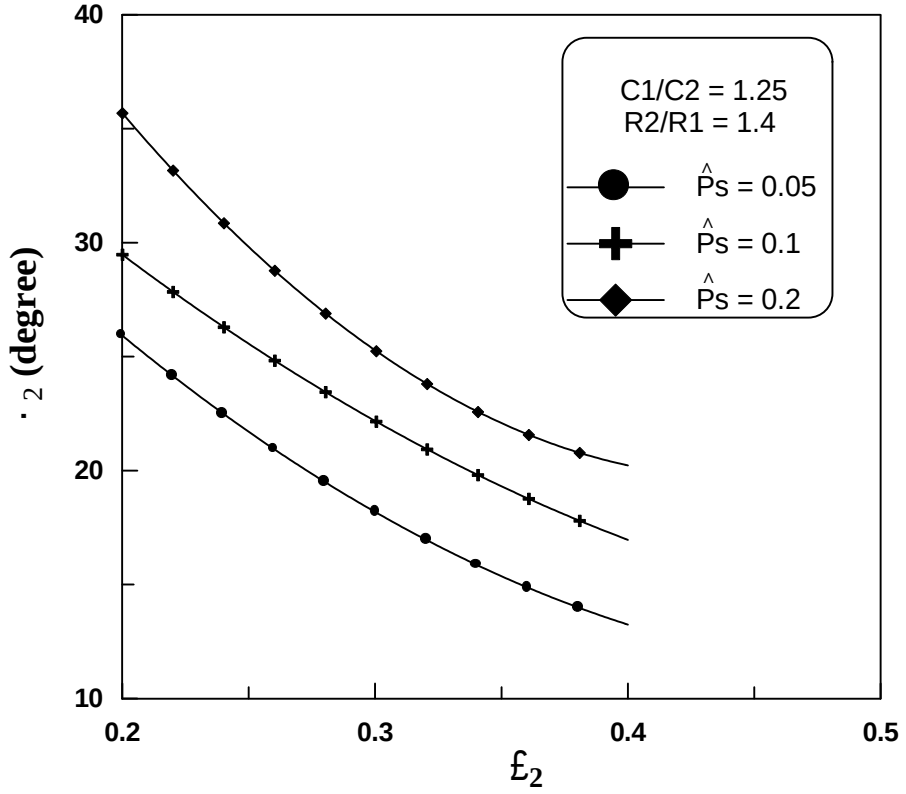

Figure (5-47), Attitude Angle of Outer Oil – Film Versus Ring Eccentricity Ratio for Various Values of Dimensionless Oil – Feed Pressure.

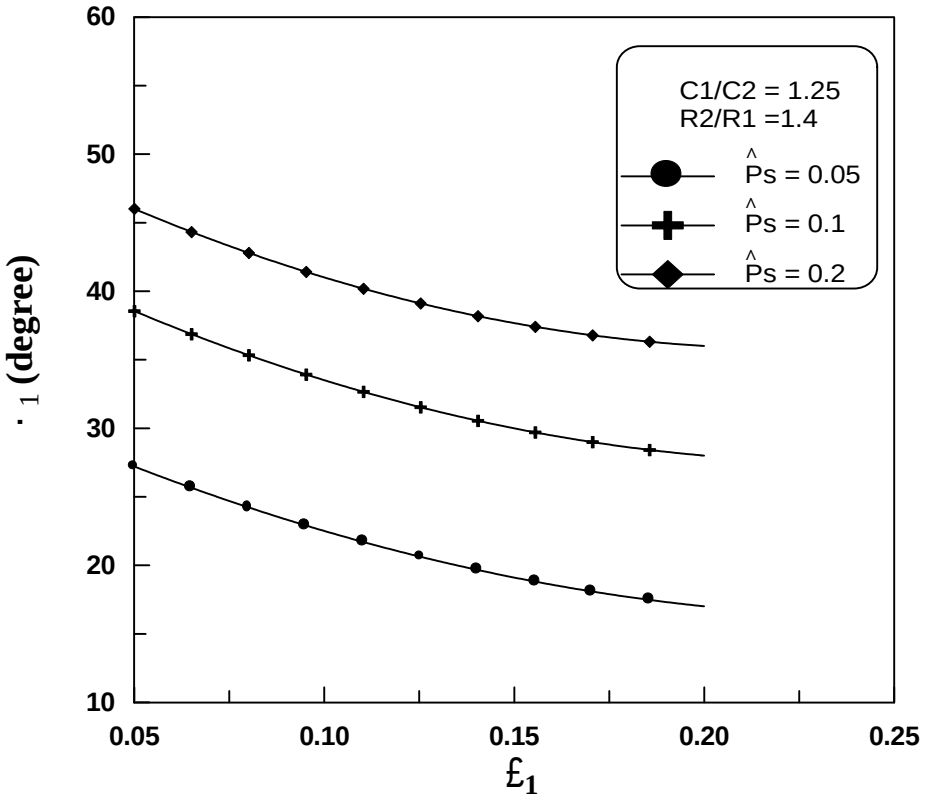

Figure (5-48), Attitude Angle of Inner Oil – Film Versus Journal Eccentricity Ratio for Various Values of Dimensionless Oil – Feed Pressure.

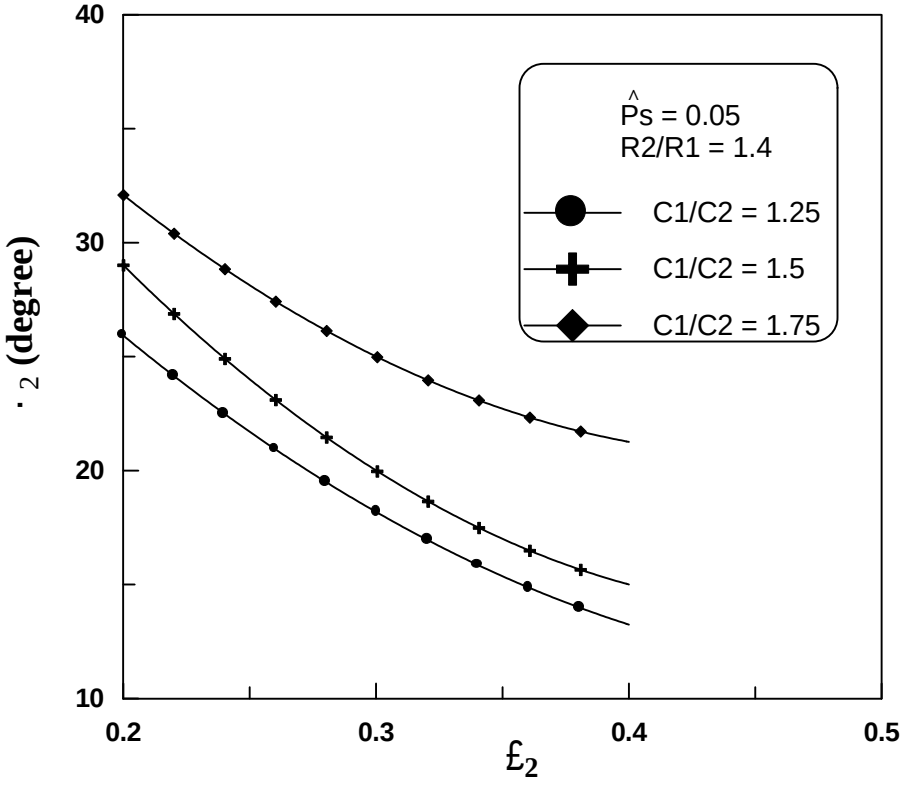

Figure (5-49), Attitude Angle of Outer Oil – Film Versus Ring Eccentricity Ratio for Various Values of Clearance Ratios.

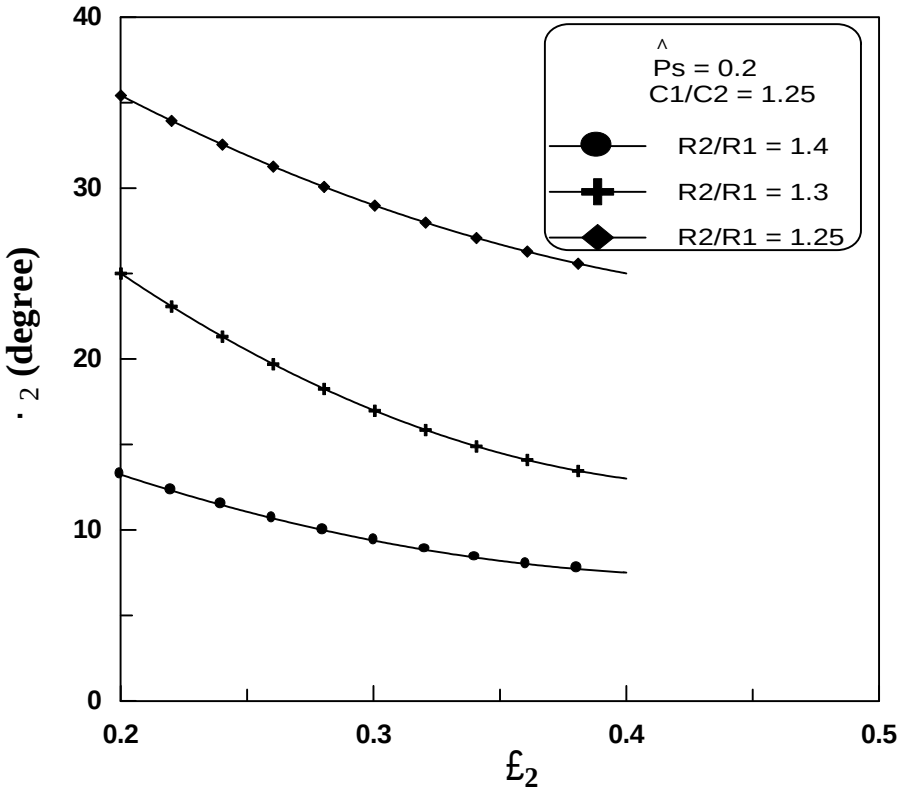

Figure (5-50), Attitude Angle of Outer Oil – Film Versus Ring Eccentricity Ratio for Various Values of Radii Ratios.

CHAPTER SIX
CONCLUSIONS AND RECOMMENDATIONS FOR FUTURE WORK

The steady state characteristics under condition of hydrodynamic lubrication conditions have been analyzed for the porous floating ring journal bearing. In view of the theoretical results obtained, the main conclusions of this work can be summarized as follows;

6.1 Conclusions

1- Sommerefeld number increases with increasing the values of the radii ratio while, decreases with increasing the supply pressure and clearance ratio

2- The load carrying capacity increases for the floating ring journal bearing working with ring has lower radii ratio.

3- The journal – ring eccentricity ratio become higher than the ring – bearing eccentricity ratio for bearings of higher permbility, clearance ratio and lower radii ratio.

4- The ring speed increases with decreasing the clearance ratio and the radii ratio.

5- The ring speed seems to be slightly affected by the supply pressure.

6- The oil – film extent increases with decreasing the values of the ring radii ratio.

7- The minimum coefficient of friction decreases with increasing the values of the supply pressure and the clearance ratio. The minimum value of the friction coefficient decreases with decreasing the values of the radii ratio.

8- The attitude angle of both films increases with increasing values of the permeability parameters, the supply pressure and the clearance ratio.

9- The attitude angle increases with decreasing the radii ratio of floating ring.

6.2 *Recommendations for Future Work*

This special type of self – lubricated bearing is not known yet as shown in the literature survey done by this work. Thus, much more is required to reveal all its performance characteristics. An additional effort is required to model this type of bearing to make it more realistic to be used by the designers. It is also suggested that further work should be carried out to account for the following points:-

1- An experimental and theoretical study concerning the steady – state and dynamic performance characteristics of the porous floating ring journal bearing.

2- An experimental and theoretical study concerning the steady – state of porous floating ring journal bearing with orthotropic permeability.

3- Theoretical study concerning the thermal effect on the performance of porous floating ring journal bearing.

4- Theoretical study concerning the steady – state and dynamic performance of porous floating ring journal bearing lubricated with Bi – phase (liquid – solid) lubricant using theory of mixtures.

5- Study of the chamfering effect on the steady – state and dynamic performance of porous floating ring journal bearing.

6- Study the steady – state characteristics of the porous floating ring journal bearing using the Elasto–hydrodynamic lubrication theory.

REFERENCES

1- Kaneko, S., 1993, "Porous Oil Bearings", Japanese J. Of Tribology, vol., 38, No. 9, Pp. 1141 – 1150.

2- Colline, R. E., 1960, "Flow of Fluid Through Porous Materials ", E.d. Charles R. Wilke, Reinhold. Publishing Corporation New York.

3- Morgan, V. T., and Cameron, A., 1957, "Study of the Design Criteria for Porous Metal Bearings", Conference on Lubrication and Wear, Institution of Mechanical Engineers, London, paper No. 88, pp. 405 – 408.

4- Kaneko, S., 1989, "Application of Porous Materials to Annular Plain Seals: Part 1 – Static Characteristics", Journal of Tribology, October, vol. 111, pp. 655 – 660.

5- Kaneko, S., and Obara, S., 1990, "Experimental Investigation of Mechanism of Lubrication in Porous Journal Bearings: Part 1- Observation of Oil Flow in Porous Matrix", Transaction of ASME, October, vol. 112, pp. 618 – 622.

6- Kaneko, S., Inoue, H., and Ushio, k., 1994, "Experimental Study on Mechanism of Lubrication in Porous Journal Bearings (Oil Film Formed in Bearing Clearance)", JSME International Journal, Series C, vol. 37, No.1, pp. 185 – 191.

7- Kaneko, S., Ohkawa, Y., Hashimoto, Y., 1994, "A Study of Mechanism of Lubrication in Porous Journal Bearings: Effect of Dimensionless Oil –

Feed Pressure on Static Characteristics Under Hydrodynamic Lubrication Conditions", Transactions of the ASME, July, vol. 116, pp. 606 – 610.

8- Kaneko, S., and Hashimoto, Y., 1995, "A Study of the Mechanism of Lubrication in Porous Journal Bearings: Effect Dimensionless Oil – Feed Pressure on Frictional Characteristics", Journal of Tribology, April, vol. 117, pp. 291 – 295.

9- Kanko, S., Kamei, H., Yanagisawa, Y., and Kawahra, H., 1998, "Experimental Study on Static and Dynamic Characteristics of Annular Plain Seals with Porous Materials", Journal of Tribology, April, vol. 120, pp. 165 – 172.

10- Shah, Rajesh, C., and Bhat, M. V., 2003, "Analysis of a porous exponential Slider Bearing Lubricated with a Ferro – Fluid Considering Slip Velocity", ABCM, July – September, vol. xxv, No. 3, pp. 264 – 267.

11- Gordon, S., Beavers and Daniel, D., Joaseph, 1967, "Boundary Conditions at a Naturally Permeable Wall", J. Fluid Mech., vol. 30, Part 1, pp. 197 – 207.

12- Prakash, J., and Vij, S., K., 1973, " Hydrodynamic Lubrication of a porous Slider", J. Mech. Eng. Sci., pp. 232 – 234.

13- Prakash, J., and Vij, S., K., 1974, "Analysis of Narrow Porous Journal Bearing Using Beavers – Joseph Criterion of Velocity Slip", Transaction of the ASME, June, pp. 348 – 354.

14- Rouleau, W. T., and Steiner, L. I., 1974, "Hydrodynamic porous Journal Bearings. Part 1 – Finite Full Bearings", Transactions of the ASME, July, pp. 346 – 352.

15- Cusano, C., 1979, "An analytical Study of Starved Porous Bearings", Transactions of the ASME, January, vol. 101, pp. 38 – 47.

16- Patel, K. C., and Cupta, J. L., 1983, "Hydrodynamic Lubrication of a Porous Slider Bearing With Slip Velocity", Wear, Vol. 85, pp. 309 – 317.

17- Kaneko, S., Inoue, H., and Ushio, k., 1994, "Experimental Study on Mechanism of Lubrication in Porous Journal Bearings (Oil Film Formed in Bearing Clearance)", JSME International Journal, Series C, vol. 37, No.1, pp. 191.

18- Kaneko, S., Hashimoto, Y., and Hiroki, I., 1997, "Analysis of Oil – Film Pressure Distribution in Porous Journal Bearings Under Hydrodynamic Lubrication Conditions Using An Improved Boundary Condition", Journal of Tribology, January, vol. 119, pp. 171 – 177.

19- Yousif, A. E., Nacy, S. M., and Abass, B. A., 1999, "An into Investigation the Bahaviour of Porous Materials in Pertinent to Elastohydrodynamic Lubrication", Conditions, Ph. D. Thesis, Mechanical Engineering Department, College of Engineering, University of Baghdad.

20- Erno¨ Baka, 2002, "Calculation of the Hydrodynamic Load Carrying Capacity of Porous Journal Bearings", Periodica Polytechnica Ser. Mech. Eng. Vol. 46, No. 1, pp. 3 – 14.

21- Saha, N., and Majumdae, B. C., 2004, "Steady – State and Stability Characteristics of Hydrostatic Two – Layered Porous Oil Journal Bearing", Proc. Instri. Mech. Engrs., Part J., J. Engineering Tribology, vol. 218, pp. 99 – 108.

22- Yung, K. M., Cameron, A., 1979, "Optical Analysis of Porous Metal Bearings", Transactions of ASME, January, vol. 101, pp. 99 – 104.

23- Braun, A. L., 1982, "Porous Bearing", Tribology International, Oct., pp. 151.

24- Terrile, R. M., 1983, "Laminar Flow in a Porous Tube", Journal of Fluid Engineering, September, vol. 105, pp. 303 – 307.

25- Yoken – Doh, 1987, "Lubrication Hand Book", Pub. Tokyo, pp. 474.

26- Kaneko, S., Inoue, H., and Ushio, K., 1991, "Experimental Study on Mechanism of Lubrication in Porous Journal Bearings 2nd Report, Oil Film Formed in Bearing Clearance", JSME Transaction, vol. 57, pp. 3927.

27- Kaneko, S., and Ohkawa, Y., 1992, "A Study on the Mechanism of Lubrication in Porous Journal Bearings, Theoretical Investigation of Oil Film Extent in Bearing Clearance under Hydrodynamic Lubrication Conditions", Trans. of the JSME, vol. 58, No. 554, pp. 3056.

28- Shaw, M. C., and Nussdorfer, Jr., T. J., 1947, "An Analysis of the Full Floating Journal Bearing", NACA Report, No. 866.

29- Kettleborough, C. F., 1954, "Frictional Experiments on Lightly – Loaded Fully Floating Ring Journal Bearing", Aust. J. of App. Sci., January, pp. 211 – 219.

30- Orcutt, F. K., and Ng. C.W. 1968, "Steady – State and Dynamic Properties of the Floating Ring Journal Bearing", ASME Journal of Lubrication Technology, vol. 90, pp. 1 – 10.

31- Tanaka, M., and Hori, Y., 1972, "Stability Characteristics of Floating Bush Bearings", ASME Journal of Lubrication Technology, July, pp. 248 – 259.

32- Rohde, S. M., and Ezzat, M. A., 1980, "Analysis of Dynamically Loaded Floating Ring Bearing for Automotive Application", ASME Journal of Lubrication Technology, July, vol. 102, pp. 271 – 276.

33- Mokhtar, M. O. A., 1981, "Floating Ring Journal Bearing: Theory, Design and Optimization", Tribology International, April, pp. 113 – 119.

34- Li, C. H., and Rohde, S. M., 1981, "On the Steady State and Dynamic Performance Characteristics of Floating Ring Bearings", ASME Journal of Lubrication Technology, July, vol. 103, pp. 389 – 397.

35- Li, C. H., 1982, "Dynamic of Rotor Bearing System Supported by Floating Ring Bearing", ASME Journal of Lubrication Technology, October, vol. 104, pp. 469 – 476.

36- Wilcock, D. F., 1983, "Load Carrying Efficiency of Floating Ring Journal Bearings", ASME, Journal of Lubrication Technology, Oct., vol. 105, pp. 605 – 608.

37- Yousif, A. E., and Abass. B. A., 1989, "Lubrication of Floating Ring Journal Bearing With Two Phase (Liquid – Solid) System", M.Sc. Thesis, Mechanical Engineering Department, College of Engineering, University of Baghdad.

38- Dong, X., and Zhao, Z., 1990, "Experimental and Analytical Research on Floating – Ring Bearing for Engine Applications", Journal of Tribology, January, vol. 112, pp. 119 – 122.

39- Yousif, A. E., and Nacy, S. M., 1993, "The Hydrodynamic Lubrication of Conical Journal Bearing", Ph.D. Thesis, Mechanical Engineering Department, College of Engineering, University of Baghdad.

40- Yeon – Min Cheong and Kyung – Wood Kim, 2001, "Operating Characteristics of Counter – rotating Floating Ring Journal Bearings", KSTLE International Journal, December, vol. 2, No. 2, pp. 127 – 132.

41- Andres, L. San, and Kerth, J., 2004, "Thermal Effect on the Performance of Floating Ring Bearings for Turbochargers", Proc. Instri. Mech. Engrs., Part J., J. Engineering Tribology, vol. 218, pp.437 – 450.

42- Quan Yong – Xin and Wang Pei – Ming, 1985, "Theoretical Analysis and Experimental Investigation of Porous Metal Bearing", Tribology International, April, vol. 18, No. 2, pp. 67 – 73.

43- Chattopadhyay , A., K. and Majumdar, B., C., 1984, "Steady State Solution of Finite Hydrostatic Porous Oil Journal Bearing With Tangential Velocity Slip ", Tribology International, December, vol. 17, No. 6, pp. 317 – 324.

Analysis of the Mechanism of Lubrication in Porous Floating – Ring Journal Bearings Working Under Different Supply Pressure.

By

Basim A. Abass , Alaa' M. Hosein
Lekaa' Hameed

Department of Mechanical Engineering, College of Engineering, Babylon University

Abstract

The static characteristics of porous floating ring journal are theoretically investigated assuming that the oil fed through outside diameter of the bearing under small supply pressure. The angular extent of the oil film formed in journal – ring and ring – bearing oil films are obtained by applying the integral momentum equation to the oil films region. Also, when the oil extent reach steady state, the in flow of oil into the bearing clearance through the porous matrix due to the feed pressure must make up for the oil leakage from the ends through the clearance gaps and that into the porous matrix due to the pressure in the oil film. Numerical results show that the dimensionless oil – fed pressure significantly influences the static characteristics of such bearings.

1- Introduction:

With the introduction of high speed turbochargers, gas turbines and compressors, vibration problems and instability were a raised. Design improvement and modifications of journal bearing arrangement were made to decrease the excessive vibration and increase the stability range; one of the arrangements is the enhancement of damping characteristics of the journal bearing by introducing a floating ring between the rotating journal and fixed bearing.

Over the past decades a considerable number of experimental and theoretical studies have been made to study the characteristics of the solid floating ring journal bearings and various information have been described in each study, Hill (1958); Pinkus (1961); Tondal (1965); Lund (1966); Orcutt (1968); Tatara (1969); Tanaka (1972); Chin – Hsiu Li et. al. (1981); Chin – Hsiu Li (1982).

Dong and Zhao (1990) carried out an experimental and analytical investigations on floating ring journal bearings for engine applications. They concluded that it is possible for the

floating – ring bearings to be used in engines, where the load is non-stationary. Yeon Min et. al. (2001) study the operating characteristics of counter rotating floating ring journal bearing which can be found in the inter shaft bearing of the front drive of the turboshaft engine. Anders and Kerth (2004) study the thermal effect on the performance of floating ring journal bearings for turbochargers applications, prediction for the exit lubricant temperature power losses and floating ring speeds agree well with the measurements obtained in automotive turbochargers.

Porous oil bearings can be defined as those bearings in which the oil comes out from pores to lubricate the friction surfaces and on shut down operation oil would penetrate back to the pores. Lubrication performance characteristics (load capacity, friction coefficient, bearing temperature. etc.) have been the object of many recent investigations, Morgan and Cameron (1957); Rouleau (1963); Goldstein and Braun (1971); Cusano (1972); Reason and Dyer (1973); Prakash and Vij (1974). In the above investigations the half Sommerfeld condition was adopted. A theoretical and experimental work done by Kaneko et. al. (1994) shows that the oil film is formed mainly in the loaded part of the bearing and the angular extent of oil film is significantly smaller than that formed in a solid journal bearing even under hydrodynamic lubrication condition. Kaneko et. al. (1997) uses improved boundary conditions to obtain the angular position of leading a trailing ends of the oil film regions. They show that the negative pressure occur before the tailing end of the oil film region.

Elsharkawy and Lotfi (2001) made an analysis to the hydrodynamic lubrication of porous bearings using a modified Brinkman – extended Darcy model. They found that the numerical model has been successfully predicting the experimental results of different researchers. Although there are number of theoretical and experimental work carried out to analyze the performance of floating ring journal bearings and porous journal bearings as described before but it seems nothing on the porous floating ring journal bearings. Hence the purpose of this study is to analyze the steady state performance of porous floating ring journal bearing under different supply pressure. Isothermal finite bearing theory with improved boundary conditions was adopted to obtain the leading and trailing ends.

2- Numerical Analysis:

2.1- Model of the Porous Floating Ring Journal Bearing:

The porous floating ring journal bearing with the coordinate system used in this analysis can be shown in figure (1). The journal rotates with a constant angular velocity (ω_j) about its axis while the porous ring rotates with an enhanced angular velocity (ω_r) about its center. The porous bearing inserted into a solid housing having a circumferential groove in the middle.

Lubricant oil at low supply pressure (P_s) is supplied to the groove in the middle. It should be noted that the present analysis also has practical limitations, since most porous bearings do not operate under the hydrodynamic condition.

2.2 Pressure Distribution in Oil Film and Porous Matrix:

The performance of the bearing inner and outer oil films are obtained from the following Reynolds' equation for finite bearings including the so – called filter term and the effect of tangential slip velocity. For constant viscosity it can be written as;

$$\frac{\partial}{\partial \bar{\theta}}\left(h^{\wedge 3}(1+\varepsilon_1)\frac{\partial P^{\wedge}}{\partial \bar{\theta}}\right)_{ii}+\left(\frac{D_{ii}}{L}\right)^2\frac{\partial}{\partial Z^{\wedge}}\left(h^{\wedge 3}(1+\varepsilon_1)\frac{\partial P^{\wedge}}{\partial Z^{\wedge}}\right)_{ii}=6\frac{\partial}{\partial \bar{\theta}}\left(h^{\wedge 3}(1+\varepsilon_0)\right)_{ii}-12\Phi_{ii}\left(\frac{\partial P^{\wedge *}}{\partial r^{\wedge}}\Big|_{r^{\wedge}=1}\right)_{jj} \quad \text{.....(1)}$$

where;

ii= 1 refer to the journal – ring oil film and $\omega_{ii}= \omega_j$

ii= 2 refer to the ring – bearing oil film and $\omega_{ii}= \omega_r$

and

jj= 1 refer to the porous ring

jj= 2 refer to the porous bearing.

$$(\varepsilon_0)_{ii}=\left(\frac{s}{(h^{\wedge}+s)}\right)_{ii} \quad \text{.....(2)}$$

$$(\varepsilon_1)_{ii}=\left(3(h^{\wedge}s+2\sigma^2 s^2)/\{h^{\wedge}(h^{\wedge}+s)\}\right)_{ii} \quad \text{.....(3)}$$

$$(s)_{ii}=\left(\Phi c/R\right)_{ii}^{1/2}/\sigma \quad \text{.....(4)}$$

$$(\Phi)_{ii}=(k_1R/c^3)_{ii} \quad \text{.....(5)}$$

$$(P^{\wedge}=c^2P/(R^2\eta\omega))_{ii} \quad \text{.....(6)}$$

$$(P^{\wedge}=c^2P/(R^2\eta\omega))_{ii} \quad \text{.....(7)}$$

$$Z^{\wedge}=\frac{Z}{L/2} \quad \text{.....(8)}$$

$$r_{ii}^{\wedge} = \frac{\Delta r}{R_{ii}} \qquad \text{.....(9)}$$

$$\left(h^{\wedge}\right)_{ii} = h_{ii} / c_{ii} = \left(1 + \pounds \cos(\theta)\right)_{ii} \qquad \text{.....(10)}$$

The slip coefficient (α) is a dimensionless parameter which depends on the porous material. In the present analysis a value of (0.1) is assumed for (α) as done in the pervious studies, Cusano (1979); Quan and Wang (1985); Kaneko et. al. (1994).

The governing equation of the oil pressure in the porous ring and bearing is given in dimensionless form as;

$$\frac{1}{r_{\mathrm{ii}}^{\wedge}} \frac{\partial}{\partial r^{\wedge}} \left(r^{\wedge} \frac{\partial P^{\wedge *}}{\partial r^{\wedge}} \right)_{jj} + \frac{1}{r_{ii}^{\wedge 2}} \left(\frac{\partial^2 P^{\wedge *}}{\partial \theta^2} \right)_{jj} + \left(\frac{D_{ii}}{L} \right)^2 \left(\frac{\partial^2 P^{\wedge *}}{\partial Z^{\wedge 2}} \right)_{jj} = 0 \qquad \text{.....(11)}$$

2.3 Circumferential Boundary Conditions for the Oil Films Pressure:

The following Circumferential Boundary Conditions are used through the solution. The pressure at the inlet and trailing ends of the oil film can be taken as;

$$\left(P^{\wedge}\right)_{ii} = 0 \quad \text{at} \quad \theta = \left(\theta_1\right)_{ii} \quad \text{and} \quad \theta = \left(\theta_2\right)_{ii} \qquad \text{.....(12)}$$

$$\left(P^{\wedge *}\right)_{jj} = 0 \quad \text{at} \quad \theta = \left(\theta_1\right)_{ii} \quad \text{and} \quad \theta = \left(\theta_2\right)_{ii} \qquad \text{.....(13)}$$

where (θ_1) in both oil films are determined by extending the boundary condition used by Kaneko et. al. (1997), as follows;

$$\left(M_{\theta_1} - M_{\theta_2} - M_{\theta_c} - M_{\theta_b} \right)_{ii} = 0 \qquad \text{.....(14)}$$

where;

$M_{\theta_1}, M_{\theta_2}, M_{\theta_c}$ and M_{θ_b} are the circumferential momentum flow rates across the control surfaces of the oil films, as shown in figure (2). The momentum flow rates are given as follows;

$$\left(M_{\theta_1}\right)_{ii} = 2 \int_0^{L/2} \int_0^{\left(h_{\theta_1}\right)_{ii}} \rho \left[\left(u_{\theta} \big|_{\theta_1} \right)^2 \right]_{ii} dy dz \qquad \text{.....(15)}$$

$$\left(M_{\theta_2}\right)_{ii} = 2 \int_0^{L/2} \int_0^{\left(h_{\theta_1}\right)_{ii}} \rho \left[\left(u_{\theta} \big|_{\theta_2} \right)^2 \right]_{ii} dy dz \qquad \text{.....(16)}$$

$$\left(M_{c}\right)_{ii} = 2\left(r_{ii}\right)\int_{1}^{2}\int_{0}^{(h)_{ii}} \circ \left[\left(u * u_{z}\right)\right|_{z=L/2}\Big]_{ii} dyd \qquad \text{.....(17)}$$

$$\left(M_{b}\right)_{ii} = 2\left(r_{ii}\right)\int_{0}^{L/2}\int_{(1)_{ii}}^{(2)_{ii}} \circ \left[\left(u_{m}\right)_{ii} * \left(u_{r}^{*}\right)_{jj}\right]_{r=(r)_{ii}} d dz \qquad \text{.....(18)}$$

where $\circ$ the density of oil film and its value is is assumed to be constant. The velocity components in circumferential and axial directions in the first and second oil films are, $(u)_{ii}$ and $(u_z)_{ii}$, while $(u_r^*)_{jj}$ is the velocity component of the oil inside the porous matrix in the bearing and the floating ring. The different velocity components at the oil films and the porous matrix can be expressed as follows;

$$(u)_{ii} = \frac{1}{2}\left(\frac{\partial P}{r\,\partial}\right)_{ii}(y - h_{ii})\left(y + \frac{1}{3}h_{ii}, 1x\right) + \left(\frac{r\mu}{h}\right)_{ii}\left(y(1 - , 0x) + h, 0x\right)_{ii} \qquad \text{.....(20)}$$

$$(u_Z)_{ii} = \frac{1}{2}\left(\frac{\partial P}{\partial Z}\right)_{ii}(y - h_{ii})\left(y + \frac{1}{3}h_{ii}, 1x\right) \qquad \text{.....(21)}$$

$$\left(u_{r}^{*}\right)_{jj} = \frac{k_1}{}\left(\frac{\partial P^{*}}{\partial r}\right)_{jj} \qquad \text{.....(22)}$$

$$\left(u_{m}\right)_{ii} = \left(\frac{1}{h}\int_{0}^{h} u\, dy\right)_{ii}$$

$$= \left(-\frac{h^2}{12\,r}\frac{\partial P}{\partial}(1 + , 1)\right)_{ii} + \frac{(r\mu)_{ii}}{2}(1 + , 0) \quad \text{if} \quad \left(u_r^*\big|_{r=r_i}\right)_{jj} \geq 0 \qquad \text{.....(23)}$$

$$\left(u_{m}\right)_{ii} = -\left(\frac{k_1}{}\frac{\partial P}{\partial}\Big|_{r=r_i}\right)_{ii} \qquad \text{if} \quad \left(u_r^*\big|_{r=r_i}\right)_{jj} < 0 \qquad \text{.....(24)}$$

The values of $(\theta_1)_{ii}$ and $(\theta_2)_{ii}$ are constant in z – direction. By substituting the above velocity components into equations **(15)** to **(18)** and normalizing each momentum flow rate by $\circ L\left(cr\,\mu^{2}\right)_{ii}$, equation **(14)** can be written in dimensionless form as;

$$\left(\hat{M}_1-\hat{M}_2-\hat{M}_c-\hat{M}_b\right)_{ii}=0 \qquad \text{……(25)}$$

where;

$$\left(\hat{M}_1\right)_{ii}=\left(M_1\right)_{ii}/\left(\circ c_{ii}r_{ii}^2\mu_{ii}^2L\right)=\int_0^1\left(\left(\frac{h^5}{1080}\left(\frac{\partial P}{\partial Z}\right)^2\left(9+15,_1+10,_1^2\right)\right)_{Z=Z_1}\right)_{ii}dZ$$

$$-\int_0^1\left(\left(\frac{h^3}{36}\frac{\partial P}{\partial Z}\left(3+3,_0+2,_1+4,_{0,1}\right)\right)_{Z=Z_1}\right)_{ii}dZ+\int_0^1\left(\left(\frac{h}{3}\left(1+,_0+,_0^2\right)\right)_{Z=Z_1}\right)_{ii}dZ$$

……(26)

$$\left(\hat{M}_2\right)_{ii}=\left(M_2\right)_{ii}/\left(\circ c_{ii}r_{ii}^2\mu_{ii}^2L\right)=\int_0^1\left(\left(\frac{h^5}{1080}\left(\frac{\partial P}{\partial Z}\right)^2\left(9+15,_1+10,_1^2\right)\right)_{Z=Z_2}\right)_{ii}dZ$$

$$-\int_0^1\left(\left(\frac{h^3}{36}\frac{\partial P}{\partial Z}\left(3+3,_0+2,_1+4,_{0,1}\right)\right)_{Z=Z_2}\right)_{ii}dZ+\int_0^1\left(\left(\frac{h}{3}\left(1+,_0+,_0^2\right)\right)_{Z=Z_2}\right)_{ii}dZ$$

……(27)

$$\left(\hat{M}_c\right)_{ii}=\left(M_c\right)_{ii}/\left(\circ c_{ii}r_{ii}^2\mu_{ii}^2L\right)=-\frac{1}{72}\left(\left(\frac{D}{L}\right)^2\int_1^2 Ad\right)_{ii}$$

Where,

$$\left(\mathrm{A}=h^3\left(3+3,_0+2,_1+4,_{0,1}\right)\left.\frac{\partial P}{\partial Z}\right|_{Z=1}\right)_{ii}\le 0 \qquad \text{if} \qquad \left(\left.\frac{\partial P}{\partial Z}\right|_{Z=1}\right)_{ii}\le 0$$

$$\mathrm{A}=0 \quad \text{if} \quad \left(\left.\frac{\partial P}{\partial Z}\right|_{Z=1}\right)_{ii}>0 \qquad \text{……(28)}$$

$$\left(\hat{M}_b\right)_{ii}=\left(M_b\right)_{ii}/\left(\circ c_{ii}r_{ii}^2\mu_{ii}^2L\right)=\int_0^1\left(\int_1^2 Bd\right)_{ii}dZ$$

$$(B)_{ii} = \left(\Phi \left\{ \frac{h^{\wedge 2}}{12}(1+\text{،}_1)\frac{\partial P^{\wedge}}{\partial \bar{\ }} - \frac{1}{2}(1+\text{،}_0) \right\} \right)_{ii} \left(\left. \frac{\partial P^{\wedge *}}{\partial r^{\wedge}} \right|_{r^{\wedge}=1} \right)_{jj} \quad \text{if} \quad \left(\left. \frac{\partial P^{\wedge *}}{\partial r^{\wedge}} \right|_{r^{\wedge}=1} \right)_{jj} \leq 0$$

$$(B)_{ii} = \left(\left(\frac{c}{r} \right) \Phi^2 \frac{\partial P^{\wedge}}{\partial \bar{\ }} \right)_{ii} \left(\left. \frac{\partial P^{\wedge *}}{\partial r^{\wedge}} \right|_{r^{\wedge}=1} \right)_{jj} \quad \text{if} \quad \left(\left. \frac{\partial P^{\wedge *}}{\partial r^{\wedge}} \right|_{r^{\wedge}=1} \right)_{jj} > 0 \qquad \textbf{……(29)}$$

On the other hand the boundary at the trailing edge can be obtained by ensuring the continuity of the bulk flow a cross the boundary line at (θ_2). This continuity is expressed as in Kaneko et. al. (1994),

$$\left(q_{\bar{\ }_p} / q_{\bar{\ }_c} \right)_{ii} = 0 \qquad \textbf{……(30)}$$

where $q_{\bar{\ }_p}$ and $q_{\bar{\ }_c}$ are the flow rate a cross the trailing boundary line due to the Poiseuilles' flow and due to the Couettes' flow respectively. Equation **(30)** can be rewritten as;

$$\left(q_{\bar{\ }_p} / q_{\bar{\ }_c} \right)_{ii} = \left(\left(\frac{(1+\text{،}_1)}{6(1+\text{،}_0)} h^{\wedge 2} \int_0^1 \frac{\partial P^{\wedge}}{\partial \bar{\ }} dz^{\wedge} \right)_{\bar{\ }=\bar{\ }_2} \right)_{ii} \qquad \textbf{……(31)}$$

Knowing the values of $(\bar{\ }_1)_{ii}$ and $(\bar{\ }_2)_{ii}$ for each oil film (journal – ring and ring – bearing oil films)**,** the angular extent $(\ \ )_{ii}$ of the first and second oil films are expressed in the form;

$$(\ \ )_{ii} = (\bar{\ }_2)_{ii} - (\bar{\ }_1)_{ii} \qquad \textbf{……(32)}$$

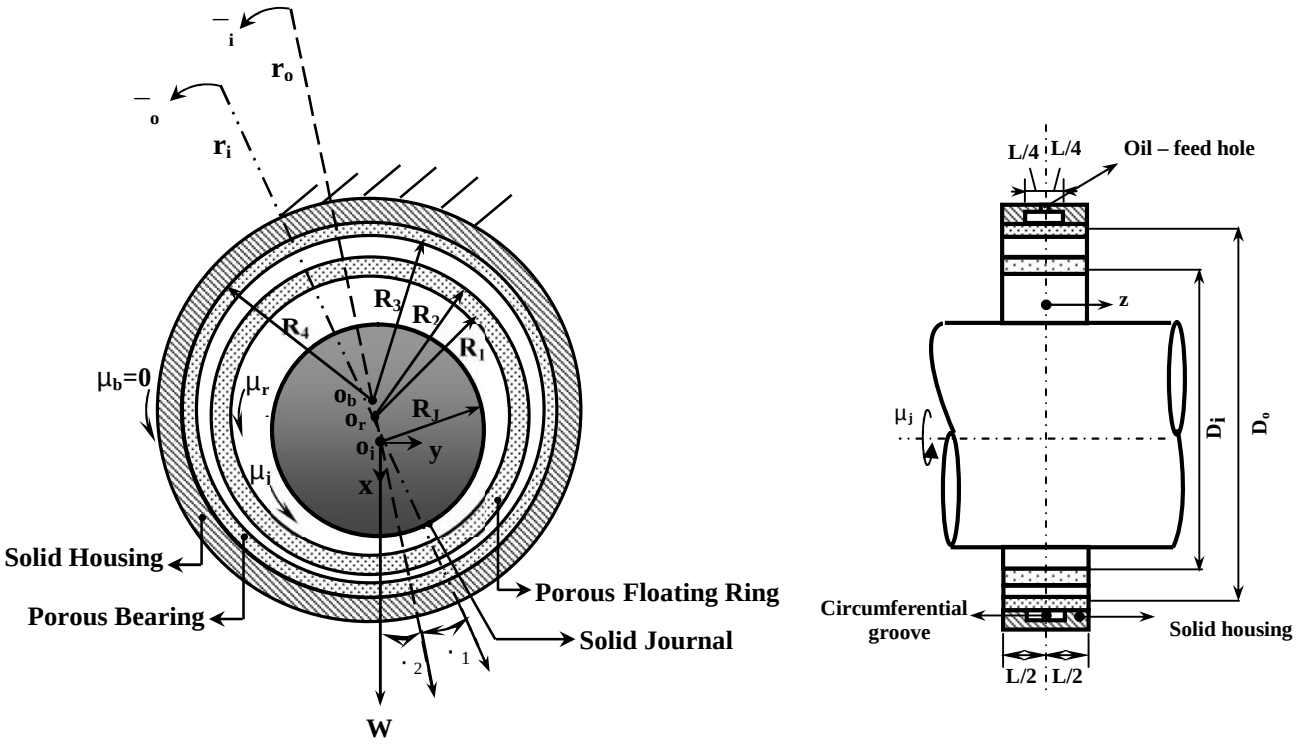

Figure (1): Oil film region and oil flow of porous floating ring journal bearing

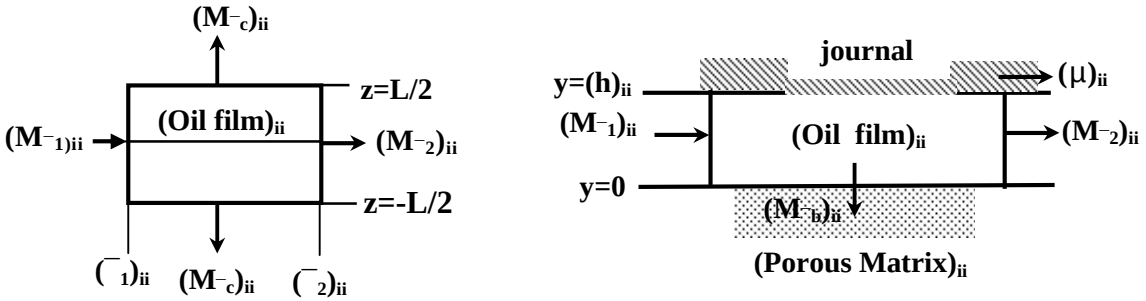

Figure (2): Circumferential momentum flow rates

3- **Bearing Parameters:**

Knowing the pressure distribution the dimensionless film force components along and perpendicular to the line of centers can be obtained, respectively as;

$$\left(W_R\right)_{ii} = -2\int_0^{L/2}\int_{-1}^{2}\left(P(\bar{\ },z)_{ii}\cos\bar{\ }\right)_{ii} d\bar{\ }dz \qquad \text{.....(33)}$$

$$\left(W_T\right)_{ii} = 2\int_0^{L/2}\int_{-1}^{2}\left(P(\bar{\ },z)_{ii}\sin\bar{\ }\right)_{ii} d\bar{\ }dz \qquad \text{.....(34)}$$

The load components can be normalized as follows;

$$\left(\hat{W}_R\right)_{ii} = (\mathrm{W_R}\ \mathrm{c}^2 / \mu R^3 L)_{ii} = -\int_0^{1}\int_{-1}^{2}\left(P^{\wedge}(\bar{\ },z)_{ii}\cos\bar{\ }\right)_{ii} d\bar{\ }dz^{\wedge} \qquad \text{.....(35)}$$

$$\left(\hat{W}_T\right)_{ii} = (\mathrm{W_T}\ \mathrm{c}^2 / \mu R^3 L)_{ii} = \int_0^{1}\int_{-1}^{2}\left(P^{\wedge}(\bar{\ },z)_{ii}\sin\bar{\ }\right)_{ii} d\bar{\ }dz^{\wedge} \qquad \text{.....(36)}$$

the total dimensionless load is;

$$\left(\hat{W}\right)_{ii} = \sqrt{\left(\hat{W}_R\right)_{ii}^2 + \left(\hat{W}_T\right)_{ii}^2} \qquad \text{.....(37)}$$

The attitude angles $(\Psi)_{ii}$ can give by;

$$(\Psi)_{ii} = \tan^{-1}\left(W_T^{\wedge} / W_R^{\wedge}\right)_{ii} \qquad \text{.....(38)}$$

The friction force on the inner surface of the ring and at outer surface of the ring can be evaluated as;

$$F_{r_1} = 2\left(\int_0^{L/2}\int_{-1}^{2} -\frac{h_1}{2}\frac{\partial P_1}{\partial\bar{\ }}d\bar{\ }dz + \int_0^{L/2}\int_{-1}^{2}\frac{h_1}{2}\frac{,_1}{3}\frac{\partial P_1}{\partial\bar{\ }}d\bar{\ }dz + \int_0^{L/2}\int_{-1}^{2}\frac{U_j R_1}{h_1}\left(1+,_0\right)d\bar{\ }dz\right) \qquad \text{.....(39)}$$

$$F_{r_2} = 2\left(\int_0^{L/2} \int_{-1}^{2} \frac{h_2}{2} \frac{\partial P_2}{\partial} d\, dz + \int_0^{L/2} \int_{-1}^{2} \frac{h_2}{2} \frac{1}{3} \frac{\partial P_2}{\partial} d\, dz + \int_0^{L/2} \int_{-1}^{2} \frac{U_r R_2}{h_2} (1+0) d\, dz \right) \quad \text{.....(40)}$$

The friction coefficient is defined as the ratio of the friction force by the total load carried;

$$\left(\hat{f} \right)_{ii} = \frac{\left(\hat{F}_r \right)_{ii}}{\left(\hat{W} \right)_{ii}} \quad \text{.....(41)}$$

if ii=1 $\left(\hat{f} \right)_{ii} = \hat{f}_1$ friction coefficient for journal –porous floating ring oil film,

and

ii= 2 $\left(\hat{f} \right)_{ii} = \hat{f}_2$ friction coefficient for porous floating ring – porous bearing oil film.

4- Steady State Performance:

For the steady – state condition, the modified Reynolds' equation **(1)** is solved simultaneously with the Darcy's equation **(11)** using an improved boundary conditions [equations **(25)** and **(31)**]. The solution yields the bearing dimensionless pressure fields, so, the above bearing parameters can be calculated. The hydrodynamic action would eventually force the ring to rotate at a speed governed by bearing assembly and bearing parameters. To calculate the load carrying capacity and the frictional torque on the journal, it is necessary to find those positions of the journal and the ring centers with respect to the bearing center at which the ring is in steady state equilibrium, that is the eccentricity ratio, attitude angles for inner and outer films and the journal speed must be established. So in steady – state, operating regimes at fixed journal speeds, i.e., the magnitude and the direction of inner and outer films loads must be equal, and the frictional torques acting on ring outer and inner surfaces must be equal and opposite thus;

$$F_{r_1} R_1 = F_{r_2} R_2 \quad \text{.....(42)}$$

By substitute equations **(39)** and **(40)** into equation **(42)** the dimensionless torques equation would be obtained as;

$$\hat{T}_{inner} = \int_0^{1} \int_{-1}^{2} \frac{-\hat{h}_1}{2} \frac{\partial \hat{P}_1}{\partial} d\, d\hat{Z} + \int_0^{1} \int_{-1}^{2} \frac{\hat{h}_1}{2} \frac{1}{3} \frac{\partial \hat{P}_1}{\partial} d\, d\hat{Z} + \int_0^{1} \int_{-1}^{2} \frac{1-0}{\hat{h}_1} d\, d\hat{Z} \quad \text{.....(43)}$$

$$T_{outer}^{\wedge} = \int_{0}^{1}\int_{-1}^{2} \frac{h_2^{\wedge}}{2}\frac{\partial P_2^{\wedge}}{\partial \bar{}}\, d\bar{}\, dZ^{\wedge} + \int_{0}^{1}\int_{-1}^{2} \frac{h_2^{\wedge}}{2}\frac{\bar{}_1}{3}\frac{\partial P_2^{\wedge}}{\partial \bar{}}\, d\bar{}\, dZ^{\wedge} + \int_{0}^{1}\int_{-1}^{2} \frac{1-\bar{}_0}{h_2^{\wedge}}\, d\bar{}\, dZ^{\wedge} \qquad \textbf{……(44)}$$

By equating the above non – dimensional torque equations the ratio of porous floating ring speed to the journal speed can be determined as follows;

$$\frac{N_r}{N_j} = \frac{T_{inner}^{\wedge}}{T_{outer}^{\wedge}} * \frac{R_1^3}{R_2^3} * \frac{c_2}{c_1} \qquad \textbf{……(45)}$$

The second equilibrium conditions which specify the steady state performance of the bearing is the load balance which state that;

$$W_1^{\wedge} = W_2^{\wedge} \qquad \textbf{……(46)}$$

5- Method of Solution:

The solution of system of partial differential equations can be greatly simplified by a well – constructed grid. The dimensionless oil film pressure distribution $\left(P^{\wedge}\right)_{ii}$ and the dimensionless oil pressure distribution through the porous matrix $\left(P^{\wedge *}\right)_{jj}$ can be obtained by simultaneously solving equations (**1**) and **(11)**.

These equations are discretized yielding the mesh size of **(N_1)** in circumferential direction, **(N_2)** across the half – width of the bearing and **(N_3)** across the thickness of the porous media. In the present analysis **(180)** divisions in circumferential direction (**N_1**) **((100)** divisions for the rupture zone **(N_{11})** and **(80)** divisions for the effective zone **(N_{12}))**, sixteen divisions in axial direction **(N_2)** and eight divisions in radial direction **(N_3)** has been adopted. The difference equations derived from this discretization are solved by successive relaxation scheme. To obtain the pressure and the location of the inlet and trailing boundary lines for the oil – film regions, the iteration is continued until the following inequalities are satisfied simultaneously,

$$\left(\frac{\sum\sum\sum \left| P_{i,j,k}^{\wedge *(n+1)} - P_{i,j,k}^{\wedge *(n)} \right|}{\sum\sum\sum \left| P_{i,j,k}^{\wedge *(n)} \right|} < 10^{-5} \right)_{jj} \qquad \textbf{……(47)}$$

$$\left(\frac{\sum\sum \left| P_{j,k}^{\wedge(n+1)} - P_{j,k}^{\wedge(n)} \right|}{\sum\sum \left| P_{j,k}^{\wedge(n)} \right|} < 10^{-5} \right)_{ii} \qquad \text{.....(48)}$$

$$\left(\left| M_{-1}^{\wedge} - M_{-2}^{\wedge} - M_{-c}^{\wedge} - M_{-b}^{\wedge} \right| / M_{-1}^{\wedge} < 10^{-3} \right)_{ii} \qquad \text{.....(49)}$$

$$\left(\left| q_{-p} / q_{-c} \right| \right)_{ii} = \left(\left| \left(\frac{(1+,1)}{6(1+,0)} h^{\wedge 2} \int_0^1 \frac{\partial P^{\wedge}}{\partial \bar{-}} dz^{\wedge} \right)_{\bar{-}=\bar{-}2} \right| < 10^{-3} \right)_{ii} \qquad \text{.....(50)}$$

To ensure the steady state performance of the bearing, the following equilibrium conditions must be satisfied;

- torque equilibrium :

$$\left| T_{inner} - T_{outer} \right| < 10^{-3} \qquad \text{.....(51)}$$

- load equilibrium :

$$\left| W_1^{\wedge} - W_2^{\wedge} \right| < 10^{-3} \qquad \text{.....(52)}$$

Always (n) and (n+1) used in above equations denote two consecutive iterations and the points i, j, k represent the grid number in radial, circumferential, and axial directions respectively.

6- Results and Discussion:

A suitable computer program was written in FORTRAN-90 to solve the governing equations. The result of the program was tested by solving the problem pf porous bearing and compared the obtain results with that published in the available literatures Kaneko et. al. (1997), as shown in figures (3) and (4).

Figures (5) and (6) present the effect of the supply pressure on the oil pressure distribution generated in both oil films. These figures show that increasing the supply pressure yields a higher pressure peak in the positive oil film pressure in both oil films and a higher oil films extent. This is

can be proposed to the higher oil flow out of the porous material with increasing the supply pressure.

The supply pressure seems to have lower effect on the speed ratio as shown in figure (7). It can be shown from this figure that slight increase in speed ratio with decreasing the supply pressure due to the increase in friction force applied to both sides of the ring in this case.

The effect of the oil supply pressure on the oil – film extent can be shown in figures (8) and (9). These figures show the variation of oil film extent with Sommerfeld number. In these figures the curves in the range $\theta < 180$ deg. correspond to the inlet end of the film extent (θ_1) while those in the range $\theta > 180$ deg. correspond to the trailing end (θ_2). The oil – film extent increases with increasing values of supply pressure, since the oil flow into the clearance gap increases in this case. Furthermore, increasing Sommerfeld number mainly decreases the oil leakage into the porous matrix due to the reduction in the magnitude of hydrodynamic pressure generated in the oil film, hence the oil film extent increases.

The effect of supply pressure on the coefficient of friction for both oil films can be shown in figures (10) and (11). Referring to these figures it is clear that the values of Sommerfeld number which gives the minimum friction coefficient decreases with increasing the supply pressure. This is due to the fact that the angular oil – film extent increases with increasing the supply pressure which allows the system to work under the hydrodynamic lubrication condition.

The attitude angle also increase with increasing the supply pressure, this is owing to an increase in the amount of the oil supplied to the clearance of the bearing through the porous matrix. as shown from figures (12) and (13). It can be shown from these figures that the attitude angle increases with increasing the supply pressure. This is attributed to the fact that the oil – film extent increases with increasing the supply pressure which allows the bearing to work under the hydrodynamic lubrication condition.

7- Conclusions:

The static characteristics of porous floating ring journal are theoretically investigated assuming that the oil fed through their outside diameter of the bearing under small supply pressure. The integral momentum theorem equation to the oil – film regions was proposed for the circumferential boundary condition of the oil – films pressure. The oil – films pressure distributions were solved numerically using the integral momentum equation and continuity equation, the present analysis yield negative pressure before the trailing ends of the oil – film regions. Numerical results obtained show that the dimensionless oil – fed pressure significantly influences the static characteristics of the porous floating ring journal bearing.

Increasing the oil supply pressure:

- Increases the value of the peak pressure of the oil – films.
- Decreases the minimum value of the coefficient of friction.
- Increasing the oil – film extent.
- It has a little effect on the ring speed.
- Increases the attitude angle.

In the present analysis a negative pressure was obtained before the trailing end.

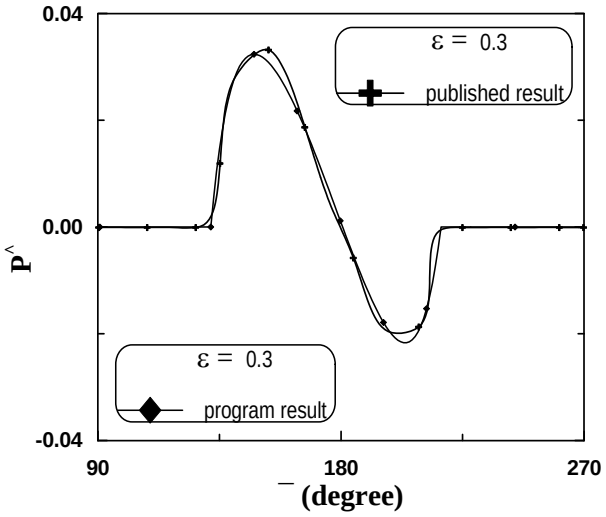

Figure (3), Comparison Between Published and Program Results for Pressure Distribution at $P^{\wedge}_S = 0.1$, $\varepsilon=0.3$

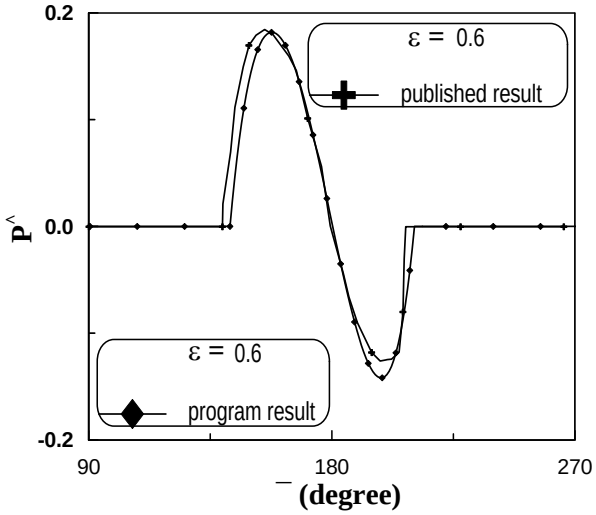

Figure (4), Comparison Between Published Program Results for Pressure Distribution at $P^{\wedge}_S = 0.1$, $\varepsilon=0.6$

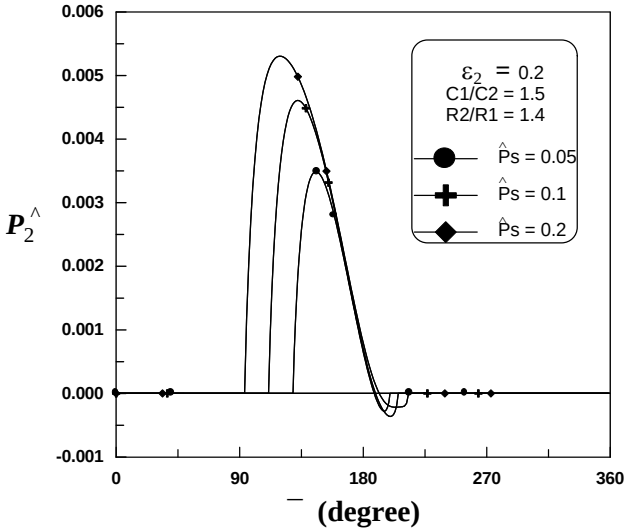

Figure (5), Computed Results for Circumferential Pressure Distribution in Ring – Bearing Clearance Gap for Various Values of Dimensionless Oil – Feed Pressure.

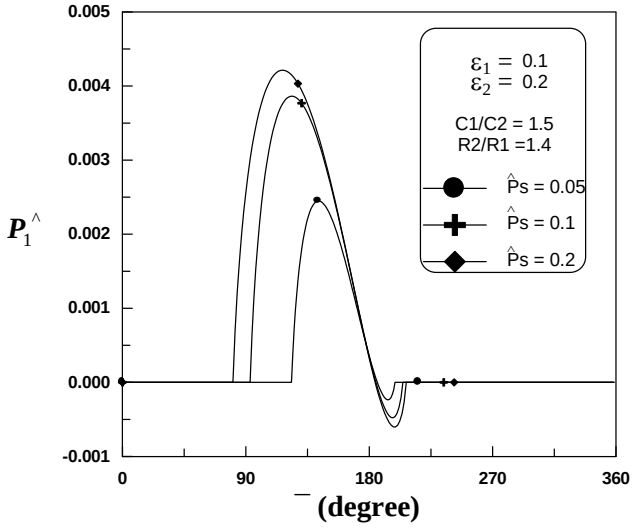

Figure (6), Computed Results for Circumferential Pressure Distribution in Journal – Ring Clearance Gap for Various Values of Dimensionless Oil – Feed Pressure.

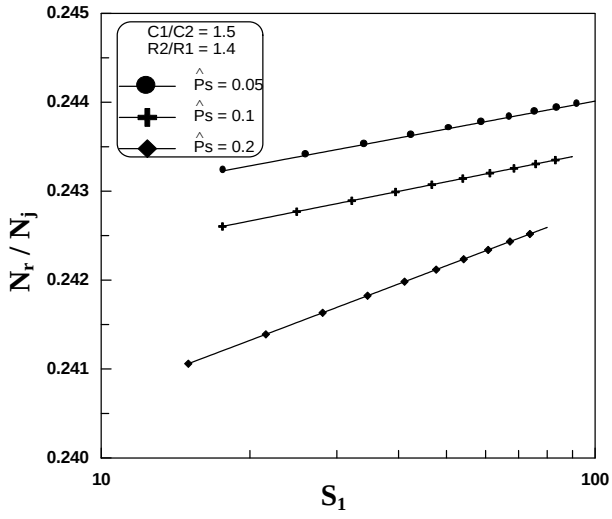

Figure (7), Computed Results Sommerfeld Number Versus Ring to Journal Speed Ratio for Various Values of Dimensionless Oil – Feed Pressure.

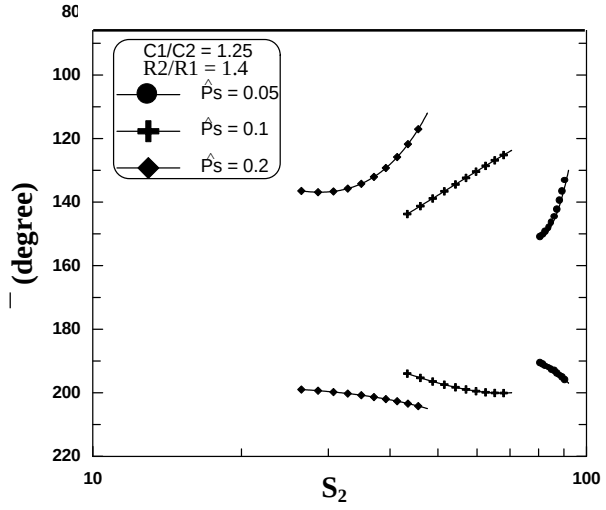

Figure (8), Computed Results for Outer Oil – Film Extent VersusSommerfeld Number for Various Values of Dimensionless Oil – Feed Pressure.

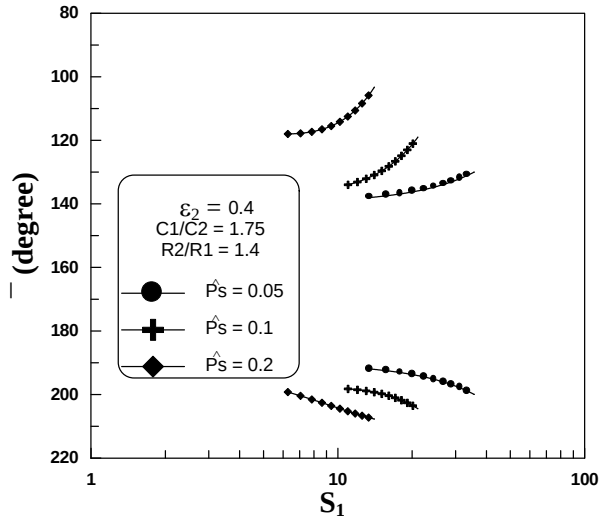

Figure (9), Computed Results for Inner Oil – Film Extent Versus Sommerfeld Number for Various Values of Dimensionless Oil – Feed Pressure.

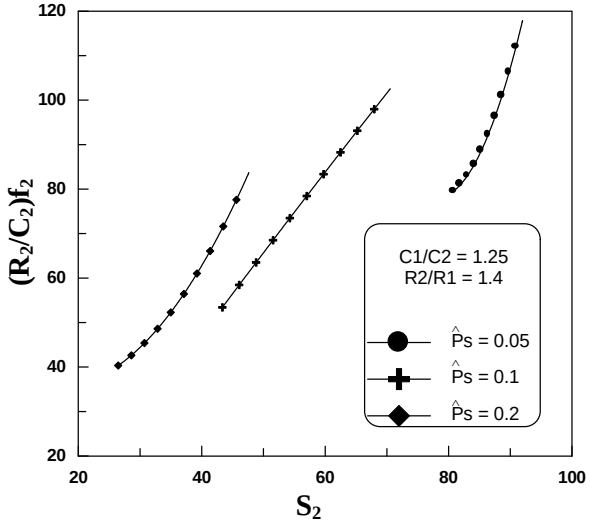

Figure (10), Friction Coefficient of Outer Oil – Film Versus Sommerfeld Number for Various Values of Dimensionless Oil – Feed Pressure.

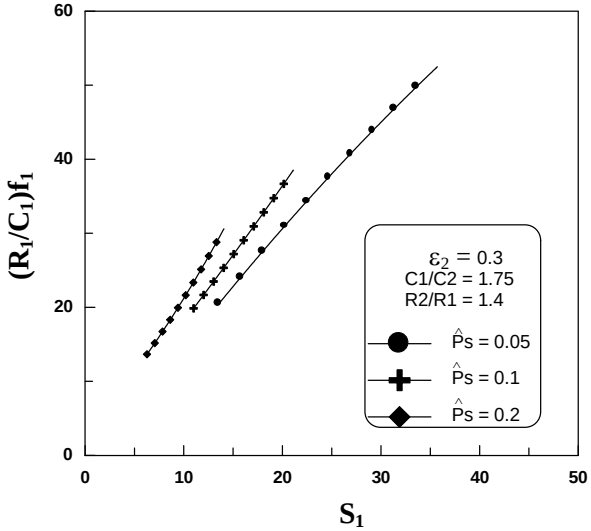

Figure (11), Friction Coefficient of Inner Oil – Film Versus Sommerfeld Number for Various Values of Dimensionless Oil – Feed Pressure.

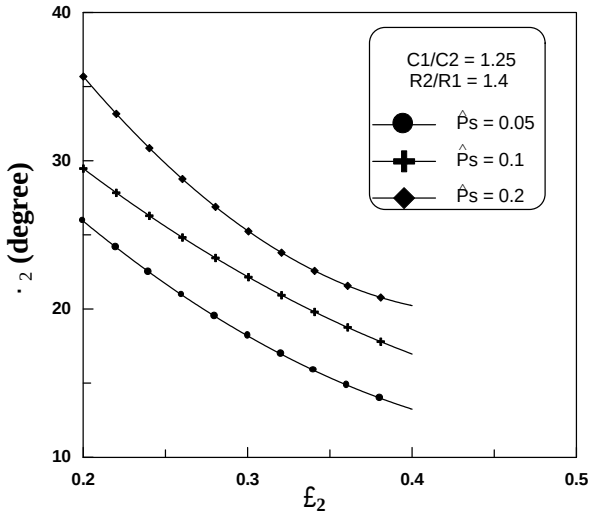

Figure (12), Attitude Angle of Outer Oil – Film Versus Ring Eccentricity Ratio for Various Values of Dimensionless Oil – Feed Pressure.

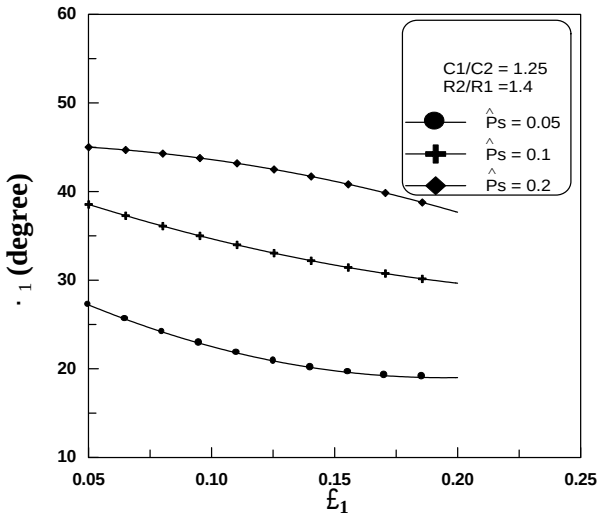

Figure (13), Attitude Angle of Inner Oil – Film Versus Journal Eccentricity Ratio for Various Values of Dimensionless Oil – Feed Pressure.

References:

Hill, H., C., 1958, "Slipper Bearing and Vibration Control in Small Gas Turbines, Trans. ASME, vol. 80, pp. 1759-1764.

Pinkus O. and Sternlicht B., 1961, "Theory of Hydrodynamic Lubrication". McGaw Hill, New York.

Tondl, A., 1965, "Some Problems of Rotor Dynamics", Chapman and Hall, London, pp. 155-160,200-201.

Lund, J., W., 1966, "Self-Excited, Stationary Whirl Orbits of a Sleeve Bearing", Ph.D Thesis, Rensselaer Polytechnic Institute.

Orcutt, F. K., and Ng. C.W. 1968, "Steady – State and Dynamic Properties of the Floating Ring Journal Bearing", ASME Journal of Lubrication Technology, vol. 90, pp. 1 – 10.

Tatara, A., 1969, "Vibration Suppressing Effect of Floating Bush Bearings", Journal of ASME vol., 72, pp. 1564-1569.

Tanaka, M. and Hori, Y., 1972, "Stability Characteristics of Floating Bush Bearings", ASME Journal of Lubrication Technology, July, vol. 94, pp. 248-259.

Li, C. H., and Rohde, S. M., 1981, "On the Steady State and Dynamic Performance Characteristics of Floating Ring Bearings", ASME Journal of Lubrication Technology, July, vol. 103, pp. 389 – 397.

Li, C. H., 1982, "Dynamic of Rotor Bearing System Supported by Floating Ring Bearing", ASME, Journal of Lubrication Technology, October, vol. 104, pp. 469 – 476.

Dong, X., and Zhao, Z., 1990, "Experimental and Analytical Research on Floating – Ring Bearing for Engine Applications", Journal of Tribology, January, vol. 112, pp. 119 – 122.

Yeon – Min Cheong and Kyung – Wood Kim, 2001, "Operating Characteristics of Counter – rotating Floating Ring Journal Bearings", KSTLE International Journal, December, vol. 2, No. 2, pp. 127 – 132.

Andres, L. San, and Kerth, J., 2004, "Thermal Effect on the Performance of Floating Ring Bearings for Turbochargers", Proc. Instri. Mech. Engrs., Part J., J. Engineering Tribology, vol. 218, pp.437 – 450.

Morgan, V. T., and Cameron, A., 1957, "Study of the Design Criteria for Porous Metal Bearings", Conference on Lubrication and Wear, Institution of Mechanical Engineers, London, paper No. 88, pp. 405 – 408.

Rouleau, W. T., 1963, "Hydrodynamic lubrication of Narrow Press-Fitted Porous Metal Bearing," ASME Journal of Basic Engineering, vol., 85 pp. 123-128.

Goldstein, M. E., and Braun, W, H., 1971, "Effect of Velocity Slip at a Porous Boundary on the Performance of an Incompressible Porous Bearing." NASA Technical Note TN D-6181.

Cusano, C., 1979, "An analytical Study of Starved Porous Bearings", Transactions of the ASME, January, vol. 101, pp. 38 – 47.

Reason, B. R., and DYER, D., 1973, "A Numerical Solution for the Hydrodynamic Lubrication of Finite Porous Journal Bearings." Proceedings of the Institution of Mechanical Engineers, vol. 187, pp. 71-78.

Prakash, J., and Vij, S., K., 1974, "Analysis of Narrow Porous Journal Bearing Using Beavers – Joseph Criterion of Velocity Slip", Transaction of the ASME, June, pp. 348 – 354.

Kaneko, S., Ohkawa, Y., Hashimoto, Y., 1994, "A Study of Mechanism of Lubrication in Porous Journal Bearings: Effect of Dimensionless Oil –Feed Pressure on Static Characteristics Under Hydrodynamic Lubrication Conditions", Transactions of the ASME, July, vol. 116, pp. 606 – 610.

Kaneko, S., Hashimoto, Y., and Hiroki, I., 1997, "Analysis of Oil – Film Pressure Distribution in Porous Journal Bearings Under Hydrodynamic Lubrication Conditions Using An Improved Boundary Condition", Journal of Tribology, January, vol. 119, pp. 171 – 177.

Abdallah A., Elsharkawy, Lotfi H., Guedouar, 2001, "Hydrodynamic Lubrication of Porous Journal Bearing Using a Modified Brinkman-Extended Darcy Model", Tribology International (34), July, pp. 767-777.

Quan Yong – Xin and Wang Pei – Ming, 1985, "Theoretical Analysis and Experimental Investigation of Porous Metal Bearing", Tribology International, April, vol. 18, No. 2, pp. 67 – 73.

Nomenclature:

The following symbols are generally used throughout the text. Others are defined as when used.

c	Mean Radial Clearance (m)
c_1	Journal – Ring Mean Radial Clearance (m)
c_2	Ring – Bearing Mean Radial Clearance (m)
$(D)_{ii}$	Inside Diameter of Ring and Bearing, $(D)_{ii} = (2*R)_{ii}$ (m)
$(h)_{ii}$	Oil – Film Thickness (m)
$(h_{\theta 1})_{ii}$	Oil – Film Thickness at Inlet End (m)
$(h_{\theta 2})_{ii}$	Oil – Film Thickness at Trailing End (m)
$(h\hat{})_{ii}$	Dimensionless Film Thickness,($h\hat{} = h/c)_{ii}$
k_1	Permeability of the Porous Matrix (m^2)
L	Length of the Ring and the Bearing Length (m)
$(M_{\theta 1})_{ii}$	Circumferential Momentum Flow Rate across Oil Film Surface at Inlet End of Oil – Film Region, i.e. at $(\theta = \theta_1)_{ii}$ (N)
$(M\hat{}_{\theta 1})_{ii}$	Dimensionless Circumferential Momentum Flow Rate across Oil – Film Surface at Inlet End of Oil–Film Region, i.e. at $(\theta = \theta_1)_{ii}$
$(M_{\theta 2})_{ii}$	Circumferential Momentum Flow Rate across Oil – Film Surface at Trailing End of Oil – Film Region, i.e. at $(\theta = \theta_2)_{ii}$ (N)
$(M\hat{}_{\theta 2})_{ii}$	Dimensionless Circumferential Momentum Flow Rate across Oil – Film Surface at Trailing End of Oil–Film Region, i.e. at $(\theta = \theta_2)_{ii}$
$(M_{\theta c})_{ii}$	Circumferential Momentum Flow Rate across Oil – Film Surface at Both Axial Ends ($z = \pm L/2$) (N)
$(M\hat{}_{\theta c})_{ii}$	Dimensionless Circumferential Momentum Flow Rate across Oil – Film Surface at Both Axial Ends i.e. at ($z = \pm L/2$)
$(M_{\theta b})_{ii}$	Circumferential Momentum Flow Rate across Oil – Film Surface

	Adjacent to Bearing (y = 0) (N)
$(M^{\wedge}_{\theta b})_{ii}$	Dimensionless Circumferential Momentum Flow Rate across Oil – Film Surface Adjacent to Bearing (y = 0)
N_j	Journal Rotational Speed (r.p.m)
N_r	Floating Ring Rotational Speed (r.p.m)
N_r/N_j	Ring to Journal Speed Ratio
$(P)_{ii}$	Oil – Film Pressure (N/m^2)
$(P^{\wedge})_{ii}$	Dimensionless Oil-Film Pressure, $(P^{\wedge} = c^2P/(R^2 \eta\omega))_{ii}$
$(P^{*})_{jj}$	Oil – Film Pressure Inside the Porous Matrix (N/m^2)
$(P^{\wedge *})_{jj}$	Dimensionless Oil – Film Pressure Inside the Porous Matrix, $(P^{\wedge *} = c^2P^{*}/(R^2\eta\omega))_{jj}$
P_s	Supply Pressure (N/m^2)
$P_s^{\wedge}$	Dimensionless Supply Pressure, $P_s^{\wedge} = P_s\ (c_2)^2/(R^2\ \eta\omega))_{ii}$
$(q_{\theta p})_{ii}$	Poiseuilles' flow (m^3/sec)
$(q_{\theta c})_{ii}$	Couettes' flow(m^3/sec)
R_j	Journal Radius(m)
R_1	Ring Inner Radius (m)
R_2	Ring Outer Radius (m)
R_3	Bearing Inner Radius (m)
R_4	Bearing Outer Radius (m)
R	Radial Coordinate with Origin at the Center of the Bearing
$(S)_{ii}$	Sommerfeld Number , $(S= (R\eta\omega L / W)*(R / c)^2)_i$
$(T)_{ii}$	Frictional Torque (N.m)
$T^{\wedge}_{inner}$	Dimensionless Frictional Torque at the Inner Surface of Ring, $T^{\wedge}_{inner}= T_{inner}\ c_1 / \eta\omega_j R^3_1 L$
$T^{\wedge}_{outer}$	Dimensionless Frictional Torque at the Outer Surface of Ring, $T^{\wedge}_{outer}= T_{outer}\ c_2 / \eta\omega_r R^3_2 L$
U_j	Journal Velocity (m/s)
U_r	Ring Velocity (m/s)
u,v,w	Oil – Film Velocity Components in θ,r,z Directions Respectively(m/s)
u^{*},v^{*},w^{*}	Oil Velocity Components inside the Porous Matrix in θ,r,z Directions Respectively (m/s)
$(u_z)_{ii}$	Axial Velocity of Oil in Clearance Gap(m/s)

$(u^*_r)_{jj}$ Radial Filter Velocity of Oil in Porous Matrix(m/s)

$(u_\theta)_{ii}$ Circumferential Velocity of Oil in Clearance Gap(m/s)

$(u_{\theta m})_{ii}$ Circumferential Velocity of Oil across the Control Surface at (y=0), (Ring and Bearing Surface)(m/s)

$(W)_{ii}$ Load Carrying Capacity (N)

$(W^\wedge)_{ii}$ Dimensionless Load Carrying Capacity, $(W^\wedge)_{ii}=(W\ c^2 / \eta\omega R^3 L)_{ii}$

$(W_r)_{ii}$ Component of Oil – Film Force Along the Line of Centers (N)

$(W^\wedge_r)_{ii}$ Dimensionless Component of Oil – Film Force Along the Line of Centers, $(W^\wedge_r)_{ii} =(W_r\ c^2 / \eta\omega R^3 L)_{ii}$

$(W_T)_{ii}$ Component of Oil – Film Force Perpendicular to the Line of Centers (N)

$(W^\wedge_T)_{ii}$ Dimensionless Component of Oil – Film Force Perpendicular to the Line of Centers, $(W^\wedge_T)_{ii} =(W_T\ c^2 / \eta\omega R^3 L)_{ii}$

z Axial Coordinate with Origin at middle of Bearing Length

y Coordinate in the Direction of Oil – Film Thickness with Origin at Inner Surface of Floating Ring and Bearing

Greek Symbols

$(\beta)_{ii}$ Angular Extent of Oil Film, $(\beta)_{ii} = (\theta_2 - \theta_1)_{ii}$ (degree)

ε Eccentricity Ratio

ε_1 Journal-Ring Eccentricity Ratio

ε_2 Ring- Bearing Eccentricity Ratio

η Absolute Viscosity of Oil(pa . s)

θ Angular Coordinate from Maximum Film Thickness Position

$(\theta_1)_{ii}$ Angle from Line of Centers to Inlet End of Oil – Film Region, (Degree)

$(\theta_2)_{ii}$ Angle from Line of Centers to Trailing End of Oil – Film Region, (Degree)

$((R/c)\mu)_{ii}$ Coefficient of Friction

$(\mu^\wedge)_{ii}$ Dimensionless Friction Coefficient

$= (R_1/c_1)\mu_1$ in case of journal / floating ring oil film

$= (R_2/c_2)\ \mu_2$ in case of floating ring /bearing oil film

ρ Density of oil (kg/m^3)

$(\hat{\tau})_{ii}$ Dimensionless Shear Stress

$(\Phi)_{ii}$ Permeability parameter, $(\Phi)_{ii} = (k_1 R / c^3)_{ii}$

ψ_1 Journal-Ring Attitude Angle (degrees)

ψ_2 Ring- Bearing Attitude Angle (degrees)

ω_j Journal Rotational Speed (rad/sec)

ω_r Floating Ring Rotational Speed (rad/sec)

Subscript

b Referring to Bearing

ii =1 referred for Journal – Ring Oil – Film

=2 referred for Ring – bearing Oil – Film

jj =1 for Porous Matrix of Floating Ring

=2 for Porous Matrix of Bearing

j Referring to Journal

i,j,k Grid Number in Radial, Circumferential and Axial Direction, Respectively

r Referring to Floating Ring

s Supply Condition

Superscript

^ Dimensionless Quantity

* Porous Parameters

APPENDIX A

Assuming steady state, thin film, negligible body forces, and an incompressible Newtonian lubricant having constant properties, the Navier – Stokes equation of the problem is reduced to

$$\frac{\partial^2 u_{ii}}{\partial y^2} = \frac{1}{\mu}\left(\frac{\partial P}{\partial x}\right)_{ii} \qquad \text{.....(A1)}$$

$$\frac{\partial P}{\partial y} = 0 \qquad \text{.....(A2)}$$

$$\frac{\partial^2 w_{ii}}{\partial y^2} = \frac{1}{\mu}\left(\frac{\partial P}{\partial z}\right)_{ii} \qquad \text{.....(A3)}$$

Equations **(A1)**,**(A2)** and **(A3)** are the equilibrium equations for the oil film of fluid in x, y, and z directions respectively, where;

ii =1 for the journal – porous floating ring oil film

ii =2 for porous floating ring – porous bearing oil film

Equation **(A1)** and **(A3)** can be integrated directly to yield general velocity distributions in x, z directions,

$$u_{ii} = \frac{1}{2\mu}\left(\frac{\partial P}{\partial x} y^2 + CC_1 y + CC_2\right)_{ii} \qquad \text{.....(A4)}$$

$$w_{ii} = \frac{1}{2\mu}\left(\frac{\partial P}{\partial z} y^2 + CC_3 y + CC_4\right)_{ii} \qquad \text{.....(A5)}$$

where CC_1,CC_2,CC_3 and CC_4 are constants to be found from the following boundary conditions,

if ii =1 at y = h_1 $u_{ii} = U_j$

at y = 0 $u_{ii} = u_{ii}(x,0,z) = u_1(x,0,z)$

if ii =2 at y = h_2 $u_{ii} = U_r$

at y = 0 $u_{ii} = u_{ii}(x,0,z) = u_2(x,0,z)$ **……(A6)**

and

if ii =1 at y = h_1 $w_{ii} = 0$

at y = 0 $w_{ii} = w_{ii}(x,0,z) = w_1(x,0,z)$ permeable floating ring interface

if ii =2 at y = h_2 $w_{ii} = 0$

at y = 0 $w_{ii} = w_{ii}(x,0,z) = w_2(x,0,z)$ permeable bearing interface

……..(A7)

Substitute equations **(A6)** and **(A7)** in equations **(A4)** and **(A5)** respectively, the values of constants CC_1, CC_2, CC_3, and CC_4 can be evaluated as;

$$\left.\begin{aligned} CC_1 &= \frac{u_{ii} - u_{ii}(x,0,z)}{h_{ii}} - \frac{h_{ii}}{2\mu}\left(\frac{\partial P}{\partial x}\right)_{ii} \\ CC_2 &= u_{ii}(x,0,z) \end{aligned}\right\} \quad \text{……(A8)}$$

$$\left.\begin{aligned} CC_3 &= -\frac{h_{ii}}{2\mu}\left(\frac{\partial P}{\partial z}\right)_{ii} - \frac{w_{ii}(x,0,z)}{h_{ii}} \\ CC_4 &= w_{ii}(x,0,z) \end{aligned}\right\} \quad \text{……(A9)}$$

Substitute equation **(A8)** in **(A4)** and equation **(A9) in (A5)** to obtain general equations of the velocity distributions in x and z directions,

$$u_{ii} = \frac{1}{2\mu}\left(\frac{\partial P}{\partial x}\right)_{ii} y(y - h_{ii}) + \frac{U_{ii} - u_{ii}(x,0,z)}{h_{ii}} y + u_{ii}(x,0,z) \qquad \textbf{.....(A10)}$$

$$w_{ii} = \frac{1}{2\mu}\left(\frac{\partial P}{\partial z}\right)_{ii} y(y - h_{ii}) - w_{ii}(x,0,z)\frac{y}{h_{ii}} + w_{ii}(x,0,z) \qquad \textbf{.....(A11)}$$

Again when

ii=1 the $h_{ii}=h_1$, $u_{ii}=U_j$, $u_{ii}(x,0,z) = u_1(x,0,z)$, $w_{ii}(x,0,z)=w_1(x,0,z)$

.....(A12)

and

ii=2 the $h_{ii}=h_2$, $u_{ii}=U_r$, $u_{ii}(x,0,z) = u_2(x,0,z)$, $w_{ii}(x,0,z)=w_2(x,0,z)$

.....(A13)

According to the slip velocity model postulated by **Beavers and Joseph, 1967, [11],** the boundary condition on u_{ii} (x,0,z) and w_{ii} (x,0,z) at the permeable floating ring and bearing films interface (y=0) are seen in Figure(A1).

$$\left|\frac{\partial u_{ii+1}}{\partial y}\right|_{y=0} = \frac{\sim}{\sqrt{k_1}}\left(u_{ii}(x,0,z) - u_{ii}^{*}(x,0,z)\right) \qquad \textbf{.....(A14)}$$

$$\left|\frac{\partial w_{ii+1}}{\partial y}\right|_{y=0} = \frac{\sim}{\sqrt{k_1}}\left(w_{ii}(x,0,z) - w_{ii}^{*}(x,0,z)\right) \qquad \textbf{.....(A15)}$$

Using the assumption that within the oil film the radial pressure gradient $\partial P/\partial x$ and the axial pressure gradient $\partial P/\partial z$ are independent of the film thickness, according to the Darcy's law and continuity equation of

pressure at the interface between the porous (floating ring and bearing) and the oil film, we obtain ;

$$u_{ii}^{*}(x,0,z) = -\frac{k_1}{\text{¦}}\left(\frac{\partial P^{*}}{\partial x}\right)_{jj} \qquad \textbf{.....(A16)}$$

$$w_{ii}^{*}(x,0,z) = -\frac{k_1}{\text{¦}}\left(\frac{\partial P^{*}}{\partial z}\right)_{jj} \qquad \textbf{.....(A17)}$$

Different equations **(A10)** and **(A11)** with respect to y at y=0, substituting the results of equations **(A16)** and **(A17)** in equations **(A14)** and **(A15)**, $u_{ii}(x,0,z)$ and $w_{ii}(x,0,z)$ can be found as;

$$u_{ii}(x,0,z) = \left(\frac{h\sqrt{k}}{h\sim + \sqrt{k}}\left(-\frac{1}{2\text{¦}}\frac{\partial P}{\partial x}\left(h + 2\sim\sqrt{k}\right) + \frac{U}{h}\right)\right)_{ii} \qquad \textbf{.....(A18)}$$

$$w_{ii}(x,0,z) = \left(\frac{h\sqrt{k}}{h\sim + \sqrt{k}}\left(-\frac{1}{2\text{¦}}\frac{\partial P}{\partial z}\left(h + 2\sim\sqrt{k}\right)\right)\right)_{ii} \qquad \textbf{.....(A19)}$$

Substituting for $u_{ii}(x,0,z)$ and $w_{ii}(x,0,z)$, in equation **(A10)** and **(A11)** can be written as;

$$u_{ii} = \frac{1}{2\text{¦}}\left(\frac{\partial P}{\partial x}\right)_{ii}(y - h_{ii})\left(y + \frac{1}{3}h_{ii\text{,}1x}\right) + \frac{U_{ii}}{h_{ii}}\left(y(1-\text{,}_{0x}) + h\text{,}_{0x}\right)_{ii} \qquad \textbf{.....(A20)}$$

$$w_{ii} = \frac{1}{2\text{¦}}\left(\frac{\partial P}{\partial z}\right)_{ii}(y - h_{ii})\left(y + \frac{1}{3}h_{ii\text{,}1z}\right) \qquad \textbf{.....(A21)}$$

where;

$$(,_{0x})_{ii} = \frac{\left(\sqrt{k_1}/\sim\right)}{\sqrt{k}_1/\sim + h_{ii}} \qquad \textbf{.....(A22)}$$

$$(,_{1x})_{ii} = (,_{1z})_{ii} = \frac{3\left(2k_1 + h_{ii}\sqrt{k}_1/\sim\right)}{h_{ii}\left(\sqrt{k_1}/\sim + h_{ii}\right)} \qquad \textbf{.....(A23)}$$

The Reynolds' equation is formed by introducing these expressions into the continuity equation and integrated with respect to (y), with limits from y=0 to y=h_{ii} . The integral for steady state becomes;

$$\int_0^{h_{ii}} \frac{\partial}{\partial x}(\circ u_{ii})dy + \int_0^{h_{ii}} \frac{\partial}{\partial z}(\circ w_{ii})dy + \int_0^{h_{ii}} \frac{\partial}{\partial y}(\circ v_{ii})dy = 0 \qquad \textbf{.....(A24)}$$

which can be rewritten as

$$\int_0^{h_{ii}} \frac{\partial}{\partial x}(\circ u_{ii})dy + \int_0^{h_{ii}} \frac{\partial}{\partial z}(\circ w_{ii})dy + \circ v\Big|_0^{h_{ii}} = 0 \qquad \textbf{.....(A25)}$$

The third term of left hand of equation **(A25)** can be written as;

$$\circ\left(vh_{ii} - v_0\right) \qquad \textbf{.....(A26)}$$

$$\because\ v_{h_{ii}} = 0 \qquad \textbf{.....(A27)}$$

and the velocity of fluid equals the volume of flow per unit area,

$$v_0 = -\frac{k_1}{\vdots}\left(\frac{\partial P_{jj}^*}{\partial r}\right)_{r=r_{ii}} \qquad \textbf{.....(A28)}$$

Substituting equation **(A20), (A21), (A27)** and **(A28)** into the continuity equation **(A25)** and integrating the result over the film thickness, the modified Reynolds' equation with slip velocity can be written as;

$$\frac{\partial}{\partial x}\left(h^3\left(1+\beta_{1x}\right)\frac{\partial P}{\partial x}\right)_{ii}+\frac{\partial}{\partial z}\left(h^3\left(1+\beta_{1x}\right)\frac{\partial P}{\partial z}\right)_{ii}=6U_{ii}\frac{\partial}{\partial x}\left(h\left(1+\beta_{0x}\right)\right)_{ii}-12k_1\left(\left.\frac{\partial P^*}{\partial y}\right|_{y=0}\right)_{jj}$$

……..(A29)

The modified Reynolds' equation as in **(A29)** by using the cylindrical coordinates and dimensionless form can be rewritten as **[18]**;

$$\frac{\partial}{\partial\bar{}}\left(h^{\wedge 3}\left(1+\beta_1\right)\frac{\partial P^{\wedge}}{\partial\bar{}}\right)_{ii}+\left(\frac{D_{ii}}{L}\right)^2\frac{\partial}{\partial Z^{\wedge}}\left(h^{\wedge 3}\left(1+\beta_1\right)\frac{\partial P^{\wedge}}{\partial Z^{\wedge}}\right)_{ii}=6\frac{\partial}{\partial\bar{}}\left(h^{\wedge}\left(1+\beta_0\right)\right)_{ii}-12\Phi_{ii}\left(\left.\frac{\partial P^{\wedge *}}{\partial r^{\wedge}}\right|_{r^{\wedge}=1}\right)_{jj}$$

……(A30)

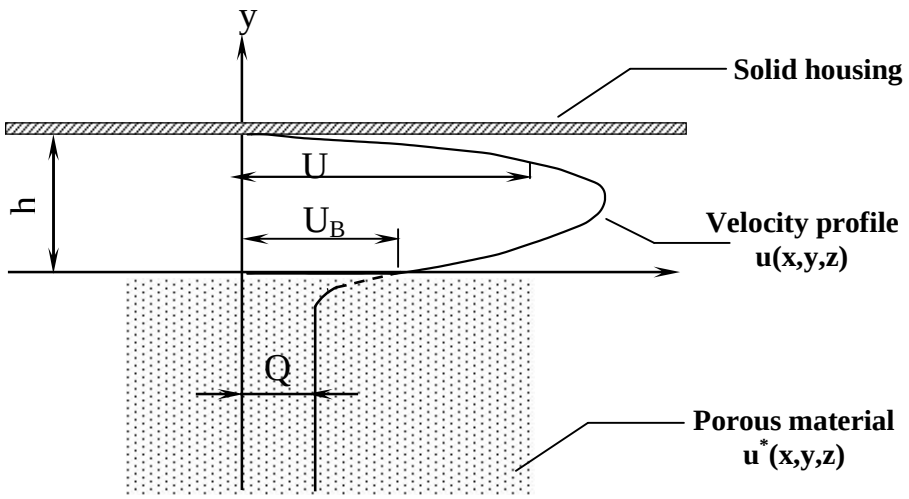

Figure (A1), The Torn Velocity Profile in Oil – Film

APPENDIX B

To derive the momentum equations and the momentum flow rates, starting from mass flow rate law which state;

$$\dot{m} = \rho Q \qquad \text{.....(B1)}$$

but,

$$Q = VA \qquad \text{.....(B2)}$$

the equation **(B2)** can be rewritten as;

$$\dot{m} = \rho VA \qquad \text{.....(B3)}$$

Therefore;

$$F = \rho V^{2} A \qquad \text{.....(B4)}$$

where;

ρ : The density of oil – film,

A: Cross section area,

$\dot{m}$: mass flow rate (kg/sec),

and

V : velocity of flow (m/sec.)

So;

$$\sum F = \sum M \qquad \text{.....(B5)}$$

i.e.

$$momentum = \rho V^2 \, dA \qquad \text{.....(B6)}$$

Figure (B-1) represents a cross sectional area of the porous matrix. From this figure it can be shown that;

$$dA = dy * dz \quad \text{for} \quad M_1 \text{ and } M_2 \qquad \text{.....(B7)}$$

$$dA = dy * d\bar{} \quad \text{for} \quad M_c \qquad \text{.....(B8)}$$

$$dA = d\bar{} * dz \quad \text{for} \quad M_b \qquad \text{.....(B9}$$

$\therefore$ M_1 can be calculated as **[18]**;

$$\left(M_1\right)_{ii} = 2\rho\left(\int_0^{L/2}\int_0^{h_1}\left(u\right)^2\Big|_1 dydz\right)_{ii} \qquad \text{.....(B10)}$$

where;

$$\left(u\right)_{ii} = \frac{1}{2\mu}\left(\frac{\partial P}{r\,\partial\theta}\right)_{ii}\left(y - h_{ii}\right)\left(y + \frac{1}{3}h_{ii,1x}\right) + \left(\frac{r\omega}{h}\right)_{ii}\left(y\left(1-\varepsilon_{0x}\right) + h_{\varepsilon,0x}\right)_{ii} \qquad \text{.....(B11)}$$

Substitute equation **(B11**) into equation **(B10)** to get;

$$\left(M_1\right)_{ii} = \left(2\rho\int_0^{L/2}\int_0^{h_1}\frac{1}{4\mu^2 r_{ii}^2}\left(\frac{\partial P}{\partial\theta}\right)_{ii}^2\left(y - h_{ii}\right)^2\left(y + \frac{1}{3}h_{\varepsilon,1}\right)_{ii}^2 + \frac{1}{\mu r_{ii}}\left(\frac{\partial P}{\partial\theta}\frac{r\omega}{h}\left(y - h\right)\right)_{ii}\right.$$

$$\left.\left(y + \frac{1}{3}h_{\varepsilon,1}\right)_{ii}\left(y\left(1-\varepsilon_{,0}\right) + h_{\varepsilon,0}\right)_{ii} + \left(\frac{r^2\omega^2}{h^2}\right)_{ii}\left(\left(y\left(1-\varepsilon_{,0}\right) + h_{\varepsilon,0}\right)^2\right)_{ii}\right)dydz$$

$$\text{.....(B12)}$$

Integrate equation **(B12)** with respect to (y) and substitute with ($h_{\theta 1}$) as;

$$\left(M_{-1}\right)_{ii}=\left(2\circ\int_{0}^{L/2}\frac{h_{ii}^{5}}{4\mu^{2}r_{ii}^{2}}\left(\frac{\partial P}{\partial x}\right)_{ii}^{2}\left(\frac{9+15\lambda_{1}+10\lambda_{1}^{2}}{270}\right)_{ii}-\frac{\mu_{ii}}{\mu}\left(\frac{\partial P}{\partial x}\right)_{ii}\frac{h_{ii}^{3}}{36}\left(3+3\lambda_{0}+2\lambda_{1}+4\lambda_{1}\lambda_{0}\right)_{ii}\right.$$

$$\left.+\left(r^{2}\mu^{2}\frac{h}{3}\left(1+\lambda_{0}+\lambda_{0}^{2}\right)\right)_{ii}\right)dz \qquad \text{.....(B13)}$$

Using dimensionless form for each term of **(B14)**, $\left(M_{-1}\right)_{ii}$ can be written as dimensionless form as follows **[18]**;

$$\left(\hat{M}_{-1}\right)_{ii}=\left(M_{-1}\right)_{ii}/\left(\circ c_{ii}r_{ii}^{2}\mu_{ii}^{2}L\right)=\int_{0}^{1}\left(\left(\frac{h^{\wedge 5}}{1080}\left(\frac{\partial P^{\wedge}}{\partial x}\right)^{2}\left(9+15\lambda_{1}+10\lambda_{1}^{2}\right)\right)_{x=x_{1}}\right)_{ii}dZ^{\wedge}$$

$$-\int_{0}^{1}\left(\left(\frac{h^{\wedge 3}}{36}\frac{\partial P^{\wedge}}{\partial x}\left(3+3\lambda_{0}+2\lambda_{1}+4\lambda_{0}\lambda_{1}\right)\right)_{x=x_{1}}\right)_{ii}dZ^{\wedge}+\int_{0}^{1}\left(\left(\frac{h^{\wedge}}{3}\left(1+\lambda_{0}+\lambda_{0}^{2}\right)\right)_{x=x_{1}}\right)_{ii}dZ^{\wedge}$$

.....(B14)

Similarly $\left(M_{-2}\right)_{ii}$ can be calculated;

$$\left(\hat{M}_{-2}\right)_{ii}=\left(M_{-2}\right)_{ii}/\left(\circ c_{ii}r_{ii}^{2}\mu_{ii}^{2}L\right)=\int_{0}^{1}\left(\left(\frac{h^{\wedge 5}}{1080}\left(\frac{\partial P^{\wedge}}{\partial x}\right)^{2}\left(9+15\lambda_{1}+10\lambda_{1}^{2}\right)\right)_{x=x_{2}}\right)_{ii}dZ^{\wedge}$$

$$-\int_{0}^{1}\left(\left(\frac{h^{\wedge 3}}{36}\frac{\partial P^{\wedge}}{\partial x}\left(3+3\lambda_{0}+2\lambda_{1}+4\lambda_{0}\lambda_{1}\right)\right)_{x=x_{2}}\right)_{ii}dZ^{\wedge}+\int_{0}^{1}\left(\left(\frac{h^{\wedge}}{3}\left(1+\lambda_{0}+\lambda_{0}^{2}\right)\right)_{x=x_{2}}\right)_{ii}dZ^{\wedge}$$

.....(B15)

From figure (B-1) $(M_c)_{ii}$ can be evaluated as **[18]**;

$$(M_c)_{ii} = 2(r_{ii}) \int_{-1}^{2} \int_{0}^{(h)_{ii}} \left[(u * u_z)|_{z=L/2} \right]_{ii} dy dz \quad \text{.....(B16)}$$

where;

$$(u_Z)_{ii} = \frac{1}{2\mu} \left(\frac{\partial P}{\partial Z} \right)_{ii} (y - h_{ii}) \left(y + \frac{1}{3} h_{ii}, 1x \right) \quad \text{.....(B17)}$$

In equation **(B16)** $(u_z)_{ii}$ at z=L/2 takes negative value, i.e., $\left(\partial P/\partial z|_{z=L/2}\right)_{ii} > 0$ and $(u_\theta)_{ii}$ at z=L/2 is assumed to be zero, since $(u)_{ii}$ would be zero just outside the axial end of the oil film. It yields **[18]**;

$$\left(u|_{z=L/2}\right)_{ii} = 0 \quad \text{if} \quad \left(u_z|_{z=L/2}\right)_{ii} < 0 \quad \left(\partial P/\partial z|_{z=L/2}\right)_{ii} > 0 \quad \text{.....(B18)}$$

$$\text{So,} \quad (M_c)_{ii} = 0 \quad \text{at} \quad \left(\partial P^{\wedge}/\partial z|_{z^{\wedge}=1}\right)_{ii} > 0 \quad \text{.....(B19)}$$

Substituted equations **(B11**) and **(B17)** into **(B16)**, therefore, $(M_c)_{ii}$ cane be evaluated as;

$$(M_c)_{ii} = \left(2 * r \int_{-1}^{2} \int_{0}^{h} \frac{r\mu}{h} \{y - y, 0 + h, 0\} * \frac{1}{2\mu} \frac{\partial P}{\partial z} (y - h) \left(y + \frac{1}{3} h, 1 \right) dy dz \right)_{ii} \quad \text{.....(B20)}$$

Equation **(B20)** can be integration with respect to (y) and simplified to equal;

$$(M_c)_{ii} = \frac{\pi}{\mu} \left(\mu r^2 \int_{-1}^{2} h^3 \frac{\partial P}{\partial z} \frac{-3\{3 + 3, 0 + 2, 1 + 4, 1, 0\}}{108} dz \right)_{ii} \quad \text{.....(B21)}$$

Multiply and divide equation **(B21)** by (L/2), then use dimensionless form for each term, so, $(M_c)_{ii}$ can be rewritten as **[18]**;

$$\left(\hat{M}_c\right)_{ii} = (M_c)_{ii} / \left(c_{ii} r_{ii}^2 \mu_{ii}^2 L\right) = -\frac{1}{72}\left(\left(\frac{D}{L}\right)^2 \int_{-1}^{2} A\, d\right)_{ii} \qquad \text{.....(B22)}$$

where,

$$\left(A = h^3 (3 + 3_{,0} + 2_{,1} + 4_{,0,1}) \frac{\partial P}{\partial Z}\Big|_{Z=1}\right)_{ii} \le 0 \qquad \text{if} \qquad \left(\frac{\partial P}{\partial Z}\Big|_{Z=1}\right)_{ii} \le 0$$

Finally $\left(\hat{M}_b\right)_{ii}$ can be found as **[18]**;

$$(M_b)_{ii} = 2(r_{ii}) \int_0^{L/2} \int_{(-1)_{ii}}^{(2)_{ii}} \left[(u_m)_{ii} * (u_r^*)_{jj}\right]_{r=(r)_{ii}} d\, dz \qquad \text{.....(B23)}$$

where;

$$(u_r^*)_{jj} = \frac{-k_1}{\mu}\left(\frac{\partial P^*}{\partial r}\right)_{jj} \qquad \text{.....(B24)}$$

The circumferential velocity component u_m across the control surface at (y=0) i.e. (ring and bearing surface) is given for both the case where the oil in the clearance gap flows into the porous matrix and the case where the oil in the porous matrix flows into the clearance gap. It expressed as;

$$\left(\bar{u}_m\right)_{ii} = \left(\frac{1}{h}\int_0^h \bar{u}\, dy\right)_{ii}$$

$$= \left(-\frac{h^2}{12\mu r}\frac{\partial P}{\partial \bar{\theta}}(1+\varepsilon_1)\right)_{ii} + \frac{(r\mu)_{ii}}{2}(1+\varepsilon_0) \quad \text{if} \quad \left(\left(u_r^*\right)_{jj}\Big|_{r=r_i}\right) \geq 0 \qquad \textbf{.....(B25)}$$

$$\left(\bar{u}_m\right)_{ii} = -\frac{k_1}{\mu}\left(\frac{\partial P}{r\partial \bar{\theta}}\Big|_{r=r_i}\right)_{ii} \qquad \text{if} \quad \left(u_r^*\Big|_{r=r_i}\right)_{jj} < 0 \qquad \textbf{.....(B26)}$$

So; for $\left(\left(u_r^*\right)_{jj}\Big|_{r=r_i}\right) < 0$

$$\left(M_b\right)_{ii} = \left(2 * r_{ii}\int_0^{l/2}\int_{\bar{\theta}_1}^{\bar{\theta}_2}\left\{-\frac{k_1}{\mu}\frac{\partial P}{\partial \bar{\theta}}\Big|_{r=r_i}\right\}_{ii} * \left\{-\frac{k_1}{\mu}\frac{\partial P^*}{\partial r}\right\}_{jj}\right) d\bar{\theta}\, dz \qquad \textbf{.....(B27)}$$

if dimensionless form using equation **(B27)** can be written as;

$$\left(\hat{M}_b\right)_{ii} = \left(M_b\right)_{ii} / \left(\Delta c_{ii} r_{ii}^2 \mu_{ii}^2 L\right) = \left(\int_0^{1}\int_{(\bar{\theta}_1)_{ii}}^{(\bar{\theta}_2)_{ii}}\left(\frac{c}{r}\right)_{ii}\Phi_{ii}^2\left(\frac{\partial P^{\wedge}}{\partial \bar{\theta}}\right)_{ii}\left(\frac{\partial P^{\wedge *}}{\partial r^{\wedge}}\Big|_{r^{\wedge}=1}\right)_{jj}\right) d\bar{\theta}\, dz^{\wedge} \textbf{.... (B28)}$$

but where $\left(\left(u_r^*\right)_{jj}\Big|_{r=r_i}\right) \geq 0$

$$\left(M_b\right)_{ii} = \left(2 * r_{ii}\int_0^{L/2}\int_{\bar{\theta}_1}^{\bar{\theta}_2}\left\{-\frac{h^2}{12\mu r}\frac{\partial P}{\partial \bar{\theta}}(1+\varepsilon_1) + \frac{r\mu}{2}(1+\varepsilon_0)\right\}_{ii} * \left\{-\frac{k_1}{\mu}\frac{\partial P^*}{\partial r}\right\}_{jj}\right) d\bar{\theta}\, dz$$

.....(B29)

Use dimensionless form and simplified equation **(B29)** to get;

$$\left(\hat{M}_{b}\right)_{ii} = \left(M_{b}\right)_{ii} / \left(c_{ii} r_{ii}^{2} \mu_{ii}^{2} L\right) = \int_{0}^{1} \int_{(\theta_1)_{ii}}^{(\theta_2)_{ii}} \left(\Phi \left\{ \frac{h^{2}}{12} (1+\lambda_1) \frac{\partial P}{\partial \theta} - \frac{1}{2} (1+\lambda_0) \right\} \right)_{ii} \left(\left. \frac{\partial P^{*}}{\partial r} \right|_{r=1} \right)_{jj} d\theta dz \qquad \text{.....(B30)}$$

Applying the momentum theorem to the oil – film region, which is considered as a control volume, the integral momentum equation is given by see Figure (B-1);

$$\left(M_{1} - M_{2} - M_{c} - M_{b}\right)_{ii} = \left(F_{p2} - F_{p1} + F_{zb} - F_{zj}\right)_{ii} \qquad \text{.....(B31)}$$

Since the pressure at $(\theta_1)_{ii}$ and $(\theta_2)_{ii}$ is ambient pressure so;

$$F_{p2} = F_{p1} = 0 \qquad \text{.....(B32)}$$

The shear forces on the control surface at (y=0) equal the shear forces on the control surface at $(y=h)_{ii}$ which mean that;

$$F_{zb} = F_{zj} \qquad \text{.....(B33)}$$

If equation **(B32)** and **(B33)** are substituted in equation **(B31)**, the sum of the external forces becomes zero, i.e. [**18];**

$$\left(M_{1} - M_{2} - M_{c} - M_{b}\right)_{ii} = 0 \qquad \text{.....(B34)}$$

Dividing each momentum flow rate by $\left(\circ c_{ii} r_{ii}^2 \mu_{ii}^2 L\right)$, equation **(B34)** can be written in dimensionless form as;

$$\left(\hat{M}^{-}_{1} - \hat{M}^{-}_{2} - \hat{M}^{-}_{c} - \hat{M}^{-}_{b} \right)_{ii} = 0 \qquad \text{.....(B35)}$$

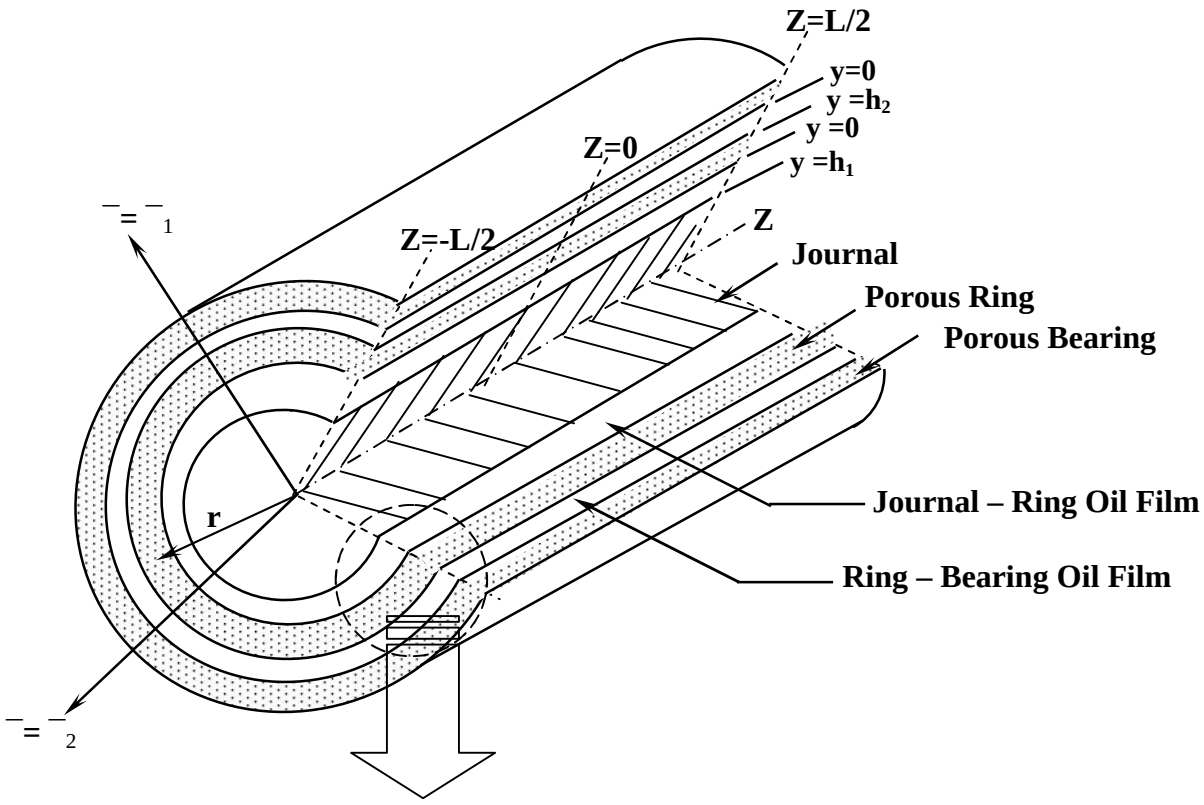

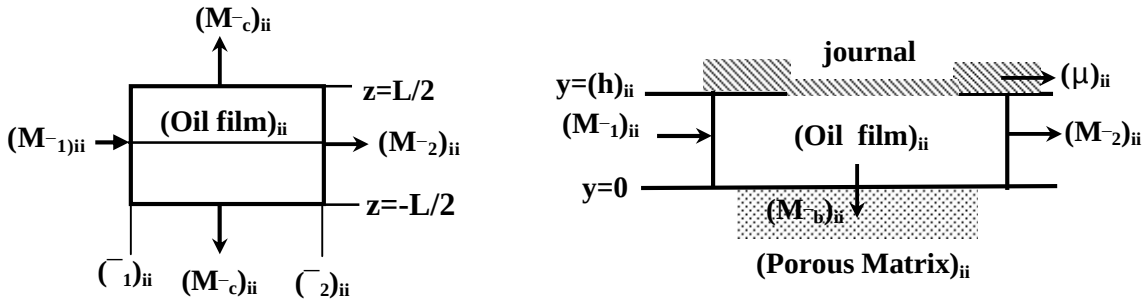

Figure (B1), Circumferential Momentum Flow Rates

APPENDIX C

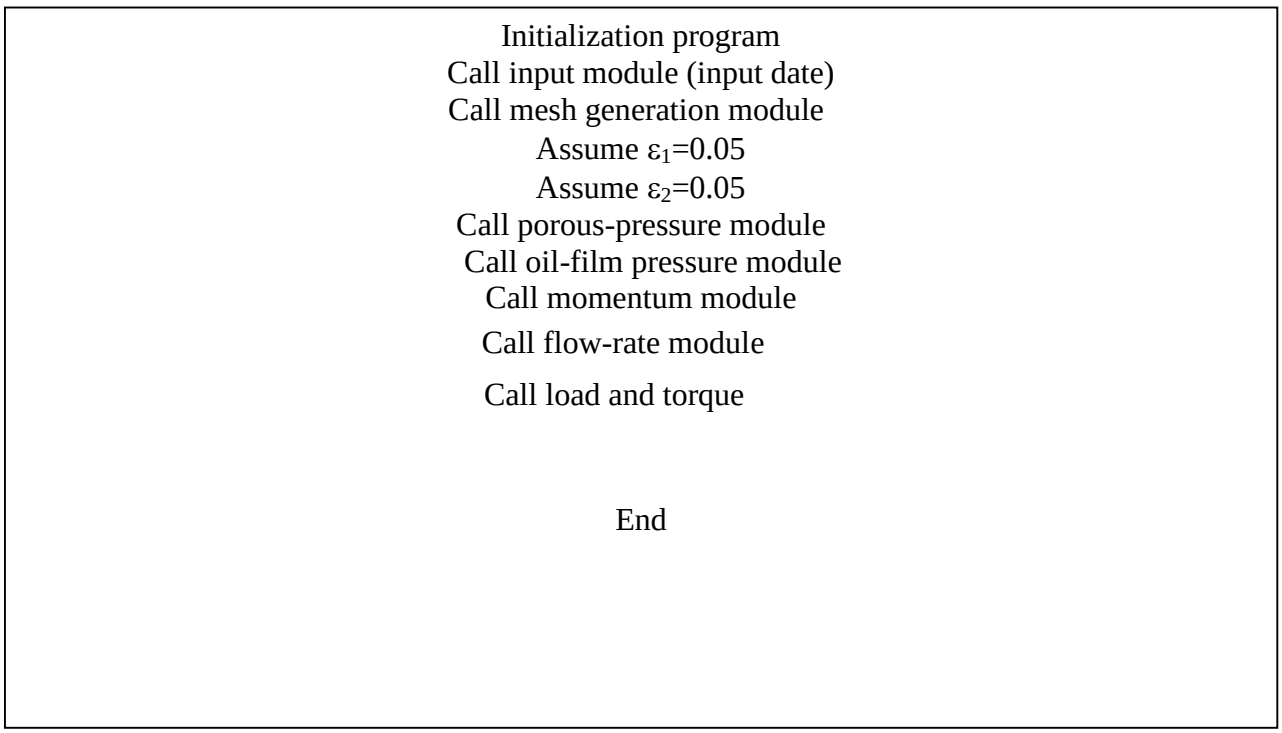

Figure (C-1) Structure Chart of the Main Program

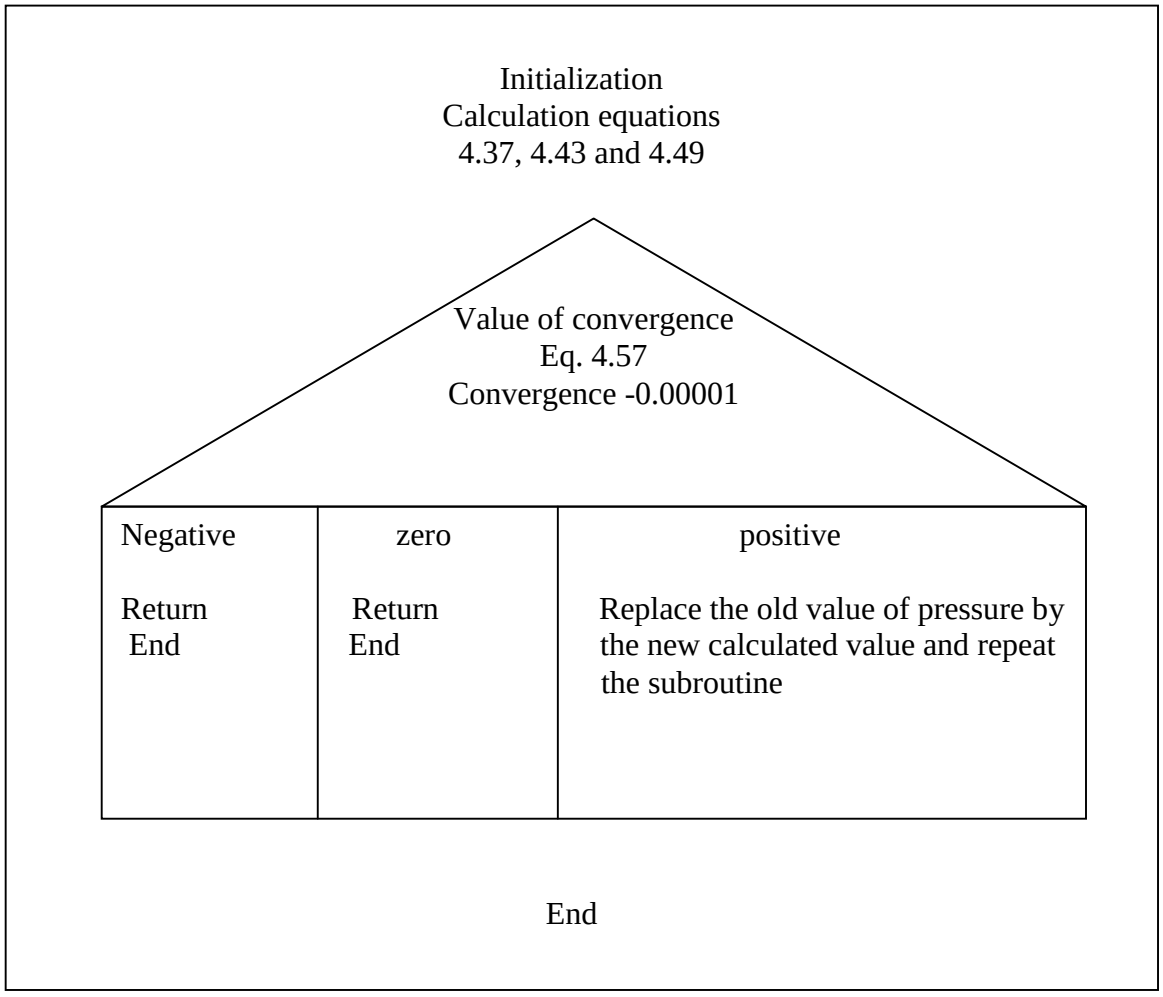

Structure chart of porous-pressure subroutine

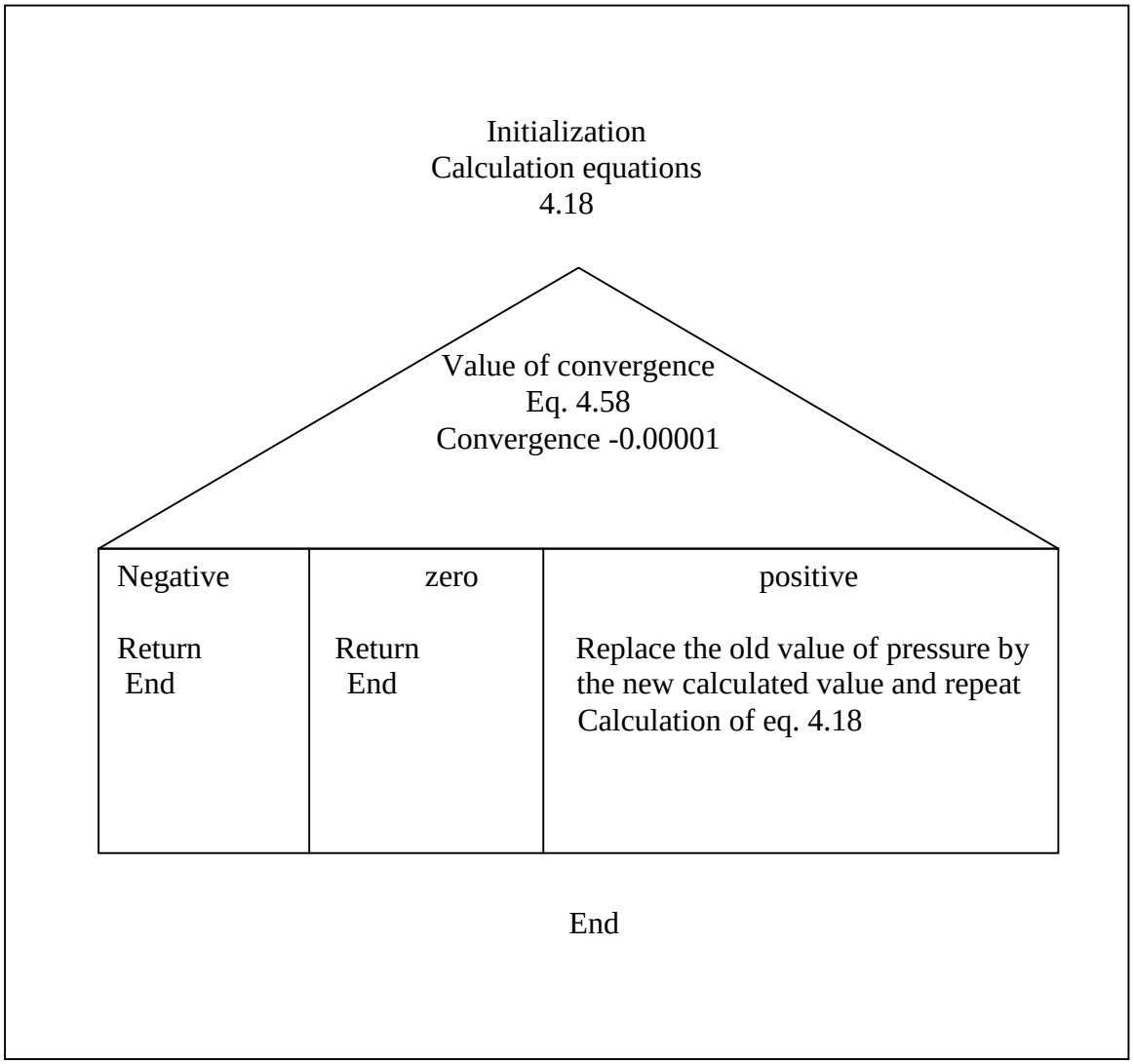

Structure chart of oil – film pressure subroutine

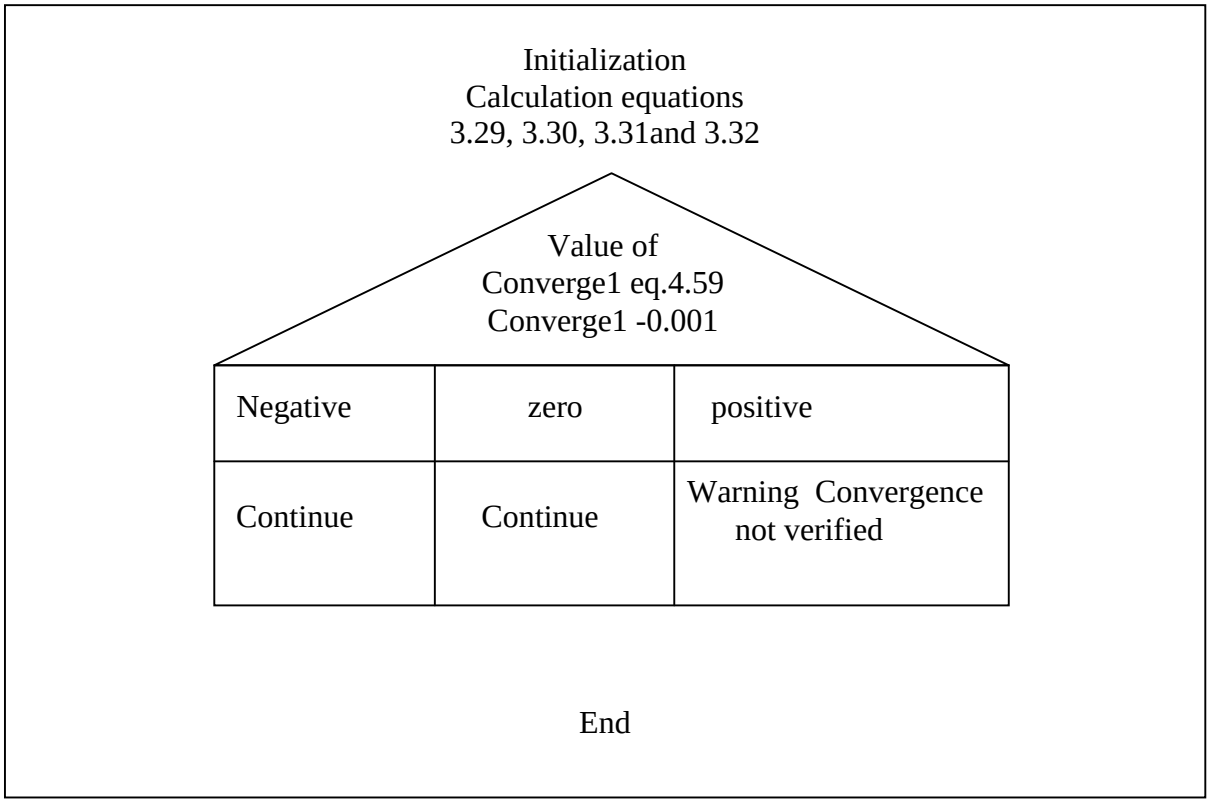

Structure chart of momentum subroutine

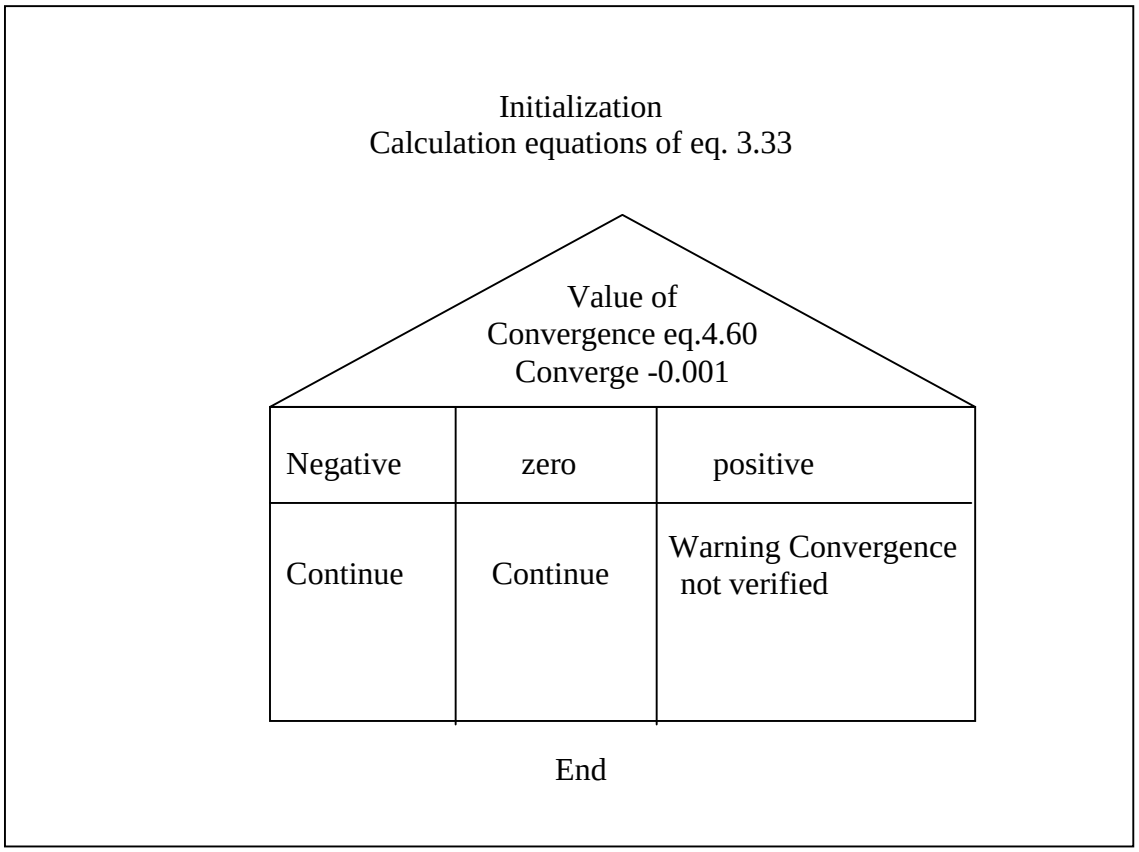

Structure chart of flow-rate subroutine

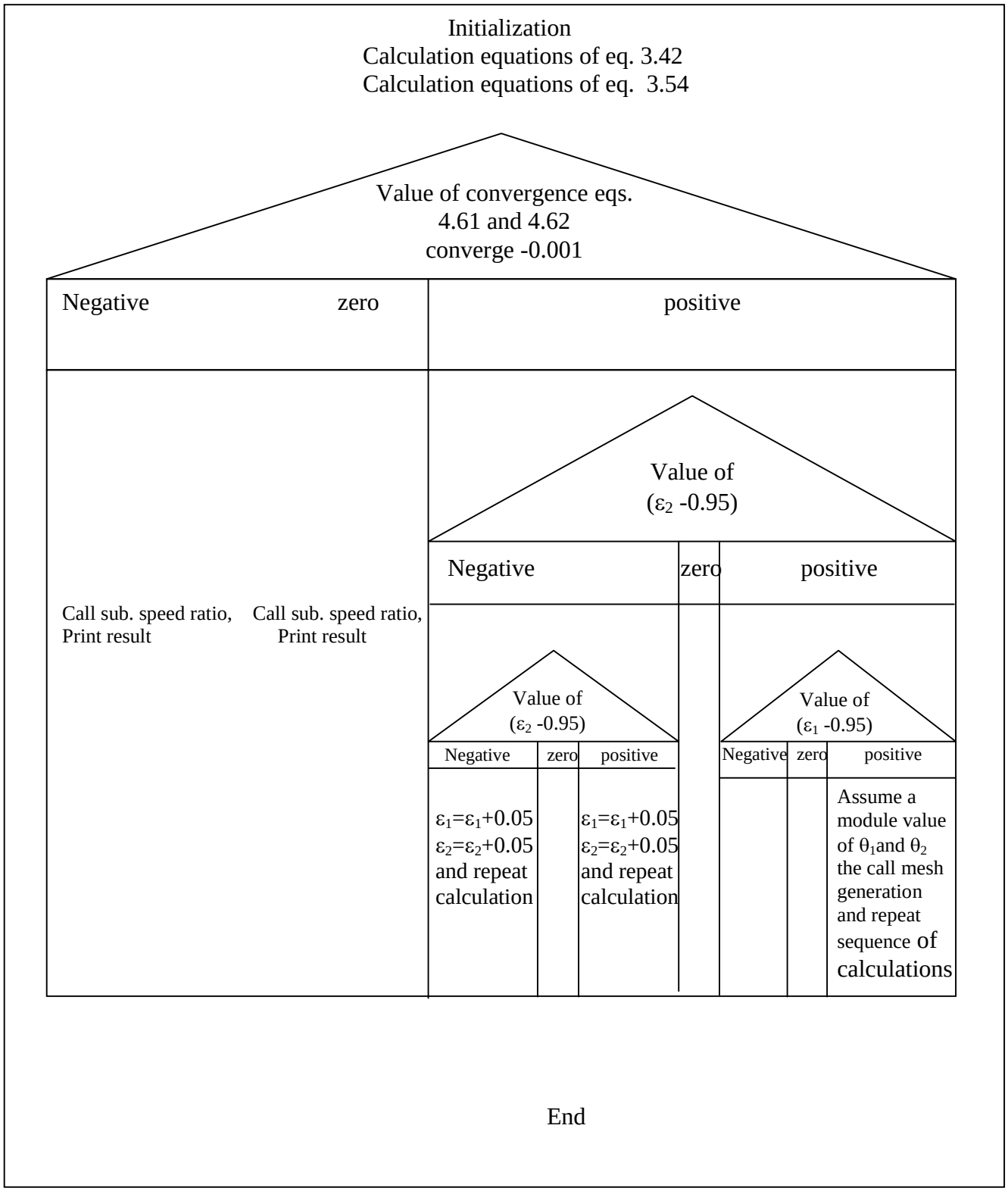

Structure chart of load and torque subroutine

جمهورية العراق

وزارة التعليم العالي والبحث العلمي

جامعة بابل

دراسة سلوك المساند ذاتية التزييت ذات الحلقة العائمة باستخدام شروط حدية محسنة

رسالة

مقدمة إلى كلية الهندسة في جامعة بابل وهي جزء من متطلبات نيل درجة ماجستير علوم في الهندسة الميكانيكية

(ميكانيك تطبيقي)

أعدت من قبل

لقاء حميد عبد الشهيد الجبوري

بكالوريوس هندسة ميكانيكية(1996)

(تشرين الثاني 2005)

1426 هـ

2005 م

الخلاصة

يتضمن هذا البحث دراسة نظرية للخصائص السكونية للمساند ذاتية التزييت ذات الحلقة العائمة. تم اعتماد نظرية الركائز المحددة الطول والتي تعمل تحت ظروف ثبوت درجة الحرارة لغرض أجراء هذه الدراسة.

لغرض ضمان عمل الركيزة تحت الظروف الهيدروديناميكية فقد تم افتراض بان الركيزة تجهز بالزيت من القطر الخارجي للركيزة تحت ضغط تجهيز منخفض. تضمنت المعالجة النظرية للموضوع حل المعادلات الحاكمة عدديا تحت دراسة تأثير مختلف العوامل التي تؤثر على أداء الركيزة وهي النفاذية, ضغط التجهيز, أبعاد الحلقة والركيزة.

تم دراسة الخصائص الساكنة للركيزة عن طريق حل معادلة رينولدز التي تحكم ضغط الزيت خلال طبقة الزيت, ومعادلة دارسي التي تحكم جريان الزيت داخل المادة المسامية بالإضافة إلى الشروط الحدية التي تستخدم لتحديد بداية ونهاية طبقة الزيت. تم أعداد برنامج مكتوب بلغة الفورتران (90) لحل المعادلات الحاكمة أعلاه آنيا.

لقد تم تحديد بداية ونهاية طبقة الزيت باستخدام معادلة الزخم التكاملية لتحديد بداية طبقة الزيت ومعادلة استمرارية الجريان لتحديد نهاية طبقة الزيت. لقد أظهرت نتائج الدراسة بان ضغطا سالبا يتولد قبل نهاية طبقة الزيت كما هو متوقع عند مقارنة النتائج مع تلك المنشورة لبعض الباحثين الذين عملوا على دراسة تصرف المساند ذاتية التزييت. كما أظهرت النتائج بان أداء المسند يتأثر بمختلف العوامل وهي ضغط التجهيز, النفاذية, نسبة اللاتمركز, نسبة الخلوص, ونسبة أنصاف أقطار الحلقة.